1973

Electroanalytical determination of antimony using electrocatalytic and enhancement phenomena

Larry Robert Taylor
Iowa State University

Electroanalytical determination of antimony using electrocatalytic and enhancement phenomena

by

Larry Robert Taylor

A Dissertation Submitted to the
Graduate Faculty in Partial Fulfillment of
The Requirements for the Degree of
DOCTOR OF PHILOSOPHY

Department: Chemistry
Major: Analytical Chemistry

Approved:

Signature was redacted for privacy.

In Charge of Major Work

Signature was redacted for privacy.

For the Major Department

Signature was redacted for privacy.

For the Graduate College

Iowa State University
Ames, Iowa

1973

TABLE OF CONTENTS

I. INTRODUCTION

Recent developments in automatic instrumentation and construction of solid electrodes have been combined to develop a rapid, selective, sensitive, and inexpensive electrochemical detector applicable to forced-flow column chromatography. In the development of the electrochemical detector, parameters such as concentration, flux of electroactive species to the electrode surface, effects of electrode pretreatment, and dependence on the supporting electrolyte were investigated. The effects of these parameters on the electrochemical reactions were studied using a rotating, platinum-disk electrode (RPDE). After preliminary investigation with the RPDE, the electrochemical detector was evaluated in terms of its sensitivity, reproducibility, detection limit, and selectivity.

An amperometric technique for the determination of Sb(III) in acidic media was investigated. In solutions of H_2SO_4, Sb(III) is not electroactive at platinum electrodes and an indirect technique was required. The catalysis of the oxidation of Sb(III) in aqueous solutions of H_2SO_4-NaBr by electrogenerated Br_2, i. e. catalytic enhancement, was investigated at an RPDE, and the results were used to choose suitable conditions for the detection of Sb(III) with the electrochemical detector.

Recently it was discovered that iodide adsorbed at the surface of the platinum electrode electrocatalyzes the direct electrochemical oxidation of Sb(III) in dilute HCl (40). The effect

of incomplete surface coverages by adsorbed iodide on the direct electrochemical oxidation of Sb(III) was investigated at an RPDE. The amperometric determination of Sb(III) using the electrocatalyzed mechanism was concluded to be a more suitable basis for chemical analysis than the determination using enhancement. The determination of Sb(III) was made in a variety of matrices using forced-flow liquid chromatography with electrochemical detection.

II. LITERATURE REVIEW

Measurements of the formal potential of the Sb(V)/Sb(III) couple were made in aqueous solutions of a large variety of supporting electrolytes at solid electrodes (7, 8, 59, 76, 81, 83, 123, 129, 180, 181, 206, 214). The polarographic reduction or oxidation of Sb(III) and the reduction of Sb(V) in various supporting electrolytes at a dropping mercury electrode (DME) have been studied by many investigators (1, 12, 14, 15, 24, 29, 35, 37, 46, 47, 50-53, 61, 67, 68, 71, 72, 74, 78-81, 91, 93, 96, 101, 107, 119, 124, 126, 129, 136, 140, 141, 142, 154-156, 160, 162, 164, 165, 167, 173, 175, 183, 200-202, 211, 213, 217, 225, 226, 228, 230, 231, 238, 239). Other polarographic techniques, such as A. C. and derivative polarography, have been used to investigate the direct electrochemical reactions of Sb(III) and Sb(V) at solid and mercury electrodes (25-27, 32, 41, 49, 73, 75, 84, 85, 105, 111, 134, 145, 176, 186, 208, 216).

Antimony has also been determined by controlled potential electrolysis at mercury (55) and platinum cathodes (171). Coulometric determinations with electrogeneration of Br_2 at constant current in 2 M HCl were reported by Brown and Swift (28). Lingane and Bard (130) and Wise and Williams (234) coulometrically determined Sb(III) at pH 7-8 using electrogenerated I_2. Kostromin and Akhmentov (120) determined Sb(III) in 2 M H_2SO_4 and 1 M HCl with electrogeneration of $Cr_2O_7^{2-}$.

Polarographic, coulometric, and amperometric methods have

all been used to determine antimony in a variety of inorganic matrices. Polarographic analyses have been used primarily for the determination of antimony in ores and alloys (41, 48, 49, 67, 74, 124, 142, 145, 154, 173, 175, 183, 212, 225). In his book entitled "Amperometric Titrations", Stock listed some of the applications of amperometry for the determination of Sb(III) (197). Rechnitz reviewed the applications of controlled potential electrolysis (171). The available electrochemical techniques described are generally subject to interference from metal ions such as As (154, 162, 225), Bi (173), Cu (145), Fe (145), Pb (142, 145, 212), and Sn (154). Elimination of the interfering species is usually done by precipitation (154, 237) or with masking agents (87, 124, 142).

III. INSTRUMENTATION

A. Electronic Circuitry

1. Three-electrode Potentiostat.

A schematic of the three-electrode potentiostat is shown in Figure III. 1. A variable voltage source was constructed by applying a ±3.6 V signal to a 10-turn, 10 KΩ potentiometer. The variable voltage signal was applied to the input of control amplifier A-1 and the output of this amplifier was connected to the counter electrode. A voltage follower with high input impedance, amplifier A-2, was placed between the reference electrode and the negative input of amplifier A-1, and a second amplifier with high input impedance, A-3, was used for the current follower.

The output of the current follower was fed to a voltage divider consisting of a 100 KΩ resistor in series with a 10-turn, 10 KΩ potentiometer. For most experiments, a 1:10 reduction in the signal was required. The output from the voltage divider was used to drive a strip chart recorder and operate an electronic integrator.

Feedback resistors for the current follower were calibrated by the Iowa State University Physics Instrument Shop. The RC constant of the integrator was determined by applying a 0.250 V signal across a 10 KΩ resistor to the negative input of amplifier A-3.

2. Four-Electrode Potentiostat.

The electronic instrument used was that for the simultaneous and independent potentiostatic control of two electrodes described

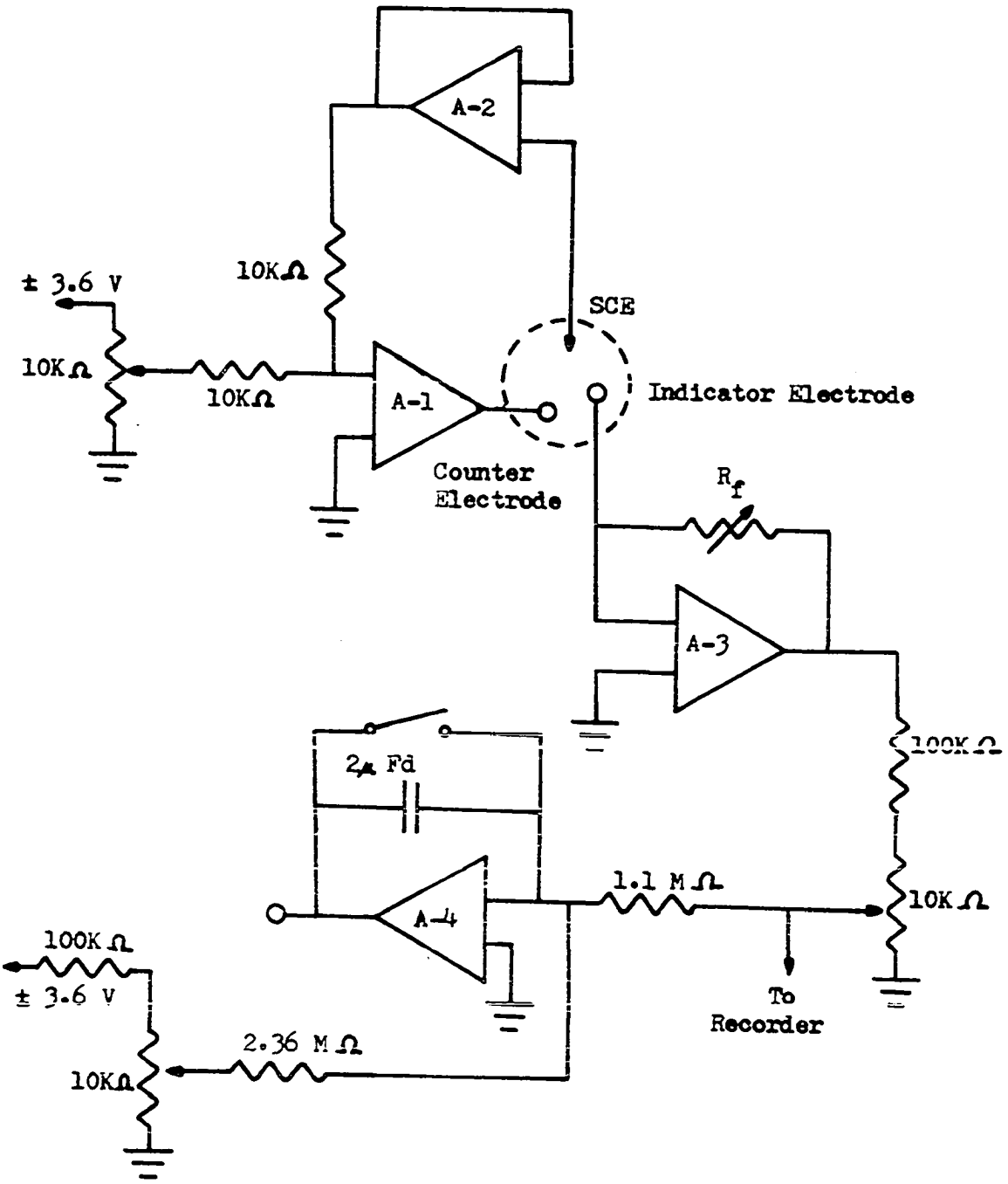

Figure III. 1. Schematic for three-electrode potentiostat

in Reference 148. The portion of the circuit for potentiostatic control of electrode I-1 in Figure 1 of Reference 148 was modified according to the design described in Reference 29. The modification permitted the control of potential or current in electrode I-1 with simultaneous potentiostatic control of electrode I-2. The circuit was constructed in our laboratory but an equivalent instrument is available commercially from Pine Instrument Co. of Grove City, Pennsylvania. Rather than use a recorder with a potentiometric input for recording the current in electrode I-2, as described in Reference 148, a difference amplifier was used to monitor the difference in the voltages at the outputs of amplifiers A-2 and F-2.

Voltages were measured using a digital voltmeter, Model 345, from Data Technology, Inc., of Palo Alto, California. The voltmeter was equipped with BCD output and was interfaced to a digital printer, Model DP12, from Mechanics For Electronics, Inc., of Wilmington, Massachusetts. Current-potential curves were recorded using an X-Y recorder, Model 815, from Bolt, Beranek, and Newman, Inc., of Santa Ana, California. Instruments used for determining values of current, voltage, and resistance were calibrated using standards from the Physics Instrument Services of Iowa State University.

3. Circuitry for Automatic End Point Shut Off.

A circuit which automatically monitors the indicator electrode current and shuts off a clock timer and the constant current in the coulometric electrode is described schematically

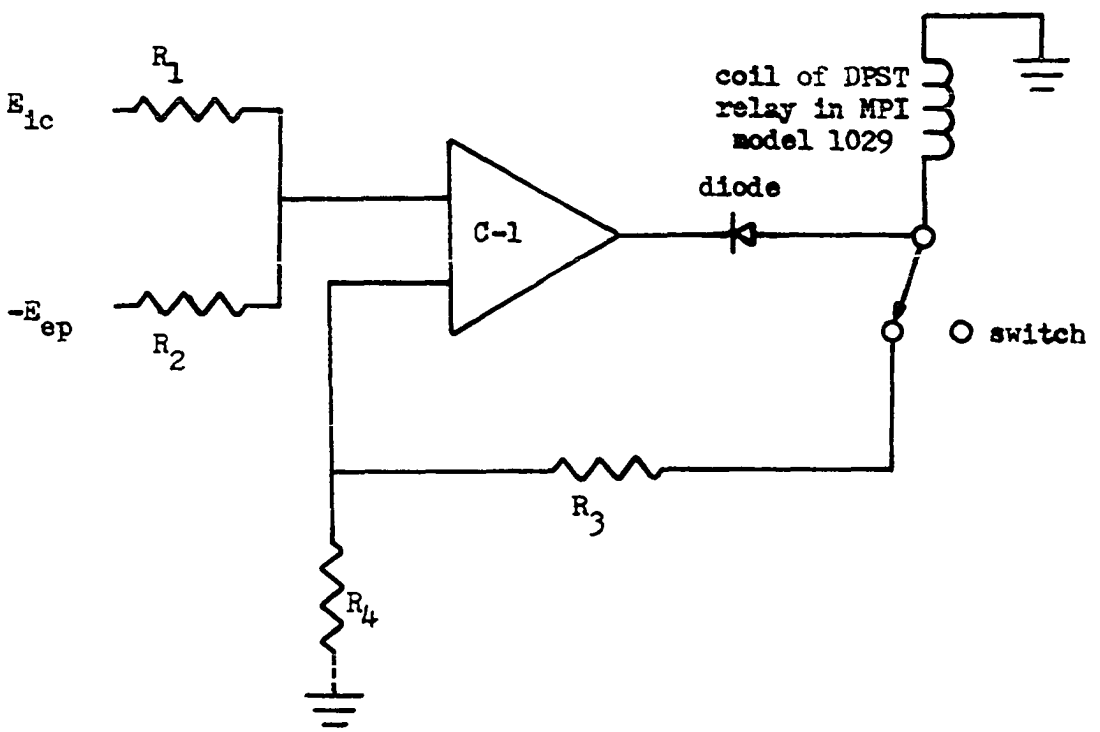

$R_1 = R_2 = R_3 = R_4 = 20{,}000$ ohms

Figure III. 2. Device for automatic detection of end point

in Figure III. 2. The clock timer used was Model 1029 from McKee Pederson Instruments of Danville, California.

A positive voltage proportional to the indicator current, E_{ic}, was continuously applied to resistor R_1 by the output of the difference amplifier described in Section III. A. 2. At the end point, $E_{ic} = E_{ep}$. The control amplifier, C-1, was wired with positive feedback with the result that the output was stable only at the saturation limits, ±12 V. A bias voltage equal to $-E_{ep}$ was applied to resistor R_2. Before the end point, $E_{ic} < E_{ep}$ and the output state of C-1 was +12 V. At an infinitesimal time past the end point, $E_{ic} > E_{ep}$ resulting in the state of the output of C-1 changing to -12 V. Electrical current was then conducted by the diode actuating a relay which stopped the timer and shut off the current in the generator electrode. At the beginning of a coulometric determination, $E_{ic} < E_{ep}$ and the momentary opening of the switch resulted in the output voltage of C-1 reverting to +12 V. The clock timer and flow of current in the generator electrode were thus started.

B. Coulometric Detector

A tubular platinum electrode, having an inside diameter of 0.28 cm and a length of 1.5 cm, was provided by Pine Instrument Co. The electrode is shown in its Teflon housing by the schematic in Figure III. 3. The interior of the electrode was packed by John LaRochelle in the following manner: each end of the tubular electrode was packed with a wad of 32 gauge platinum wire and the

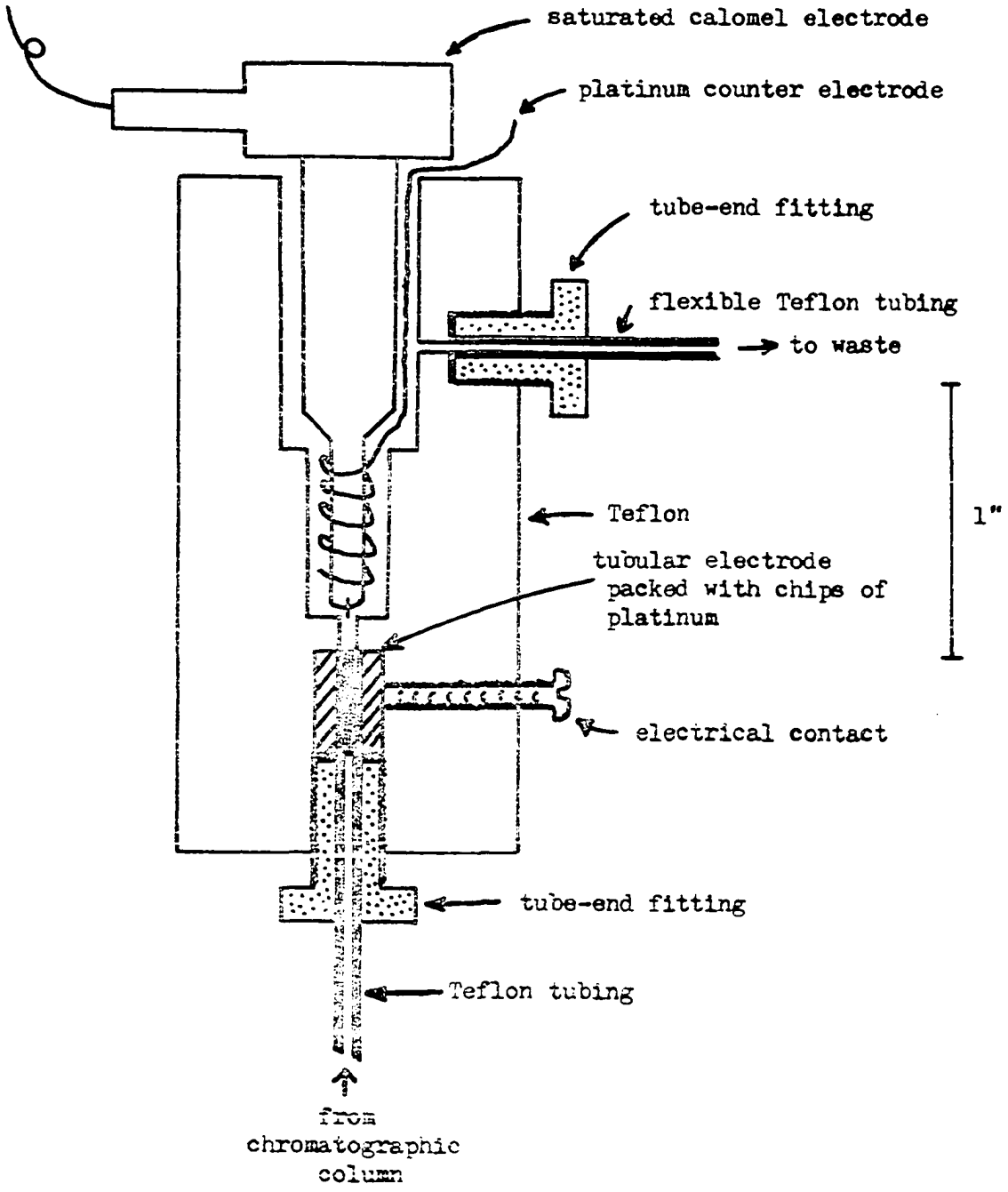

Figure III. 3. Cross-Section of Coulometric Electrode

center was filled with finely chopped platinum wire ranging from 26 to 32 gauge. A coil of platinum wire, which served as the counter electrode, was wrapped around a Beckman SCE and both were inserted into the chamber above the tubular electrode.

C. Liquid Chromatograph

1. Chromatographic Design.

The liquid chromatograph was constructed according to the design described by Seymour, Sickafoose, and Fritz (240). Teflon tubing, sample injection valves, eluent selection valves, and the chromatographic column were obtained from Gilmont Instruments, Inc. A synchronous, screw-driven syringe pump and Teflon mixing chamber were built by Pine Instrument Co. Eluent tanks, nylon intake and exhaust manifolds, and brass-to-Teflon adapters were built by the Iowa State University Chemistry Shop. A schematic of the liquid chromatograph used is shown in Figure III. 4.

2. Measurement of Flow Rates.

When compressed helium was used for pumping eluents, flow rates were controlled by restricting the fluid flow through the Teflon tubing with a screw clamp. The flow rate was related to the flow meter readings by preparing a calibration curve of flow meter reading *versus* flow rate. To measure flow rates, the eluent was diverted into a 10-ml buret and the length of time required to deliver a particular volume was determined.

The syringe pump had a variable speed motor which was controlled by a 10-turn potentiometer. The flow rate was measured as a

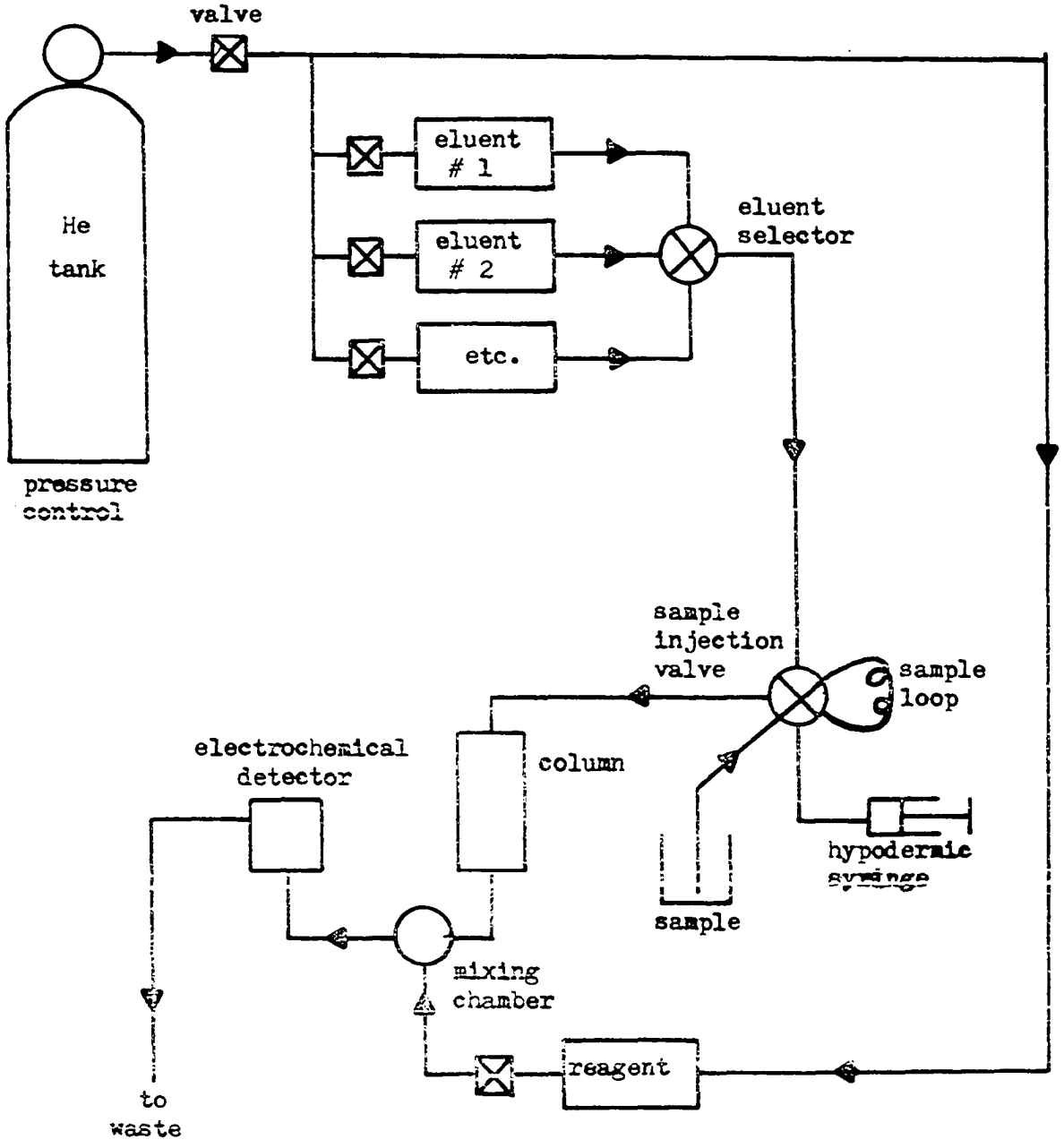

Figure III. 4. Diagram of Forced-Flow Liquid Chromatograph

function of the potentiometer setting. Flow rates were measured by the same method as used for the pumping by compressed helium. Calibrations for both pumping systems are shown in Figure III. 5.

3. Volume of Sample Loops.

The exact volume delivered using the 0.5-ml. sample loop volume was determined by comparing the volume of 0.10 M NaOH titrant required to titrate 1.0 ml aliquots of 5.0 M $HClO_4$, delivered from a calibrated pipet, to the amount of 0.10 M NaOH titrant required to titrate two 0.5 ml aliquots of 5.0 M $HClO_4$ delivered by the sample loop. The volume was determined to be 0.5065 ± 0.0017 ml.

The 2.0-ml sample loop volume was measured by delivering an aliquot of 0.0100 M As(III) into a coulometric cell containing 4.0 M H_2SO_4 and 0.10 M NaBr. The As(III) was titrated by electrogenerating Br_2 at a constant current of 10.00 mA using the circuitry described in Sections III. A. 2 and III. A. 3. The sample loop volume was found to be 2.017 ± 0.0035 ml.

D. Ultra-Violet Spectra

Spectra in the UV region of the electromagnetic spectrum between 200 nm and 350 nm were obtained using a Bausch and Lomb Spectronic 600 dual beam spectrophotometer equipped with a Sargent Model SRLG recorder to record the transmittance versus wavelength.

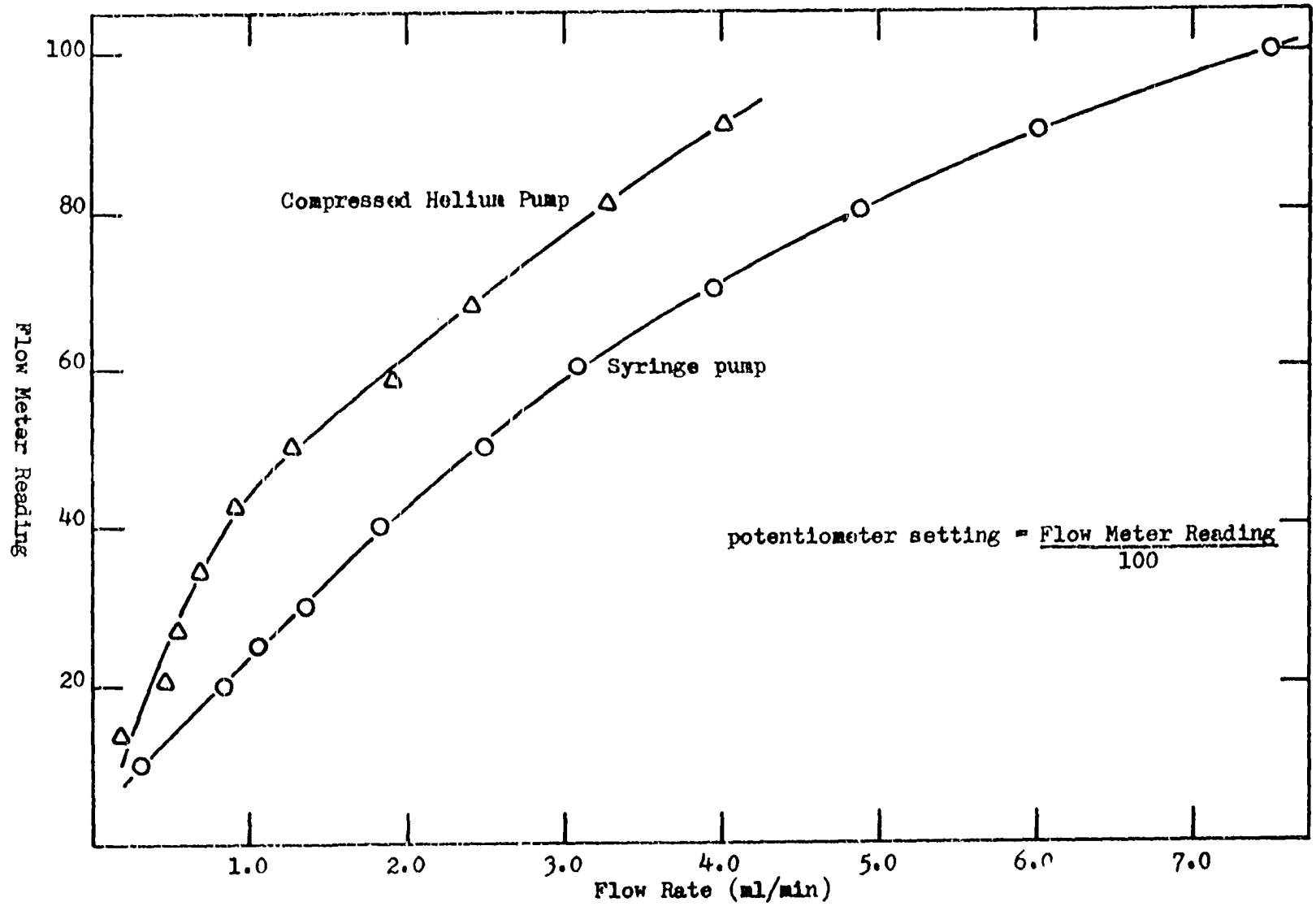

Figure III. 5. Flow Rate Calibration Curves for Compressed Helium and Syringe Pumping Systems.

IV. INVESTIGATION OF THE PHENOMENON OF CATALYTIC ENHANCEMENT

A. Introduction

To be applicable for in-stream analysis, the electrochemical detector must be capable of continuous operation at high stream velocities. For the electrochemical detector, a dropping mercury, hanging mercury drop, or mercury pool electrode was judged to be unsuitable because of the physical instability of the mercury electrode at high stream velocities. Random motions of the electrode surface would result in charging currents which would prevent application of the detector for trace determinations.

A solid electrode, such as platinum, is preferred as a detector material for in-stream analysis. One disadvantage, however, is that the reduction of Sb(III) plates the electrode, thus changing the electrode properties. Also, if hydrogen evolution occurs simultaneously with the deposition of antimony, some stibine may be produced (171). An amperometric method was developed which utilized the electrogeneration of an intermediate which reacts rapidly and quantitatively with the non-electroactive species in solution. The technique is based on the measured increase, caused by Sb(III), of the limiting current for the oxidation of Br^- to Br_2 in acidic media. The mechanism for the Faradaic reaction is described by Equation IV. 1 and IV. 2. According to this mechanism, Br^- serves essentially as a catalyst for the electrolysis of Sb(III). Such a phenomenon is commonly known as a "catalytic enhancement". The use of catalytic

enhancement for electroanalytical determinations of electroinactive species was described by Mairanovskii (135).

Platinum electrode: $2Br^- \longrightarrow Br_2 + 2e^-$ (IV. 1)

Diffusion layer: $Sb(III) + Br_2 \longrightarrow 2Br^- + Sb(V)$ (IV. 2)

This investigation of the catalytic enhancement by Sb(III) of the limiting current for the oxidation of Br^- was made using an RPDE. This electrode was chosen because the rates of convective transport can be precisely controlled and easily changed by controlling the rate of rotation of the electrode (125). It is necessary to study the effect of variations of fluid velocity on the applicability of any detector used in a fluid stream. If the rate of the forward reaction in Equation IV. 2 is fast relative to the rate of mass transport in the vicinity of the electrode, and if the equilibrium constant for the homogeneous reaction is large, the concentrations of Br^- and Sb(III) at the surface of the electrode equal zero for an electrode potential in the region of the limiting anodic wave for Br^-. Thus, the total current in the electrode is limited by the rates of convective-diffusional transport of Br^- and Sb(III) and independent of the rate constant as described by Equation IV. 3. For a rotating disk electrode,

$$I_{\ell,tot} = n_{Br^-}F(\text{flux } Br^-) + n_{Sb(III)}\,F(\text{flux } Sb(III)) \quad \text{(IV. 3)}$$

Equation IV. 3 is written as Equation IV. 4. In Equation IV. 3 and IV. 4,

$$I_{\ell,tot} = 0.62\,FA\nu^{-1/6}\omega^{1/2}(n_{Br^-}D_{Br^-}^{2/3}C_{Br^-}^{b} + n_{Sb(III)}D_{Sb(III)}^{2/3}C_{Sb(III)}^{b}) \quad \text{(IV. 4)}$$

I = Faradaic current limited by rate of convective-diffusional mass transport

F = Faraday's constant

A = area of the disk electrode

ν = kinematic viscosity of the solution

ω = angular velocity of electrode rotation

n_i = number of electrons transferred in reaction of the i^{th} species

D_i = diffusion coefficient of the i^{th} species

C_i^b = concentration of the i^{th} species in the bulk of the solution

If k for Equation IV. 2 is zero, the observed current is due only to the oxidation of Br^- and is predicted by Equation IV. 5.

$$I_{\ell,tot} = I_{\ell,Br^-}$$
$$= 0.62\, FA\nu^{-1/6}\omega^{1/2} n_{Br^-} D_{Br^-}^{2/3} C_{Br^-}^b \qquad \text{(IV. 5)}$$

The solution of the equation of convective-diffusion for the case of intermediate values of k has been discussed by Haberland and Landsberg (77) and by Prater and Bard (163). It has been found that Equation IV. 4 is applicable for the catalytic enhancement of Sb(III) in 4.0 $\underline{M}$ H_2SO_4 for low values of ω when $C_{Sb(III)}^b$ $C_{Br^-}^b$.

B. Experimental

1. Chemicals and Reagents.

Stock solutions of As(III) were prepared using Primary Standard As_2O_3 from the National Bureau of Standards. Stock

solutions of Sb(III) were prepared using Technical Grade metal from Coleman and Bell Co. and Reagent Grade from J. T. Baker, Inc. All water used was triply distilled with a deionization between the first and second distillation, the second being from alkaline permanganate.

Coulometric determinations of Sb(III) with electrogenerated Br_2 in 4.0 M H_2SO_4 were performed for two standard alloys from the National Bureau of Standards and two standard alloys prepared by Dr. John D. Verhoeven of the Department of Metallurgy at Iowa State University and Ames Laboratory of the Atomic Energy Commission. The certificate values of the standards were as follows: NBS-54D contained 88.57% Sn, 7.04% Sb, 3.62% Cu, 0.62% Pb, and 0.1% of As, Bi, Fe, Ag, and Ni. NBS-53 contained 78.87% Pb, 10.91% Sn, 10.09% Sb, and 0.1% of Bi, Cu, Fe, and As. ISU-1 contained 96.00% Pb and 4.00% Sb. ISU-2 contained 56.00% Sn, 40.00% Pb, and 4.00% Sb.

2. Preparation of Solutions.

a. As_2O_3. Standard solutions of As(III) were prepared as follows: Sufficient Primary Standard As_2O_3 to prepare 1.0 l of 5 mM As(III) was dissolved in 20 ml of 5 M NaOH. The solution was transferred to a volumetric flask and 200 ml of water was added. 225 ml of concentrated H_2SO_4 were added with mixing, the solution cooled to room temperature, and diluted to the proper volume with distilled water.

b. Sb and Sb_2O_3. Stock solutions of Sb(III) were prepared

using sufficient Sb metal or Sb_2O_3 to prepare 1.0 l of 5 mM Sb(III) which was dissolved in 30 ml of concentrated H_2SO_4 at 250-275° C. Prepurified N_2 was bubbled through the solution during cooling to remove dissolved SO_2. The solution was transferred to a volumetric flask and 200 ml of distilled water added while vigorously stirring to prevent the hydrolysis and precipitation of Sb(III). 225 ml of concentrated H_2SO_4 were added, the solution was cooled and diluted to the proper volume with distilled water.

c. Pb-Based Alloys (Procedure A). The procedure for dissolution of alloys designated ISU-1 and NBS-53 was similar to methods described for lead-based alloys in References 236 and 227. Sufficient alloy to prepare a solution 3-5 mM in Sb(III) was dissolved in 30 ml of concentrated H_2SO_4 at 250-275° C. After cooling to room temperature, 70 ml of water were added slowly with vigorous stirring and the solution was again cooled. The solution was decanted from the precipitate of $PbSO_4$ and heated to gentle boiling to remove dissolved SO_2. The $PbSO_4$ was boiled with 10 ml of concentrated HCl until the gray precipitate of $PbSO_4$ was converted to white, crystalline $PbCl_2$. The process resulted in the dissolution of all Sb(III). The $PbCl_2$ was removed by filtration with Whatman No. 41 paper and rinsed with 50 ml of 40% H_2SO_4. The combined filtrate was diluted with sufficient H_2SO_4 and H_2O so that the final acidity was 4.0 M H_2SO_4.

d. Sn-Based Alloys (Procedure B). The procedure for dissolution of alloys designated NBS-54D and ISU-2 was as follows: Sufficient sample to prepare a solution 3-5 mM in Sb(III) was dissolved in 30 ml of concentrated H_2SO_4 at 250-275° C. 70 ml of water were added and N_2 bubbled through the solution during cooling to remove dissolved SO_2. The solution was transferred to a volumetric flask and diluted with concentrated H_2SO_4 and H_2O, while vigorously stirring, so that the final acidity was 4.0 M H_2SO_4.

Solutions of Sn-based alloys prepared according to Procedure B developed a yellow color within a few days of preparation and a yellow precipitate after 2 to 4 weeks. The yellow color and precipitate were concluded to be the products of the slow hydrolysis of Sn(IV) since the same phenomena occurred for solutions containing only Sn(IV) prepared by dissolving Sn according to Procedure B. Solutions of Sn-based alloys were stable if 5-10 ml of concentrated HCl were added after the first addition of water. The modification of Procedure B with the use of HCl will be referred to as Procedure B + HCl.

3. Standardization of Solutions.

Coulometric determinations of As(III) and Sb(III) by electrogeneration of Br_2 at constant current were performed using a glass cell constructed with three chambers separated by fritted glass disks. The larger chamber contained a platinum generator electrode, a microplatinum indicating electrode, and a Beckman

Model 39270 Saturated Calomel Electrode. The solution of electrolyte in this chamber was 0.10 M NaBr in 4.0 M H_2SO_4. A coil of 21 gauge platinum wire in 4.0 M H_2SO_4 was used as the counter electrode. The chamber for the counter electrode was separated from the chamber containing the generator electrode by an intermediate compartment filled with 6.0 M H_2SO_4.

Coulometric determinations were made using the circuit described in Section III. A. 2 with galvanostatic control of the generator electrode and simultaneous potentiostatic control of the platinum indicating electrode. An electrical current of approximately 20.0 mA was used for the electrogeneration of Br_2 with the exact value determined at the time of each analysis by measuring the IR-drop produced by the current across a standard resistor. The electrolyte in the generator compartment was stirred during the coulometric analyses using a magnetic stirrer and a Teflon-coated bar. The current of the indicating electrode was typically 0.02 μA throughout the coulometric determinations. The current corresponding to the end point was arbitrarily taken as 0.10 μA and was due to the reduction of excess Br_2. The circuitry used to automatically shut off the constant current in the generator electrode and the clock timer was described in Section III. A. 3.

4. Experimental Procedures.

Voltammetric studies of catalytic enhancement were performed using the circuitry described in Section III. A. 2 and an RPDE from Pine Instrument Co. The geometric area of the disk electrode

was 0.3135 cm^2. The RPDE was rotated using a variable speed rotator, Model PIR, from Pine Instrument Co. A description of the glass cell used for volumetric studies is given in Reference 98. The cell was thermostated by circulating water from a bath at constant temperature through the water jacket. The temperature was controlled within $\pm 0.2^{\circ}$ C.

The RPDE was polished with Beuhler Handimet 600 paper stripe followed by 30 μ, 6 μ, and 1 μ Beuhler AB Metadi Diamond on nylon lubricated with Beuhler Metadi Fluid. Following each step in the procedure, the electrode was washed carefully with detergent using a cotton swab and was then rinsed thoroughly with distilled water. At the beginning of each experimental day, the electrode was polished with 0.3 μ alumina on Beuhler microcloth using distilled water as a lubricant and the electrode was cleaned as described above. The electrode was then potentiostated in 4.0 M H_2SO_4 for 3 minutes at +1.5 V, -1.5 V, and 0.0 V.

All solutions were deaerated using Air Products, prepurified (99.999%) nitrogen. All potentials of the electrode were measured and are reported in V vs. SCE. Following pretreatment of the electrode, the potential was set to 0.300 V and the voltage range scanned between the pre-set scan limits. When the voltage returned to 0.300 V, the voltage scan was held until the current fell to less than 2 μ A. This procedure was repeated for every I-E curve obtained.

Values of the limiting current for oxidation of Br^- in the absence and presence of Sb(III) were obtained using a potential-step method. Following the pretreatment of the electrode, the potential was set at 0.300 V and the residual current allowed to decrease to less than 2 μ A. The potential was then stepped to 1.100 V which is in the region of the limiting current for oxidation of Br^-. The currents for charging of the double layer and oxidation of the platinum surface were allowed to decay and the value of current printed. The potential was then returned to 0.300 V. All additions of reagents were made with the potential of the electrode at 0.300 V.

C. Results and Discussion

1. Coulometry.

a. Stock solutions of As(III) and Sb(III). The current efficiency for the electrogeneration of Br_2 in 4.0 M H_2SO_4 was determined by coulometric titration of the solution of NBS Primary Standard As_2O_3. Each aliquot contained from 25 to 50 μ moles of As(III). A total of 29 determinations were made over a period of 5 months. The average efficiency was 100.0% with a relative standard deviation of 2 ppt.

Table IV. 1 contains the results for the coulometric standardization of the stock solutions of Sb(III). The concentration of Sb(III) found for the solutions prepared with technical grade Sb were consistently less than the calculated values, undoubtedly because of impurities. The concentration of Sb(III) found for

the solution prepared from reagent grade Sb_2O_3 was equal to the value calculated. The precision of the determinations for both stock solutions was essentially identical. The values of concentration determined coulometrically were used as the correct values.

TABLE IV. 1

Standardization of Stock Solutions of Sb(III)

Solution	Determinations	Calculated (mM)	Found (mM)	Std. Dev. (mM)
1[a]	10	4.11	4.03	0.012
2[a]	4	4.00	3.96	0.024
3[a]	5	5.00	4.95	0.015
4[b]	7	4.05	4.05	0.012

[a]Prepared from technical grade Sb metal.
[b]Prepared from reagent grade Sb_2O_3.

References 130 and 234 prescribe the use of tartaric acid when determining Sb(III) by a coulometric method in neutral and slightly basic media. The chelating properties of tartrate prevent hydrolysis and precipitation of Sb(III). The use of tartrate was not necessary in 4.0 M H_2SO_4, but when added it had no adverse effect on the results of coulometric determinations.

b. Lead and Tin-Based Alloys. The results of the coulometric determinations of Sb in the four standard alloys are summarized in Table IV. 2. The success of the procedures for dissolution and coulometric determinations is evident from an inspection of

the results. No difficulty was experienced in precisely applying Procedure A for Pb-based alloys. It was stated above that solutions of Sn-based alloys without the use of HCl were not stable because of hydrolysis of Sn(IV). The results of coulometric determinations of Sb(III) in solutions which were yellow were distinctly low perhaps due to the formation of a stable dinuclear complex between Sb(III) and the product of the hydrolysis of Sn(IV). The modification of Procedure B with

TABLE IV. 2

Determination of %Sb in Standard Alloys

Alloy	Dissolution	Certificate Value	Determinations	Found	Rel. Std. Dev.
ISU-1	Procedure A	4.00%	3	3.98%	4 ppt
NBS-53	Procedure A	10.09%	3	10.10%	2 ppt
NBS-54D	Procedure B[a]	7.04%	4	7.04%	4 ppt
NBS-54D	Procedure B[b]	7.04%	2	3.56%	---
NBS-54D	Procedure B+HCl	7.04%	4	7.03%	4 ppt
ISU-2	Procedure B+HCl	4.00%	3	4.00%	3 ppt

[a]Solution analyzed immediately after preparation.

[b]Solution analyzed 4 days after preparation.

the addition of concentrated HCl for dissolution of Sn-based samples is recommended. It was reported in Reference 236 that Cu(II) interferes in the analysis of alloys for Sb. No such interference occurred for the analysis of NBS-54D which contained 3.62% Cu.

Large positive error existed in preliminary tests of the procedures for dissolution and analysis when no special precaution was made for removal of dissolved SO_2. For the Pb-based alloys containing no Sn, SO_2 was removed by gentle boiling. The same technique was not applicable to solutions containing Sn(IV). Boiling resulted in the solutions quickly becoming yellow due to hydrolysis of Sn(IV) and subsequent coulometric analysis gave low results for Sb(III). Dissolved SO_2 was removed from solutions containing Sn(IV) by dispersing N_2 through the solution during cooling.

2. Voltammetry.

Current-potential (I-E) curves for platinum electrodes in H_2SO_4 are shown and discussed in Reference 100. I-E curves obtained with the RPDE used in this study in 4.0 M H_2SO_4 were consistent with that discussion. The I-E curves obtained in the 4 M H_2SO_4 after addition of 0.1 mM Sb(III) were virtually unchanged from those for the supporting electrolyte. The irreversibility of the oxidation of Sb(III) prevents determination of Sb(III) by a direct amperometric method other than by electrodeposition of Sb.

The anodic portion of the I-E curve obtained with the RPDE at $\omega^{1/2} = 6.47$ $(rad/sec)^{1/2}$ for 0.63 mM Br^- in 4.0 M H_2SO_4 is shown in Figure IV. 1. Following pretreatment of the electrode, the potential of the RPDE, E_d, was set at 0.300 V and the current allowed to decay to approximately 2 μA. E_d was then scanned at

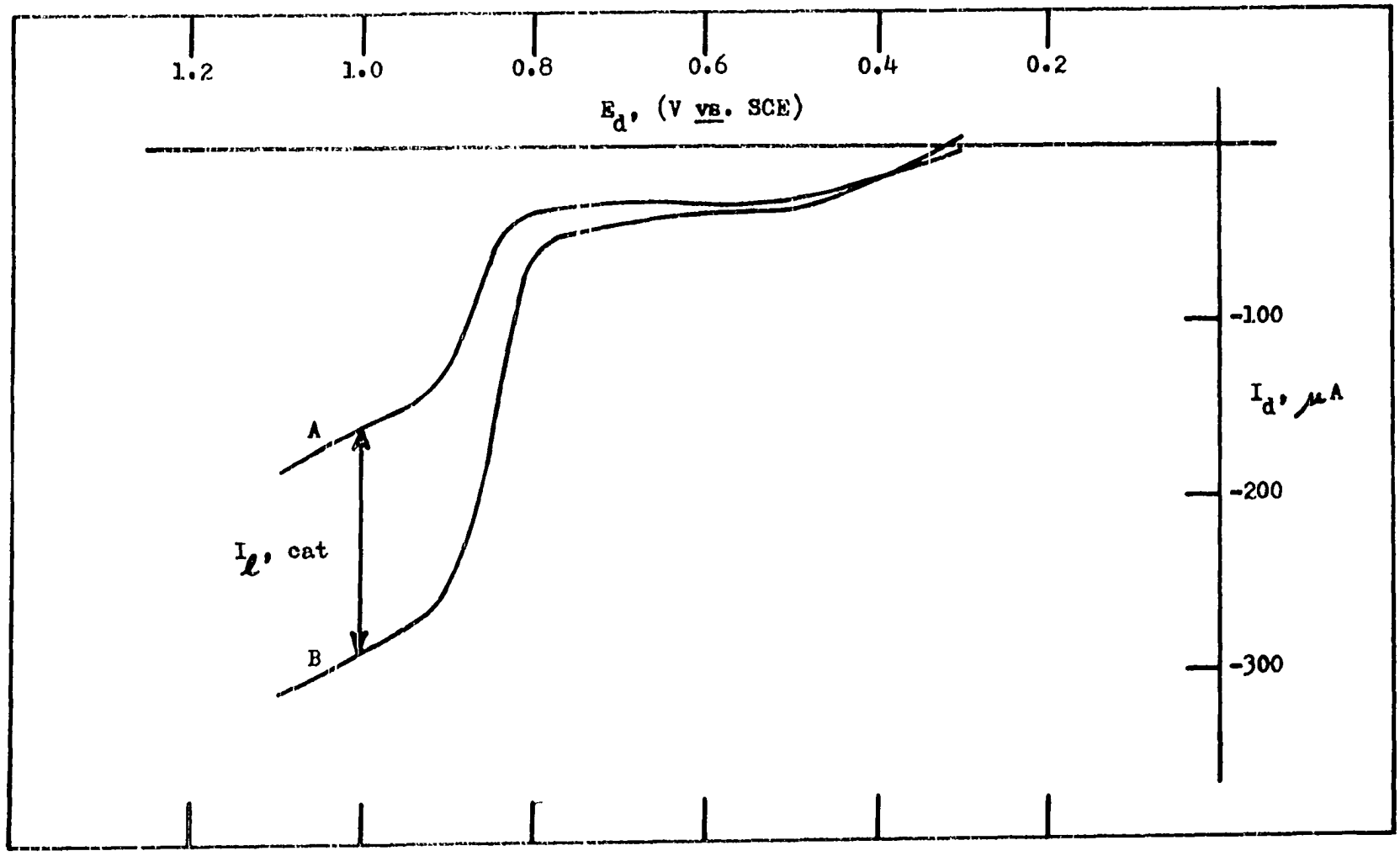

Figure IV. 1. I-E Curves for Br^- in 4.0 M H_2SO_4

Scan Rate 1.0 V/min. Temperature 24° C. Rotational Velocity 41.9 rad/sec. A - 0.63 mM Br^-. B - 0.63 mM Br^- and 0.524 mM Sb(III).

1.0 V/min and the I-E curve recorded. The oxidation of Br^- in acidic media is discussed in Reference 99. The $E_{1/2}$ for the oxidation is approximately 0.85 V and the anodic current is limited by the rate of convective-diffusional mass transport at $E_d > 0.9$ V. The process resulting in the small anodic wave at $E_d = 1.0$ V is the oxidation of the surface of the platinum electrode (99).

According to Equation IV. 5, the current for the electrochemical reaction of a species at a rate limited by convective-diffusional processes is proportional to $\omega^{1/2}$. The results of a study of the limiting current for the oxidation of Br^-, I_{ℓ,Br^-}, as a function of $\omega^{1/2}$ confirmed this dependency for 6.47 $(rad/sec)^{1/2} \leq \omega^{1/2} \leq$ 32.4 $(rad/sec)^{1/2}$ in 4.0 M H_2SO_4. These results are consistent with those reported in Reference 99. The value of D_{Br^-} was calculated using Equation IV. 5 from the slopes of the plots of I_{ℓ,Br^-} vs. $\omega^{1/2}$. The value determined is 0.76×10^{-5} cm^2/sec in 4.0 M H_2SO_4.

The I-E curve obtained following addition of 0.524 mM Sb(III) to the 0.63 mM Br^- in 4.0 M H_2SO_4 is also shown in Figure IV. 1. The mechanism resulting in the increase of the anodic current at $E_d = 1.1$ V is given by Equations IV. 1 and IV. 2 and was discussed in Section IV. A. This increase is defined as $I_{\ell,cat}$. $I_{\ell,cat}$, for the case when k in Equation IV. 2 is large, is found by subtracting Equation IV. 5 from Equation IV. 4 as shown by Equation IV. 6.

$$I_{\ell,\,cat} = I_{\ell,tot} - I_{\ell,Br^-}$$

$$= 0.62FA\nu^{-1/6}\omega^{1/2}n_{Sb(III)}D^{2/3}_{Sb(III)}C^{b}_{Sb(III)} \qquad \text{(IV. 6)}$$

I-E curves obtained in 4.0 M H_2SO_4 for 0.633 mM Br^- and for 0.633 mM Br^- plus 0.70 mM Sb(III) are shown in Figure IV. 2. Also shown in Figure IV. 2 are the anodic portions of three consecutive I-E curves obtained after the $C^{b}_{Sb(III)}$ was increased to 1.49 mM. The anodic wave began to shift to more positive potentials and on the third and subsequent scans produced I-E curves which were identical, but not convective-diffusional controlled. I-E curves for fresh solutions of Br^- obtained at the RPDE after recording the curves in Figure IV. 2 were identical to those curves obtained after the collapse of the Br^- wave is shown in Figure IV. 2. All efforts to reactivate the electrode by repeated anodization and cathodization were futile. The electrode was removed from the solution, polished according to the procedure described previously and an I-E curve obtained for the fresh solution of 0.633 mM Br^-. Apparently, Sb(III) was adsorbed at the surface of the electrode and resulted in deactivation of the electrode.

It was found to be necessary to restrict the values of E_d if the proper functioning of the electrode was to be maintained. For $E_d < 0.3$ V, some Sb was deposited at the electrode, and although the majority of the deposit was stripped for $E_d > 0.3$ V, the electrode was deactivated. Polishing of the electrode surface

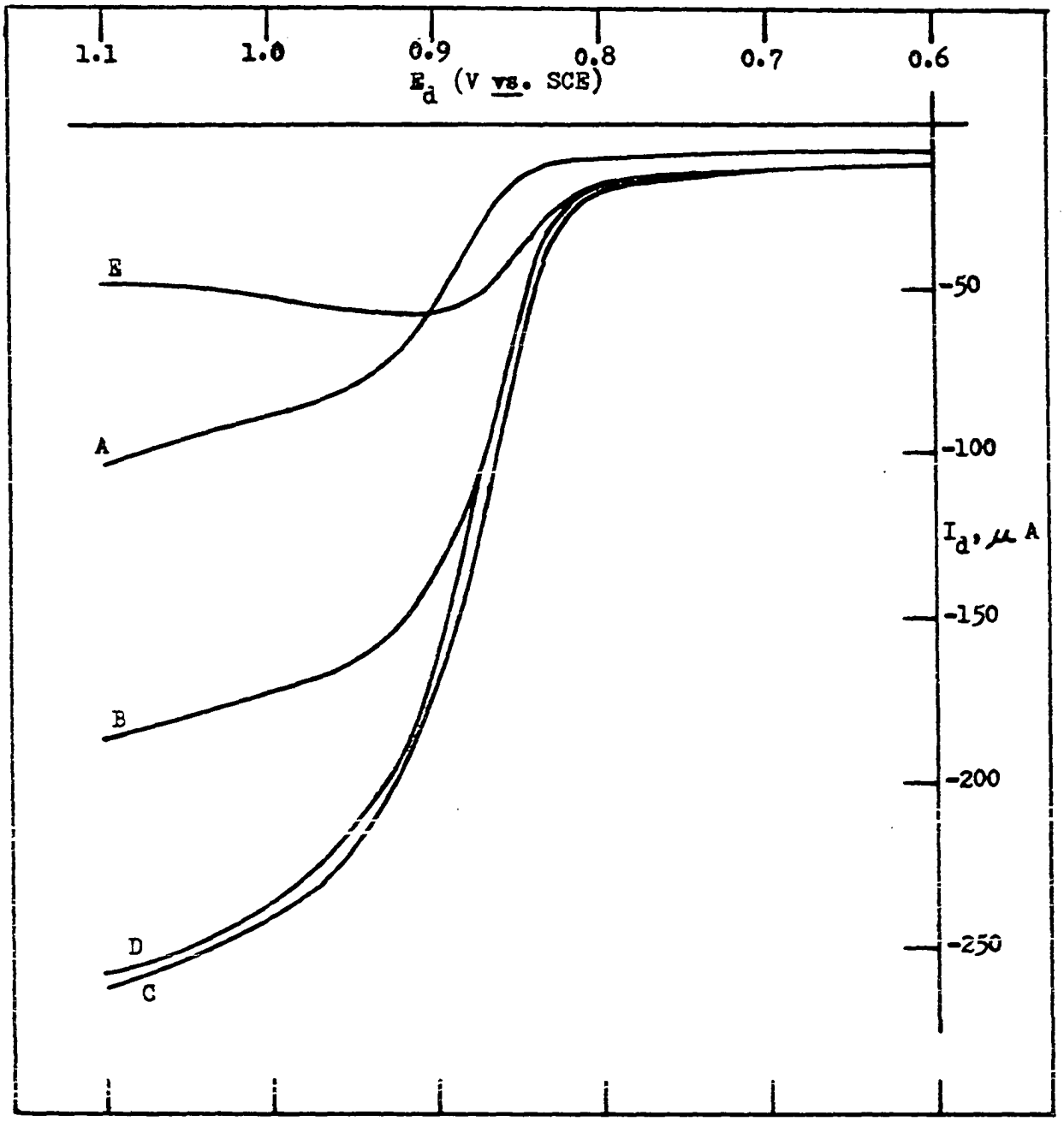

Figure IV. 2. I-E Curves for Br^- in 4.0 M H_2SO_4

Scan rate 1.0 V/min. Temperature 25° C. Rotational velocity 41.9 rad/sec. A - 0.63 mM Br^-. B - 0.63 mM Br^- and 0.70 mM Sb(III). C - 0.63 mM Br^- and 1.49 mM Sb(III), first scan. D - 0.63 mM Br^- and 1.49 mM Sb(III), second scan. E - 0.63 mM Br^- and 1.49 mM Sb(III), third scan.

was necessary to restore activity.

3. Catalytic Enhancement.

a. Effect of Br^- Concentration. Values of $I_{\ell,cat}$ obtained using the potential-step method as a function of $C^b_{Sb(III)}$, for three values of $C^b_{Br^-}$, are shown in Figure IV. 3 for 4.0 M H_2SO_4. Each plot is linear with a zero intercept for $C^b_{Sb(III)} < C^b_{Br^-}$. As $C^b_{Sb(III)}$ was made larger, deviation from linearity increased until $I_{\ell,tot}$ finally collapsed to the residual value. For larger values of $C^b_{Br^-}$ a larger value of $C^b_{Sb(III)}$ was necessary to deactivate the electrode. Johnson and Bruckenstein (99) found that Br^- is adsorbed strongly at a platinum electrode in 1.0 M H_2SO_4 and a complete coverage of the surface of the electrode is achieved for $C^b_{Br^-} > 3$ mM. Apparently the adsorption of Sb(V) is inhibited by increased surface coverage by adsorbed Br^-. Johnson and Bruckenstein showed that for $E_d > 1.1$ V, the desorption of Br^- as HOBr occurs. In 4.0 M H_2SO_4 the concentration of Sb(III) required to deactivate the electrode decreased for $E_d > 1.1$ V.

b. Effect of H_2SO_4 Concentration. Values of $I_{\ell,cat}$ were obtained using the potential-step method as a function of Sb(III) concentration in solutions of 4.0 M and 1.0 M H_2SO_4. The Br^- concentration was 0.63 mM for both H_2SO_4 concentrations. In 1.0 M H_2SO_4, the concentration of Sb(III) which caused deactivation of the electrode was 0.97 mM while in 4.0 M H_2SO_4, the concentration of Sb(III) which caused deactivation was 1.55 mM. For this reason and because stock solutions of Sb(III) in 4.0 M H_2SO_4 are stable

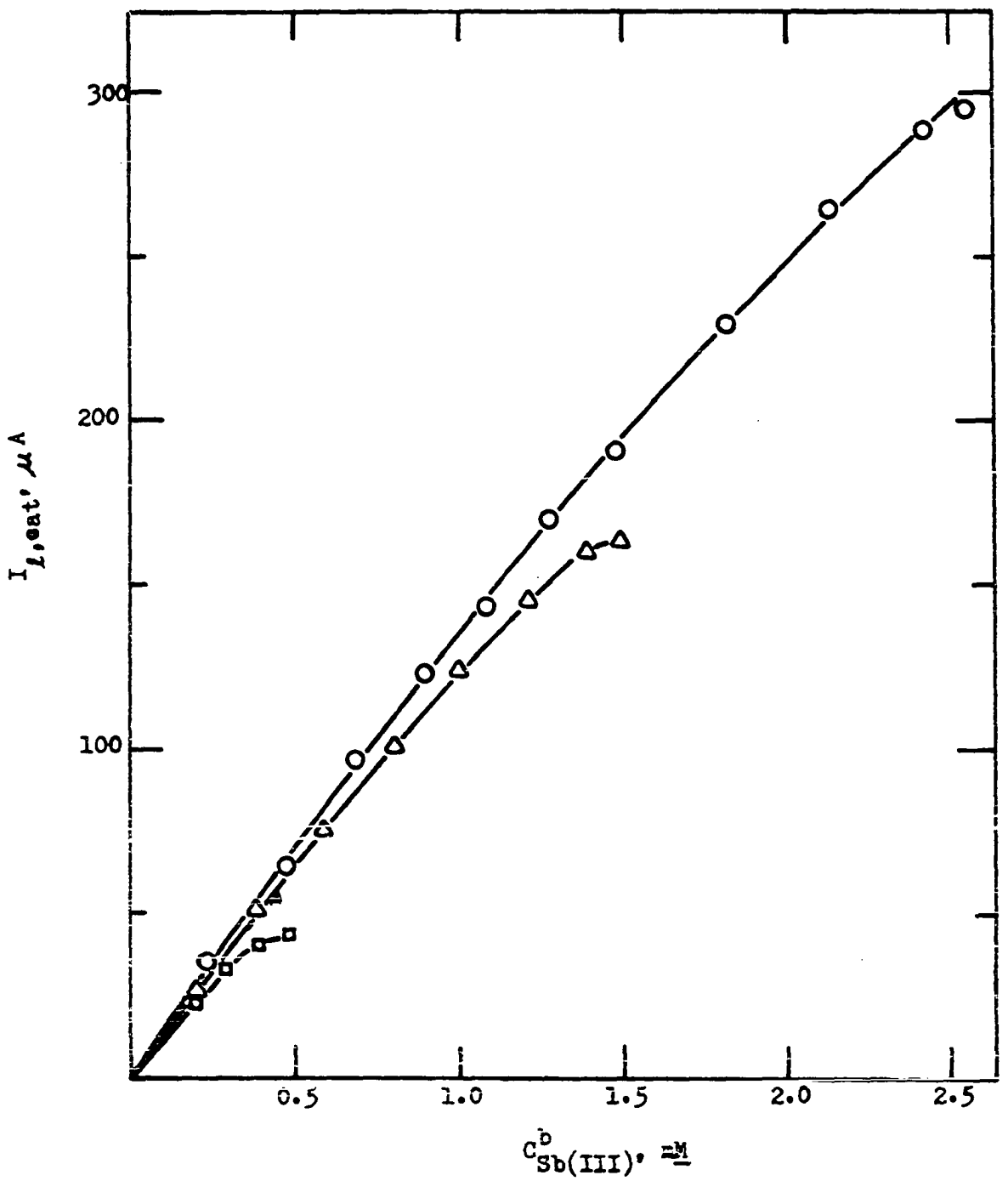

Figure IV. 3. $I_{l,cat}$ vs. $C^b_{Sb(III)}$
4.0 M K_2SO_4. Temperature 25.0° C. Rotational velocity 41.9 rad/sec. □ - 0.13 mM Br^-. △ - 0.63 mM Br^-. ○ - 1.22 mM Br^-.

for much longer periods of time, 4.0 M H_2SO_4 was chosen as the supporting electrolyte.

c. Temperature Dependence. The values of $I_{\ell,cat}$ were determined as a function of temperature using the potential-step method. The limiting current for a 1.22 mM NaBr solution in 4.0 M H_2SO_4 was measured at four values of temperature in the range 20° C $\leq$ T $\leq$ 35° C. The solution was then made 0.5 mM in Sb(III) and the total current measured at the same temperatures. For maximum precision, all measurements were made with thermostatic control to within $\pm 0.2^\circ$ C. In the temperature range investigated, a linear dependence of catalytic current, $I_{\ell,cat}$, versus temperature was observed. The magnitude of this dependence was found to be $+2.1\ \mu A/^\circ C$. in 4.0 M H_2SO_4.

d. Diffusion Coefficient of Sb(III). Plots of $I_{\ell,cat}$ as a function of $\omega^{1/2}$ were obtained using the potential-step method for 1.22 mM Br^- at two Sb(III) concentrations in 4.0 M H_2SO_4. The plots, shown in Figure IV. 4, are linear with zero intercepts only for the low values of $\omega^{1/2}$. The deviation from linearity at high values of $\omega^{1/2}$ was concluded to be the result of a slow rate of reaction between Br_2 and Sb(III) relative to the rate of convective-diffusional mass transport. For values of $C^b_{Sb(III)}$ higher than those used in Figure IV. 4, a deviation from linearity occurred at lower values of $\omega^{1/2}$.

The value of $D_{Sb(III)}$ was calculated using Equation IV. 5 and the slopes of the linear portions of the plots in Figure IV. 4.

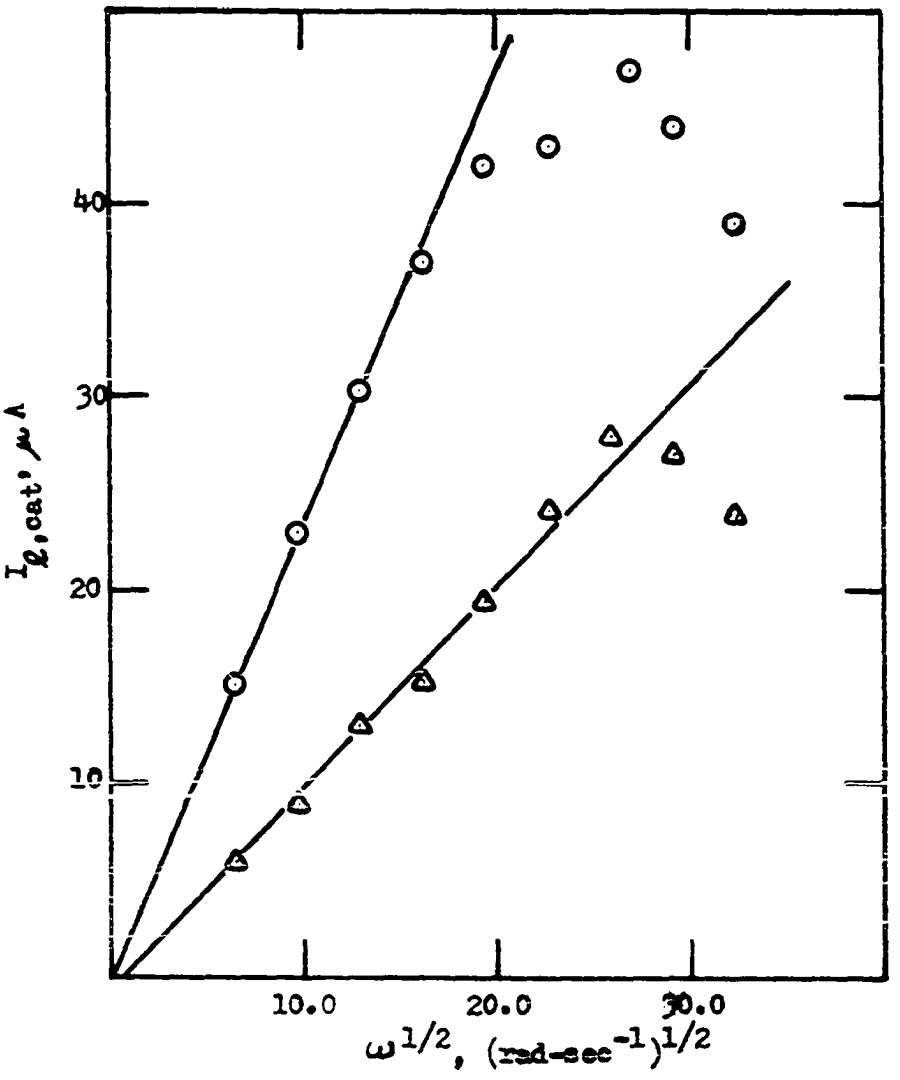

Figure IV. 4. $I_{l,cat}$ vs. $\omega^{1/2}$

4.0 M H_2SO_4. Temperature 25.0° C.

△ - 1.22 mM Br^- and 0.0964 mM Sb(III).

○ - 1.16 mM Br^- and 0.188 mM Sb(III).

In 4.0 M H_2SO_4 $D_{Sb(III)}$ was calculated to be $2.7 \pm 0.1 \times 10^{-6}$ cm^2/sec, which is in good agreement with the value of 2.7×10^{-6} cm^2/sec reported in Reference 42.

e. Precision Study. The potential-step method was used for obtaining values of $I_{\ell,cat}$ for solutions prepared by standard addition of stock solutions of Sb(III) to 1.22 mM Br^- in 4.0 M H_2SO_4. The values of $C^b_{Sb(III)}$ were determined using the calibration curve in Figure IV. 5 and the results are tabulated in Table IV. 3. The average relative error for the determinations is slightly larger than expected for electroanalytical methods and results from the fact that evaluation of $I_{\ell,cat}$ involves taking the difference of two relatively large numbers, $I_{\ell,tot} - I_{\ell,Br^-}$. The relative error decreased as $C^b_{Sb(III)}$ increased.

f. Interference Study. The interference of several cations was investigated using the potential-step method. The limiting current was measured for a 1.22 mM solution of NaBr in 4.0 M H_2SO_4 and the total current measured after addition of 0.43 mM Sb(III). Additions of stock solutions containing the interfering cations in 4.0 M H_2SO_4 were made and the total current measured after each addition. The stock solutions of Cu(II), Cd(II), Zn(II), Ni(II), and Fe(III) were 0.100 M and the Sn(IV) and Bi(III) stock solutions were 0.0100 M and 0.00500 M, respectively.

TABLE IV. 3

Analytical Applications of Calibration Curves

$\omega^{1/2} = 6.47(\text{rad/sec})^{1/2}$

$C^{b}_{Br^-} = 1.22$ mM

Temp = 25.0° C.

Tot. mg Sb added	Tot. mg Sb found	Relative Error (%)
3.01	2.87	-4.7
6.02	6.02	0.0
9.03	8.81	-2.4
12.04	11.98	-0.5
15.05	14.65	-2.7
3.01	3.14	4.3
6.02	6.07	0.8
9.03	9.00	-1.2
15.05	14.87	-1.2
	Average Relative Error	-1.8

In all instances the interferences resulted in a negative error. The concentrations of the interfering species producing a 50% change in the $I_{\ell,cat}$ are given in Table IV. 4.

TABLE IV. 4

Concentration of Interfering Species Producing a 5% Decrease in $I_{\ell,cat}$

$C^{b}_{Br^-} = 1.22$ mM

$C^{b}_{Sb(III)} = 0.43$ mM

$\omega^{1/2} = 6.47(rad/sec)^{1/2}$

Temp = 24.0° C.

Cation	Concentration (mM)
Bi(III)	0.20
Sn(IV)	0.33
Cd(II)	1.0
Fe(III)	1.2
Zn(II)	5.7
Cu(II)	6.0
Ni(II)	6.8

None of the species listed in Table IV. 4 is oxidized by Br_2. The interference was greatest for those cations forming the strongest complexes with Br^-. Because of the severe interference by Sn(IV), Sn-based alloys could not be analyzed by the catalytic method without prior separation. HCl was added to solutions of Pb-based alloys, and because Cl^- is oxidized at values of E_d in the region of the limiting wave for Br^-, these could not be analyzed. Several masking agents were used including phosphate

and oxalate. None successfully prevented interference by cations, probably because of the high acidity of the solution.

V. ELECTROCATALYSIS BY ADSORBED IODIDE

A. Introduction

The investigation of any electrode reaction must begin with a study of the electrical double layer (45). A double layer is formed at the electrode-electrolyte interface because of electrostatic and specific interactions of the charged electrode with the solvent and ions in the electrolyte (196, 209). The double layer affects the rate of electrode reactions because specific and non-specific adsorption of ions and solvent change the "outer" Helmholtz potential, ϕ (196). The potential which drives the electrode reaction is the effective potential, $E - \phi$, and not the applied potential, E (45).

The effective potential, $E - \phi$, is strongly affected by adsorption of ions and neutral molecules. The effect of the adsorption of organic molecules on $E - \phi$ has been reviewed in detail by Damaskin, Petrii, and Batrakov (38). This type of adsorption usually inhibits electrode reactions and will not be discussed further.

The adsorption of ions at electrodes cannot be treated mathematically in the same manner as the adsorption of organic molecules because of the strong interactions between the ions in the double layer (158). The mathematical treatment of ionic adsorption was developed primarily by Parsons (158, 159) and Hurwitz (90). There are many reports in the literature of the determination of adsorption isotherms for ions at a variety of

electrode materials. Only the adsorption of halides, and especially that of iodide, at platinum electrodes is of interest for this thesis. Experimental methods of measuring adsorption parameters are reviewed in detail by Gileadi and Conway (70).

The adsorption of I^- on platinum electrodes has been thoroughly investigated using several different techniques by Johnson (98); Hubbard, Osteryoung, and Anson (89); Osteryoung and Anson (153); and Trukhan, Povanov, and Lukovtsev (210). Frumkin, Petrii, and Kotlov (62); Cooper and Parsons (36); Veber, Pirtskhalova, Vasil'eva, and Bagotskii (218); and Johnson and Bruckenstein (99) studied the Br_2/Br^- adsorption at platinum electrodes. Studies of the adsorption of other halides at platinum electrodes were also reported in the literature (10, 44, 116, 178, 185).

Heyrovsky, according to deLevie, was the first to discover that adsorbed halides can promote electrode reactions of metal ions (45). He observed that the reductions of Sn(II), Bi(III), In(III), and Sb(III) at a mercury drop were electrocatalyzed by the presence of halides in the solution of electrolyte and postulated that the electron transfer occurred by a bridging mechanism (45). In his review on anion electrocatalysis and anion bridging, deLevie illustrates the general nature of the phenomenon at mercury surfaces by reviewing the cases which have been reported in the literature (45). Anson has observed that the oxidation of Co-EDTA complexes at a platinum electrode is electrocatalyzed by the presence of halides (6), but the interpretation of the results

obtained at solid electrodes is much more difficult than at mercury surfaces because of insufficient double-layer data for solid electrodes (45), and because of the difficulty in obtaining a reproducible platinum surface.

The effect of ion adsorption on electrode processes is studied by observing the effect of ion adsorption on electrode kinetic parameters such as the Tafel slope, exchange current density, and the transfer coefficient, α (194). Many methods for determining the electrochemical kinetic parameters of electrode reactions have been reported in the literature. The use of current-voltage curves to determine kinetic parameters, which is the most widely reported technique, have been described by Vetter (219, 220); Vetter and Manecke (222, 223); Vetter and Thiemke (224); Gerischer (66); Petrocelli and Paolucci (161); and Lov'ev, Molodov, and Gorodetski (132). Faradaic impedance techniques have been reported by Randles and Somerton (168); Llopis and Vazquez (131); Vetter (221); and Baticle and Perdu (11). The rotating disk electrode has been used by Jahn and Vielstich (94); Frumkin and Tedoradse (63); and Newson and Riddiford (152) to determine heterogeneous kinetic parameters. Other methods such as the galvanostatic (5, 140), potential-step (31), faradaic rectification (2), thin-layer voltammetric (88), potential sweep (195), and hydrodynamic voltammetric methods (102, 103) have also proved to be useful for the determination of kinetic parameters.

The techniques which involve the determination of kinetic parameters from current-voltage curves use the portion of the I-E curve between the limiting current and the equilibrium potential. The determination of kinetic parameters from this portion of the I-E curve requires long extrapolations leading to large uncertainties in the values of the kinetic parameters (66, 132, 161, 219, 220, 222-224).

Methods involving the RDE electrode use plots of 1/i versus $1/\omega^{1/2}$ at constant values overpotential, η, to determine kinetic parameters. No long extrapolations are used in this method, but at high exchange current densities, greater than 10 ma/cm^2, the uncertainty in the determination of kinetic parameters is large (63, 94, 152).

A method for determining kinetic parameters, such as the heterogeneous rate constant, k_o, the exchange current density, i_o, and the transfer coefficient, α, is described in this thesis. The method described involves measurement of the slope of the I-E curve at the equilibrium potential as a function of the rotational velocity of the electrode. The measurements are made for different concentrations of either the oxidized or reduced species, while the concentration of the species not varied is held constant.

If one assumes that the rate of the electrochemical reaction is not infinitely fast, and that there is no concentration polarization, the current at any point on the I-E curve is given by Equation V. 2 (196) for the oxidation-reduction reaction in

Equation V. 1.

$$O \pm ne = R \tag{V. 1}$$

$$i = nFAK_o \left[\exp\left\{ \frac{-\alpha nF}{RT} (E - E^o) \right\} C_o^o - \exp\left\{ \frac{(1-\alpha)nF}{RT} (E - E^o) \right\} C_R^o \right] \tag{V. 2}$$

Equation V. 2 is modified to include concentration polarization by substitution of Equation V. 3 to give Equation V. 4 (196).

$$E - E^o = \eta + \frac{RT}{nF} \ln \frac{C_o^b}{C_R^b} \tag{V. 3}$$

In the previous equations,

i = Faradaic current at any point on the I-E curve

E = Voltage applied to working electrode

E^o = Equilibrium potential of O/R couple

C_i^o = Concentration of i^{th} species at the electrode surface

η = Overpotential

σ = Diffusion layer thickness

$$i = nFAk_o \left[C_o^o \exp\left\{ \frac{-\alpha nF}{RT} \left(\eta + \frac{RT}{nF} \ln \frac{C_o^b}{C_R^b} \right) \right\} - C_R^o \exp\left\{ \frac{(1-\alpha)nF}{RT} \left(\eta + \frac{RT}{nF} \ln \frac{C_o^b}{C_R^b} \right) \right\} \right] \tag{V. 4}$$

Rearrangement of Equation V. 4 and substitution of Equation V. 5 (205) into Equation V. 4 gives Equation V. 6. Equation V. 5 is the fundamental equation of heterogeneous kinetics relating all kinetic parameters.

$$i_o = nFAk_o C_o^{b(1-\alpha)} C_R^{b\alpha} \tag{V. 5}$$

$$i = i_o \left[\frac{C_o^o}{C_o^b} \exp\left\{ \frac{-\alpha nF}{RT} \eta \right\} - \frac{C_R^o}{C_R^b} \exp \left\{ \frac{(1-\alpha)nF}{RT} \eta \right\} \right] \qquad (V.\ 6)$$

Equations V. 7 and V. 8 account for concentration polarization when $i \neq 0$ (128).

$$\frac{C_o^o}{C_o^b} = 1 - \frac{\sigma i}{nFADC_R^b} \qquad (V.\ 7)$$

$$\frac{C_R^o}{C_R^b} = 1 + \frac{\sigma i}{nFADC_R^b} \qquad (V.\ 8)$$

Equation V. 6 then becomes Equation V. 9.

$$i = i_o \left[\left(1 - \frac{\sigma i}{nFADC_o^b} \right) \exp\left\{ \frac{-\alpha nF}{RT} \eta \right\} - \left(1 + \frac{\sigma i}{nFADC_R^b} \right) \exp \left\{ \frac{(1-\alpha)nF}{RT} \eta \right\} \right] \qquad (V.\ 9)$$

Solving Equation V. 9 for i gives Equation V. 10.

$$i = \frac{i_o \left(\exp\left\{ \frac{-\alpha nF}{RT} \eta \right\} - \exp\left\{ \frac{(1-\alpha)nF}{RT} \eta \right\} \right)}{1 + i_o \frac{\sigma}{nFAD} \left(\frac{1}{C_o^b} \exp\left\{ \frac{-\alpha nF}{RT} \eta \right\} + \frac{1}{C_R^b} \exp\left\{ \frac{(1-\alpha)nF}{RT} \eta \right\} \right)} \qquad (V.\ 10)$$

At $\eta = 0$, $\frac{\alpha nF}{RT} < 1$ and $\frac{(1-\alpha)nF}{RT} < 1$, so the approximation that $e^x \approx 1 + x$ is valid. Equation V. 10 reduces to Equation V. 11.

$$i = \frac{-i_o \frac{nF}{RT} \eta}{1 + \frac{i_o \sigma}{nFAD} \left(\frac{1}{C_o^b} + \frac{1}{C_R^b} \right)} \qquad (V.\ 11)$$

Since $\sigma = 1.61 D^{1/3} \omega^{-1/2} \nu^{1/6}$ (125), Equation V. 11 becomes

$$i = \frac{-i_o \frac{nF}{RT}\eta}{1 + \frac{i_o}{0.62nFAD^{2/3}\nu^{-1/6}} \left(\frac{1}{C_o^b} + \frac{1}{C_R^b}\right)\omega^{-1/2}} \qquad \text{(V. 12)}$$

Taking the derivative of Equation V. 12 with respect to η and rearranging gives Equation V. 13.

$$-\left(\frac{\partial i}{\partial \eta}\right)^{-1}_{\eta=0} = \frac{RT}{nF}\left(i_o\right)^{-1} + \frac{RT(C_o^b + C_R^b)}{0.62\, n^2F^2AD^{2/3}\nu^{-1/6}C_o^bC_R^b}\,\omega^{-1/2} \qquad \text{(V. 13)}$$

A plot of $-(\partial i/\partial \eta)^{-1}_{\eta=0}$ versus $\omega^{-1/2}$ allows calculation of i_o from the intercept according to Equation V. 13. To calculate α, a plot of ln i_o versus ln C_R^b is made, and from Equation V. 5, the slope is equal to $(1-\alpha)$ when C_o^b is held constant. From the intercept, ln $(nFAk_o)$, the heterogeneous rate constant, k_o, can be calculated.

The above method was applied to the determination of the kinetic parameters for the Sb(V)/Sb(III) couple in 12 M HCl as a function of the amount of adsorbed I^- at the platinum electrode.

B. Experimental

1. Chemicals and Reagents.

A stock solution of Fe(III) was prepared from 100.00% electrolytic iron from G. Frederick Smith Chemical Co. All other solutions were prepared from J. T. Baker, Inc. reagent grade chemicals. All water used was triply distilled with a

deionization between the first and second distillation and the second distillation being from alkaline permanganate.

2. Preparation of Solutions.

a. $Fe(ClO_4)_3$, Cl^- free. Sufficient electrolytic iron to prepare one liter of 0.08 M $Fe(ClO_4)_3$ was dissolved in 85 ml of 70-72% $HClO_4$ by bringing the $HClO_4$ to a boil for five minutes. The solution was cooled slowly to room temperature while N_2 was bubbled through the solution to remove Cl_2 and prevent air from entering the solution as it cooled. If water vapor from the air were to enter the solution, the Cl_2 in the hot $HClO_4$ would disproportionate into Cl^- and ClO^- (241).

b. Sb_2O_3. A 5.00 X 10^{-3} M stock solution of Sb(III) was prepared by dissolving sufficient Sb_2O_3 powder in concentrated HCl and diluted to one liter with HCl and H_2O. The final HCl concentration was 4.0 M. A 1.0 X 10^{-2} M stock solution was prepared by dissolving sufficient Sb_2O_3 in 12 M HCl and diluting it to 100.0 ml with 12 M HCl.

c. $SbCl_5$. A 0.0414 M Sb(V) stock solution was prepared by diluting reagent grade $SbCl_5$ with concentrated HCl. The concentration of the solution was calculated using Equation IV. 5 and the measured value of I_l assuming the diffusion coefficient of Sb(V) in 12 M HCl equals the diffusion coefficient of Sb(III). This method is acceptable because the same assumption is made in calculating the kinetic parameters.

d. EDTA. Reagent grade disodium ethylenediamine tetra-

acetic acid di-hydrate was recrystallized from 50 ml volume percent ethanol-water according to the procedure described by Blaedel and Knight (18).

3. Standardization of Solutions.

a. Sb(III). The coulometric standardization of Sb(III) was performed by the procedure described in Section IV. B. 3.

b. Fe(III). The coulometric determination of Fe(III) at constant current was made using a Sargent Model IV constant current coulometer with electrogenerated UO_2^+ (128). The generator compartment of the cell (see Section IV. B. 3) was filled with a solution of 0.050 M $UO_2(CH_3COO)_2 \cdot 2H_2O$, adjusted to a pH=1.9 with $HClO_4$, and 2 drops of 5 M NaBr were added to sharpen the end point. The remaining two chambers of the cell were filled with 1 M $HClO_4$. Two platinum wires, polarized with a 10 μA current, were placed in the generator electrode chamber as indicator electrodes. The potential difference between the two electrodes, ΔE, was recorded versus time using an Electronics Associated Incorporated, Model 1131, Variplotter. As long as there was a reversible couple present, ΔE was approximately zero. At the end point, ΔE was equal to the difference between the formal potentials of the UO_2^{2+}/UO_2^+ and Fe^{3+}/Fe^{2+} couples. A spike was observed on the ΔE-t curve at the end point.

4. Experimental Procedures.

a. Voltammetry. A description of the RPDE, variable speed rotator, and cell used in this research is given in Section IV.

B. 4. The electronic circuitry is described in Section III. A. 2. The RPDE was pretreated by potentiostating the electrode in 1.0 M $HClO_4$ for two minutes at 2.5 V and -2.5 V. The potential range between 1.4 V and -0.2 V was scanned for 5 minutes before changing the supporting electrolyte to the one used to obtain the voltammetric data.

When 4.0 M and 12 M HCl were used as the supporting electrolytes, the electrode was pretreated by potentiostating for 3 minutes at 1.2 V, -0.6 V, and 0.0 V. The potential range was then scanned in a cyclic manner between the chosen limits until reproducible curves were obtained.

b. Kinetic Data, Sb(V)/Sb(III). All kinetic data was obtained at a constant concentration of Sb(III). The concentration of Sb(V) was varied by adding known volumes of a stock solution of Sb(V). The I-E curves for each mixture of Sb(V) and Sb(III) were recorded at seven rotation speeds using an expanded scale to increase the accuracy of the measurement of the slope at i=0.

C. Results and Discussion

1. Fe(III)/Fe(II) System.

Before obtaining the heterogeneous kinetic data for the Sb(V)/Sb(III) couple, the effect of traces of I^- and Br^- on the reduction of Fe(III) was investigated at an RPDE. Resnick (172) reported that the presence of traces of Cl^- in a solution containing Fe(III) and 1 M $HClO_4$ shifted the observed $E_{1/2}$ for

the cathodic wave to more positive values. I-E curves for 0.5 mM Fe(III) were obtained as a function of the rotational velocity of the RPDE in a solution of 0.10 M EDTA which contained 1.5 mM NaCl, curve A, 0.40 M NaCl, curve B, and 0.40 M NaCl-1 mM NaI, curve C. All solutions were adjusted to pH 5.1 with NaOH. Plots of I_ℓ vs. $\omega^{1/2}$ for each solution are shown in Figure V. 1. The plot for the solution containing 1.5 mM NaCl (curve A) shows a marked deviation from the linear relationship predicted by Equation IV. 5. When the NaCl concentration was increased to 0.40 M, the deviation from Equation IV. 5 became smaller. The addition of 1 mM NaI to the solution which already contained 0.40 M NaCl resulted in a linear relationship for $6.47(\text{rad/sec})^{1/2} \leq \omega^{1/2} \leq 32.4(\text{rad/sec})^{1/2}$.

The decreased curvature observed in Figure V. 1 was attributed to the increased adsorption of halides at the RPDE when the Cl^- concentration was increased, and to the adsorption of I^- instead of Cl^-. This effect is called electrocatalysis. In the pH range of 3.5 to 6.0, the concentration of EDTA and hydrogen ions has no effect on the half-wave potential of the Fe(III)/Fe(II) couple (118). In this pH range the only species which exist are FeY^- and FeY^{2-}, where Y^{4-} refers to the unassociated EDTA molecule. The formation constants of the Fe(III) and Fe(II) chloride complexes are much less than the Fe(III) and Fe(II) EDTA complexes. Therefore, chloride cannot effectively compete with the EDTA ligand (34).

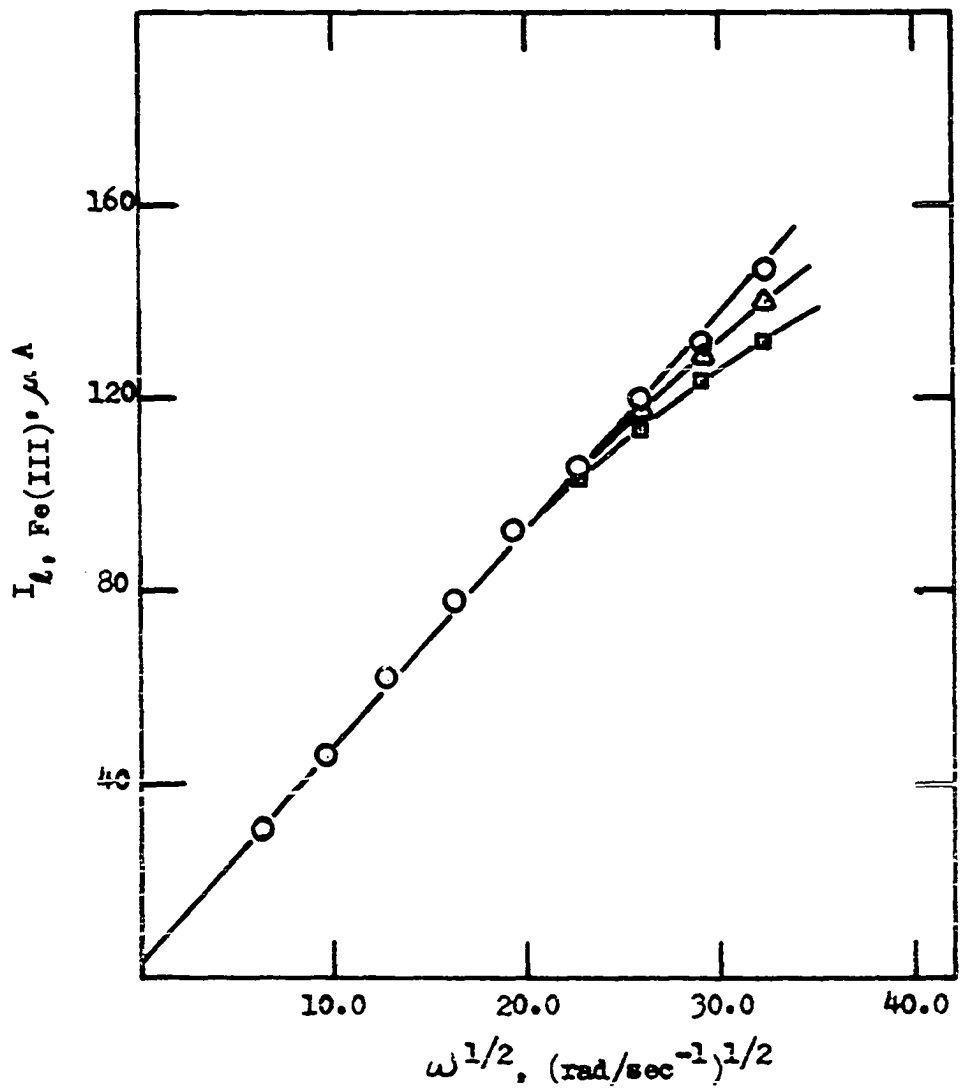

Figure V. 1. $I_{\ell,Fe(III)}$ vs. $\omega^{1/2}$

0.10 M EDTA. -0.400 V.
□ - 0.50 mM Fe(III) and 1.5 mM NaCl
△ - 0.50 mM Fe(III) and 0.40 M NaCl
○ - 0.50 mM Fe(III), 0.40 M NaCl and 1.0 mM NaI

I-E curves were obtained for various ratios of [Fe(III)]: [Fe(II)] in 0.10 M EDTA, 0.10 M NaBr, and 0.05 M $NaClO_4$ at pH 5.1. The I-E curves are shown in Figure V. 2. Fe(II) was electrogenerated by electroreduction of Fe(III) at a constant potential of -0.40 V vs. SCE using a platinum gauze electrode. In this way, the analytical concentration of iron remained constant. The ratio of Fe(III) : Fe(II) was varied between 1.0 and 0.0. Bromide was chosen to electrocatalyze the oxidation-reduction reaction because the strength of the bromide adsorption at platinum is intermediate between that of chloride and iodide (10).

The dependence of the Fe(III) reduction and the Fe(II) oxidation on the rotational velocity of the RPDE is shown in Figure V. 3. The plot of I_ℓ vs. $\omega^{1/2}$ was made for equal concentrations of Fe(III) and Fe(II). Values of I_ℓ for the oxidation and reduction of iron were chosen 0.300 V anodic and cathodic of the half-wave potential. At the same overpotential the reduction of Fe(III) was linear for $6.47(\text{rad/sec})^{1/2} \leq \omega^{1/2} \leq 12.9(\text{rad/sec})^{1/2}$, but the oxidation of Fe(II) was only linear for $6.47(\text{rad/sec})^{1/2} \leq \omega^{1/2} \leq 19.4(\text{rad/sec})^{1/2}$.

2. Sb(V)/Sb(III) System.

a. Voltammetry, 4.0 M HCl. I-E curves for 0.125 mM Sb(III) and 0.125 mM Sb(V) in 4.0 M HCl containing 2.0 M NaI are shown in Figure V. 4. During a period of approximately one hour, $I_{\ell,Sb(V)}$, measured at 0.52 V, decreased from 150 to 115 μA, a

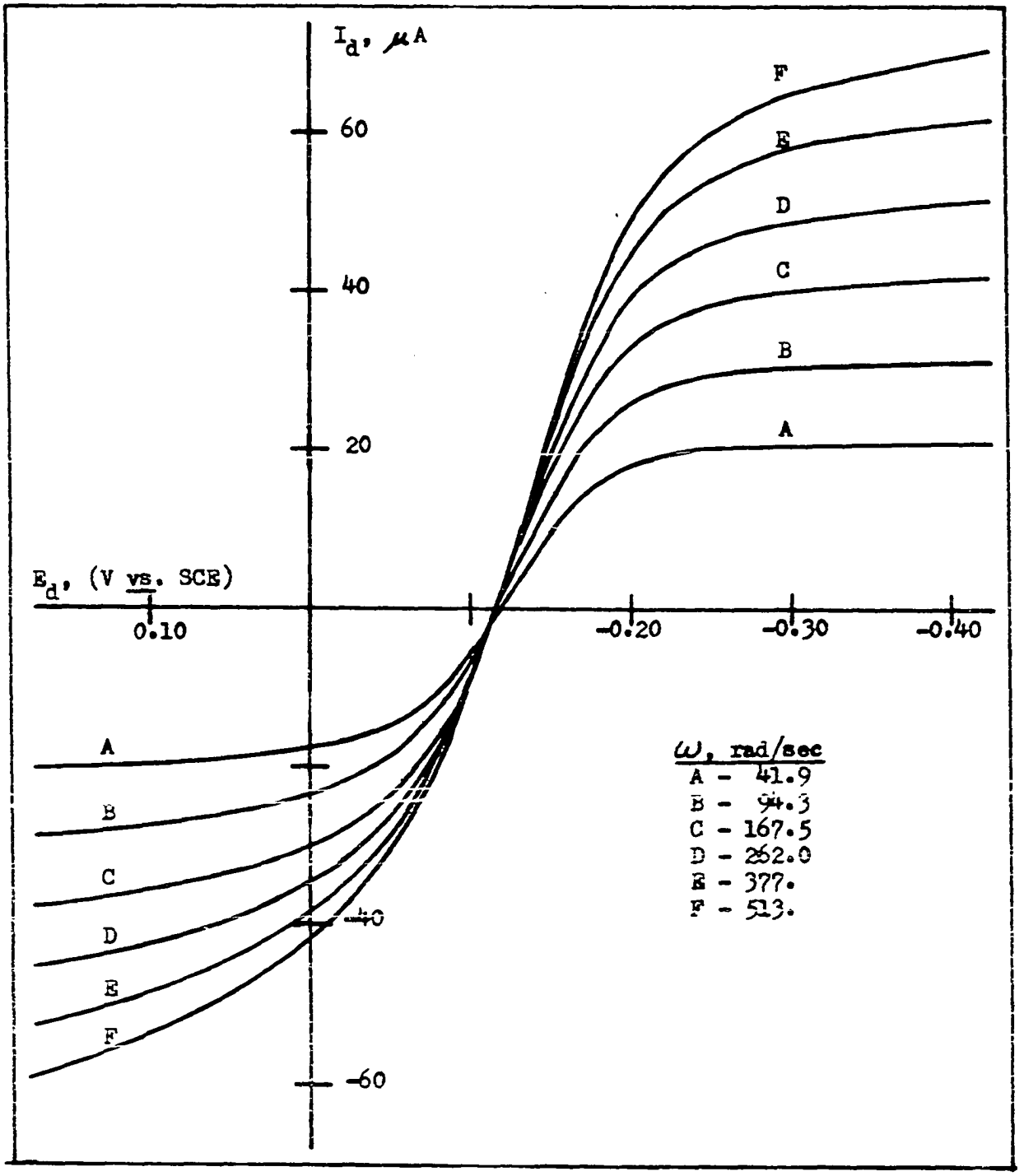

Figure V. 2. I-E Curves for Fe(III)/Fe(II) in 0.10 M EDTA. 0.05 M $NaClO_4$, and 0.10 M NaBr
0.25 mM Fe(III). 0.25 mM Fe(II). 0.5 V/min.

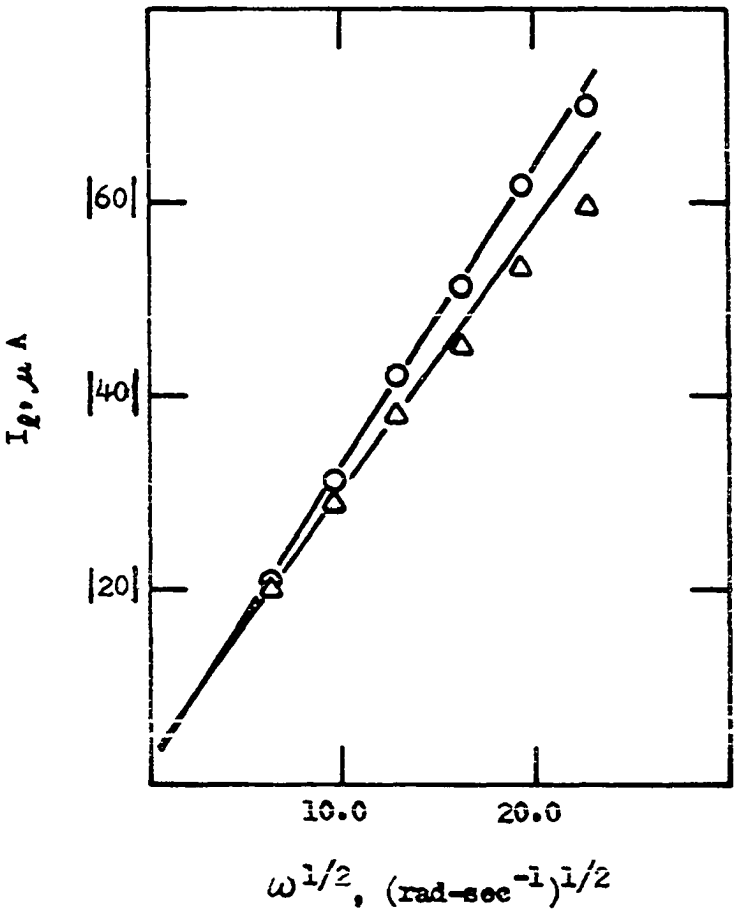

Figure V. 3. I_ℓ vs. $\omega^{1/2}$

0.10 M EDTA, 0.05 M $NaClO_4$, and 0.10 M NaBr.
O - 0.25 mM Fe(III). Δ - 0.25 mM Fe(II).

23% decrease. In the same time period, $I_{\ell,Sb(III)}$, measured at 0.80 V, decreased from 172 to 167 μA, a 2.9% decrease. The large decrease in $I_{\ell,Sb(V)}$ could be caused by inhibition of the electrode reaction from the irreversible adsorption of a species in the solution or from a change in the nature of the electroactive species in solution. Neumann (151) found that Sb(V) is slowly hydrolyzed in dilute HCl solutions and that the products are not electroactive at platinum electrodes.

The absorption spectra obtained in a solution of 4.0 M HCl containing equal concentrations of Sb(V) and Sb(III) and 2 μ M I^- are shown in Figure V. 5. I-E curves were recorded less than five minutes before the absorption spectra were obtained and the electrode potential was scanned between the limits 0.5 and 0.8 V during the entire experiment. The absorption at 260 nm, which corresponded to the absorption maximum for Sb(V), decreased with time. On the basis of the results shown in Figure V. 4 and V. 5, it was concluded that the decrease in $I_{\ell,Sb(V)}$ is related to the hydrolysis of $SbCl_6^-$. Also shown in Figure V. 5 are the absorption spectra for 5.0×10^{-6} M Sb(III) and 2×10^{-5} M Sb(V) alone.

b. Voltammetry. 12 M HCl. A study of the heterogeneous kinetics of the Sb(V)/Sb(III) couple in 4.0 M HCl was not performed because of the presence, in that media, of electroinactive forms of Sb(V). In 12 M HCl, Sb(V) and Sb(III) exist only as $SbCl_6^-$ and $SbCl_4^-$, respectively. Values of I_ℓ for the anodic and cathodic reactions in 12 M HCl were determined not to

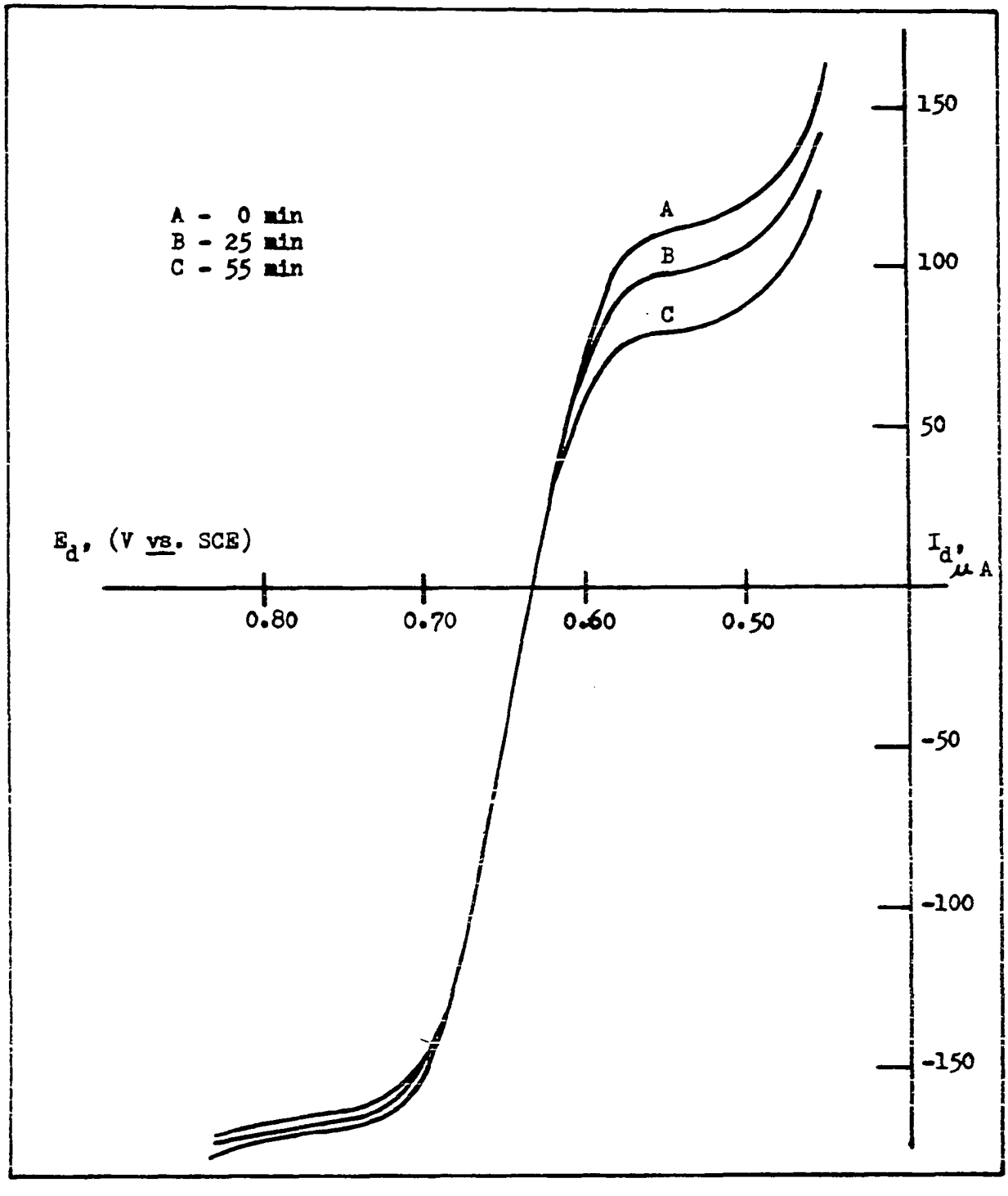

Figure V. 4. Time Dependence of I-E Curves for Sb(V)/Sb(III) in 4.0 M HCl
Sb(V) = Sb(III) = 0.125 mM. Rotational Velocity 168 rad/sec. Scan Rate 0.5 V/min.

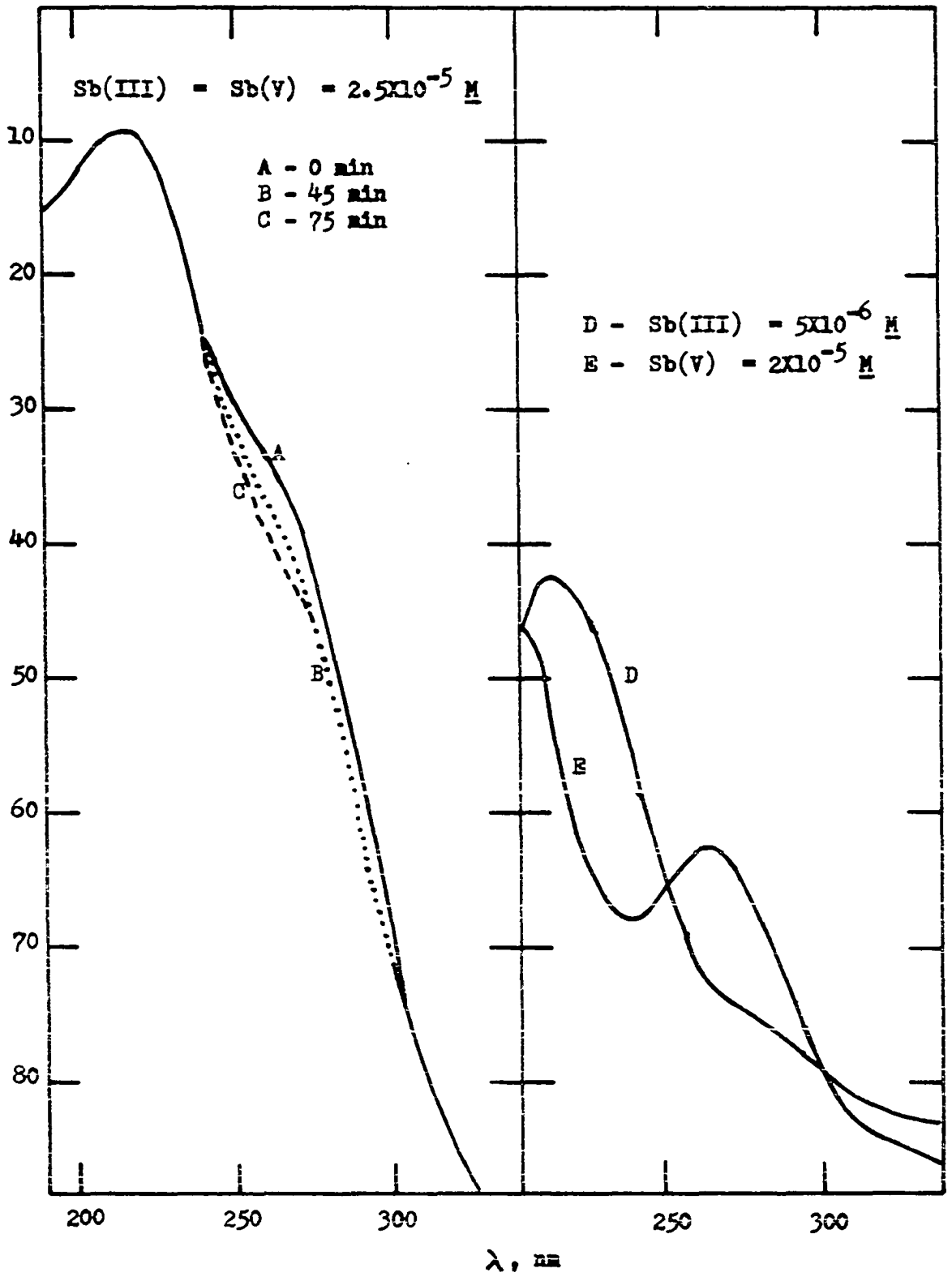

Figure V. 5. UV Spectra of Sb(III) and Sb(V) in 4.0 M HCl

decrease with time.

The I-E behavior of Sb(V)/Sb(III) mixtures was investigated as a function of the concentration of NaI added. After each addition of NaI, the potential was scanned between the limits 0.25 V and 0.80 V until no change in the I-E curve was observed. The concentration of NaI was varied from 0.0 μM to 2.0 μM and the I-E curve recorded on the anodic scan of potential. No change in the observed I-E curve was found for $[I^-] > 2.0\,\mu M$.

The rate of the heterogeneous reaction of the Sb(V)/Sb(III) couple can be varied simply by changing the iodide concentration as shown by the data in Figure V. 6. The reciprocal of the slope of the I-E curve at $\eta = 0$, $-(\partial i/\partial \eta)^{-1}_{\eta=0}$, is related to the reciprocal of the exchange current, i_o^{-1}, through Equation V. 13. If the amount of iodide adsorbed on the electrode surface is controlling the rate of the electrochemical reaction, a plot of $-(\partial i/\partial \eta)^{-1}_{\eta=0}$ vs. $[I^-]$ should be the mirror image of the adsorption isotherm for iodide. A plot of $-(\partial i/\partial \eta)^{-1}_{\eta=0}$ vs. $[I^-]$ is shown in Figure V. 7.

The isotherm for adsorption of I^- at platinum was determined experimentally. Solutions containing between 0.0 and 2.0 μM I^- in 12 M HCl were passed through the packed tubular electrode described in Section III. B. The electrode was potentiostated at 0.65 V. 1.0 M H_2SO_4 was then passed through to wash out the 12 M HCl containing I^- and the potential stepped to 1.3 V. At 1.3 V adsorbed I^- is oxidized to IO_3^- (97), and the amount of IO_3^-

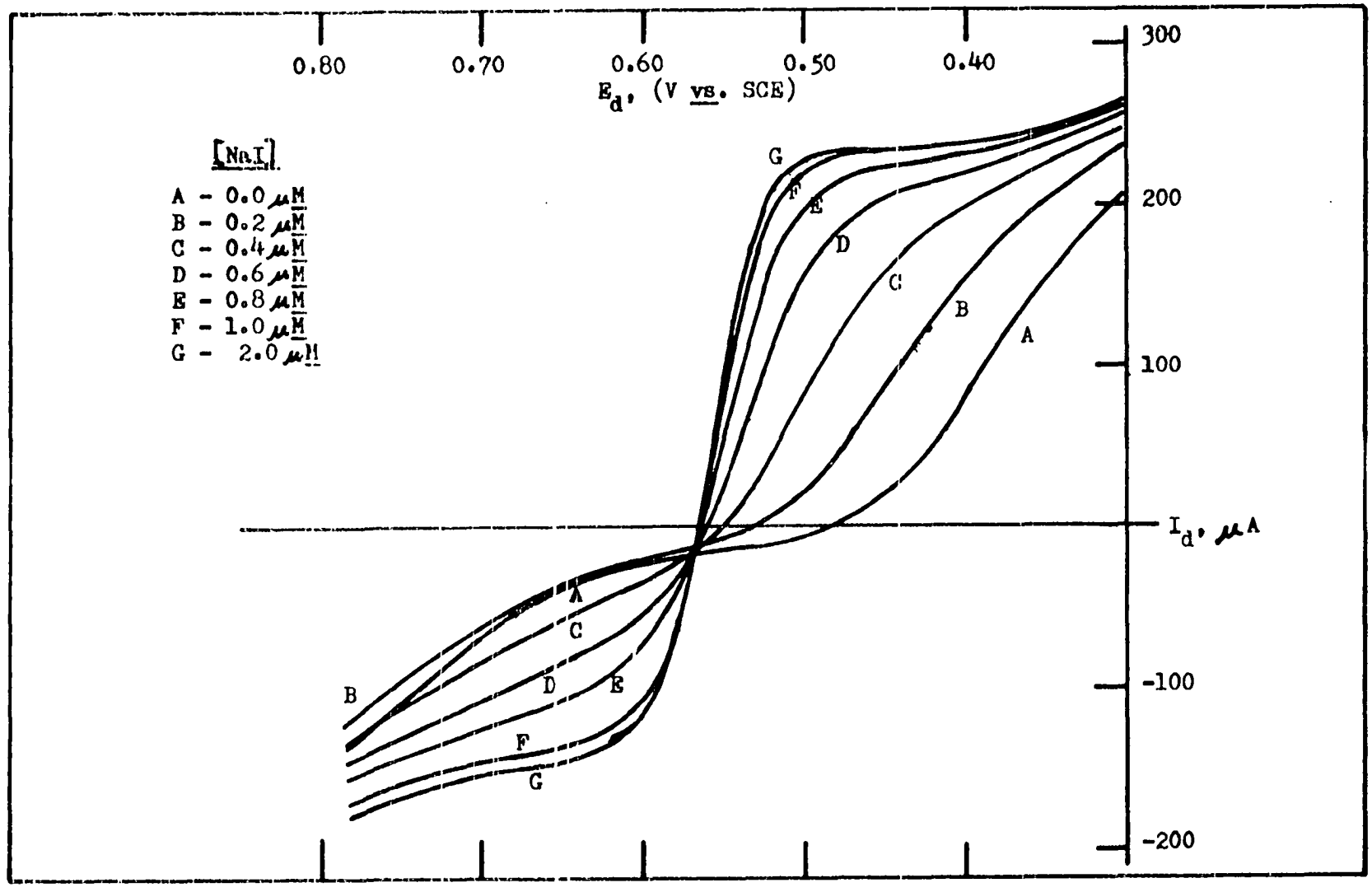

Figure V. 6. I-E Curves for Sb(V)/Sb(III) vs. the Concentration of NaI 12 M HCl. Scan Rate 0.5 V/min. Rotational Velocity 168 rad/sec.

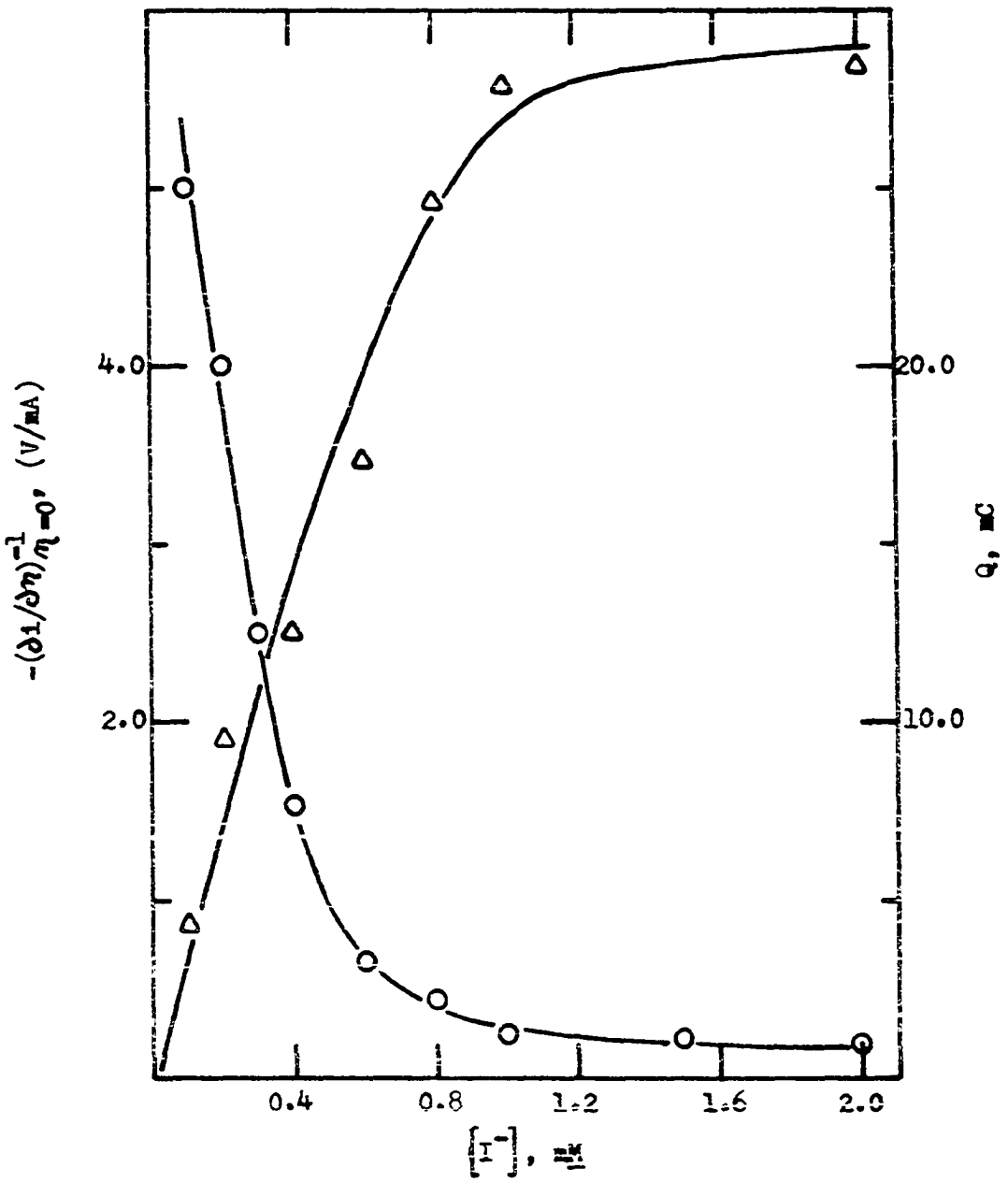

Figure V. 7 Plots of $-(\partial i/\partial \eta)^{-1}_{\eta=0}$ vs. $[I^-]$ and Coulombs of IO_3^- Found vs. $[I^-]$

O - $-(\partial i/\partial \eta)^{-1}_{\eta=0}$ Δ - Q

produced was determined from the I-t curve. A plot of the number of coulombs of IO_3^- vs. the concentrations of I^- in 12 M HCl was the adsorption isotherm for I^- in 12 M HCl. The results are plotted in Figure V. 7. The adsorption isotherms has a similar shape and reaches the limiting surface coverage at approximately the same concentration of I^- as the plot of $-(\partial i/\partial \eta)^{-1}_{\eta=0}$.

c. Determination of Kinetic Parameters. The values of i_o and k_o were determined for the heterogeneous reaction of the Sb(V)/Sb(III) couple in 12 M HCl containing two different concentrations of NaI. To find i_o the I-E curves were recorded at different rotation speeds for varying ratios of $[Sb(V)]:[Sb(III)]$, prepared keeping $[Sb(III)]$ constant and varying $[Sb(V)]$. I-E curves at 0.5 μM I^- were recorded with the potential scale expanded to make measurement of the slopes at $\eta = 0$ more accurate. The I-E curves obtained at different rotation speeds for equal concentrations of Sb(V) and Sb(III) are shown in Figure V. 8.

In Figure V. 9 a plot of $-(\partial i/\partial \eta)^{-1}_{\eta=0}$ vs. $\omega^{-1/2}$ was made for each Sb(V) concentration. The intercepts of Figure V. 9 are equal to RTi_o^{-1}/nF according to Equation V. 13. The values of i_o were calculated and used to determine α. A plot of log i_o vs. log $C^b_{Sb(V)}$ was made and is shown in Figure V. 10. The slope of this plot can be shown to be $1-\alpha$ if one takes logarithms of both sides of Equation V. 5, as shown in Equation V. 14. Since $C^b_{Sb(III)}$ does not change, $\Delta \log C^b_{Sb(III)}$ is zero. The values of α,

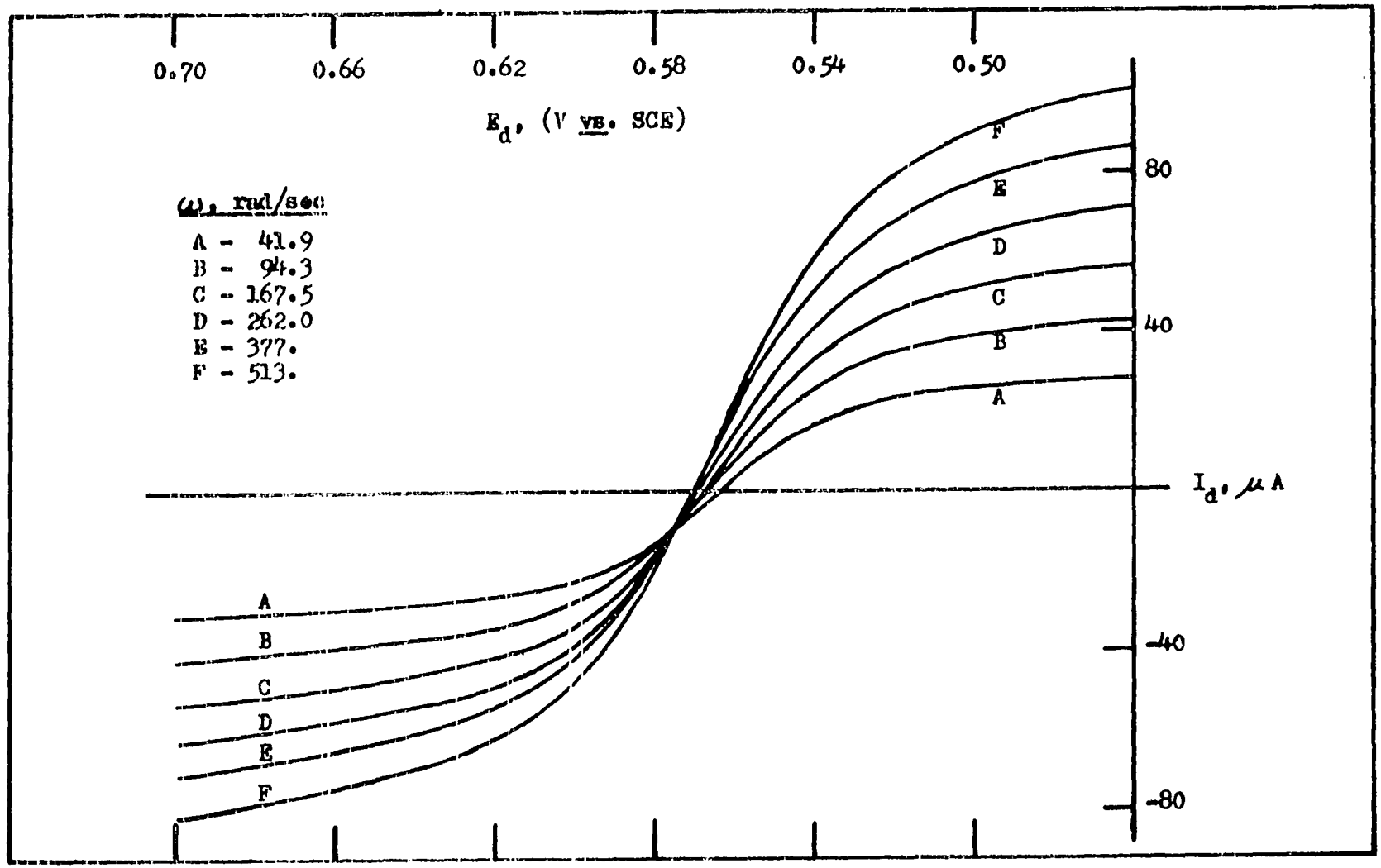

Figure V. 8. I-E Curves for Sb(V)/Sb(III) in 12 M HCl vs. Rotational Velocity
Scan Rate 1.0 V/min. 0.105 mM Sb(III). 0.079 mM Sb(V). 0.5 M NaI.

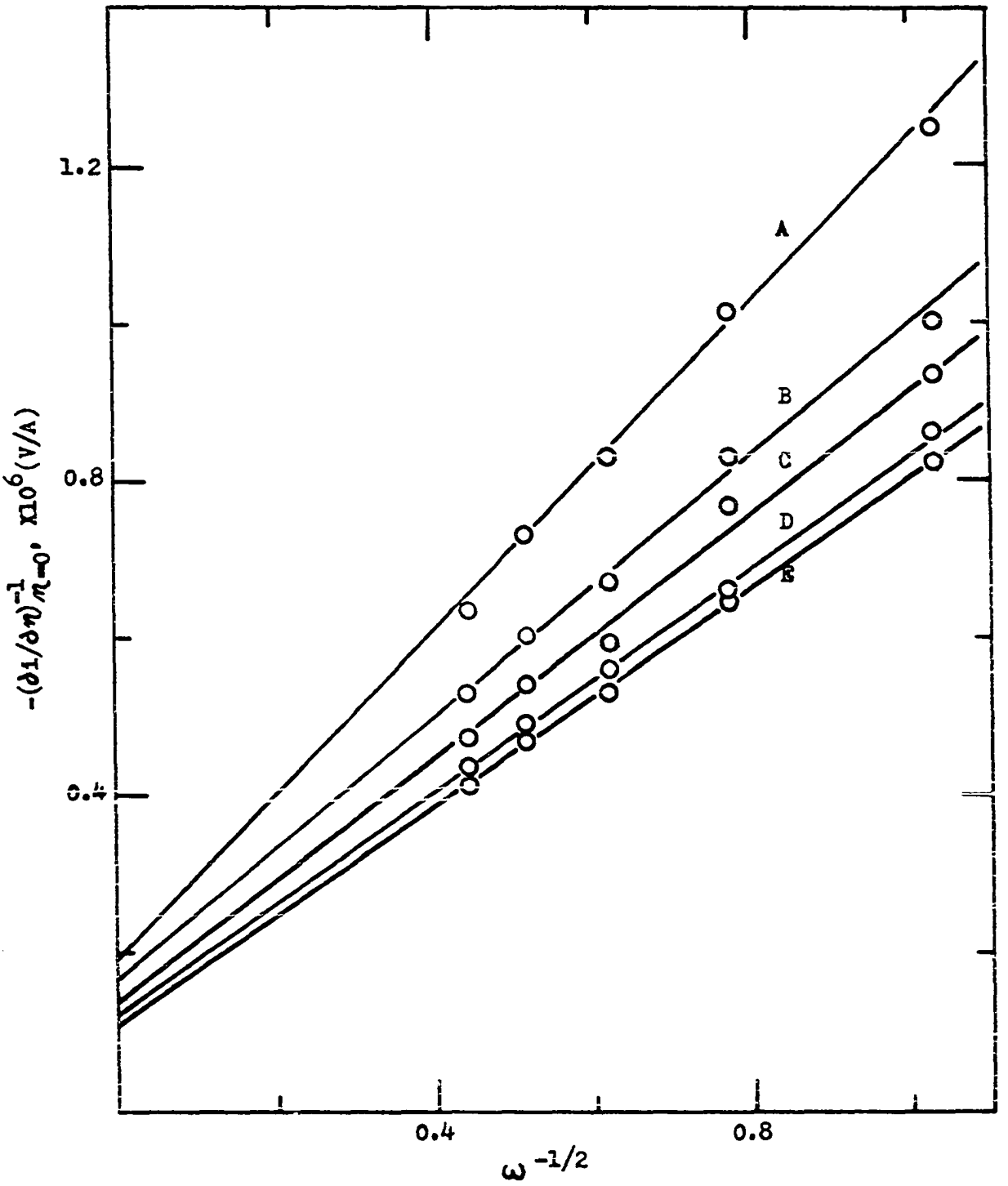

Figure V. 9. $-(\partial i/\partial \eta)^{-1}_{\eta=0}$ vs. $\omega^{-1/2}$

12 M HCl. 0.5 M NaI. 0.105 mM Sb(III). A - 0.079 mM Sb(V). B - 0.120 mM Sb(V). C - 0.158 mM Sb(V). D - 0.197 mM Sb(V). E - 0.236 mM Sb(V).

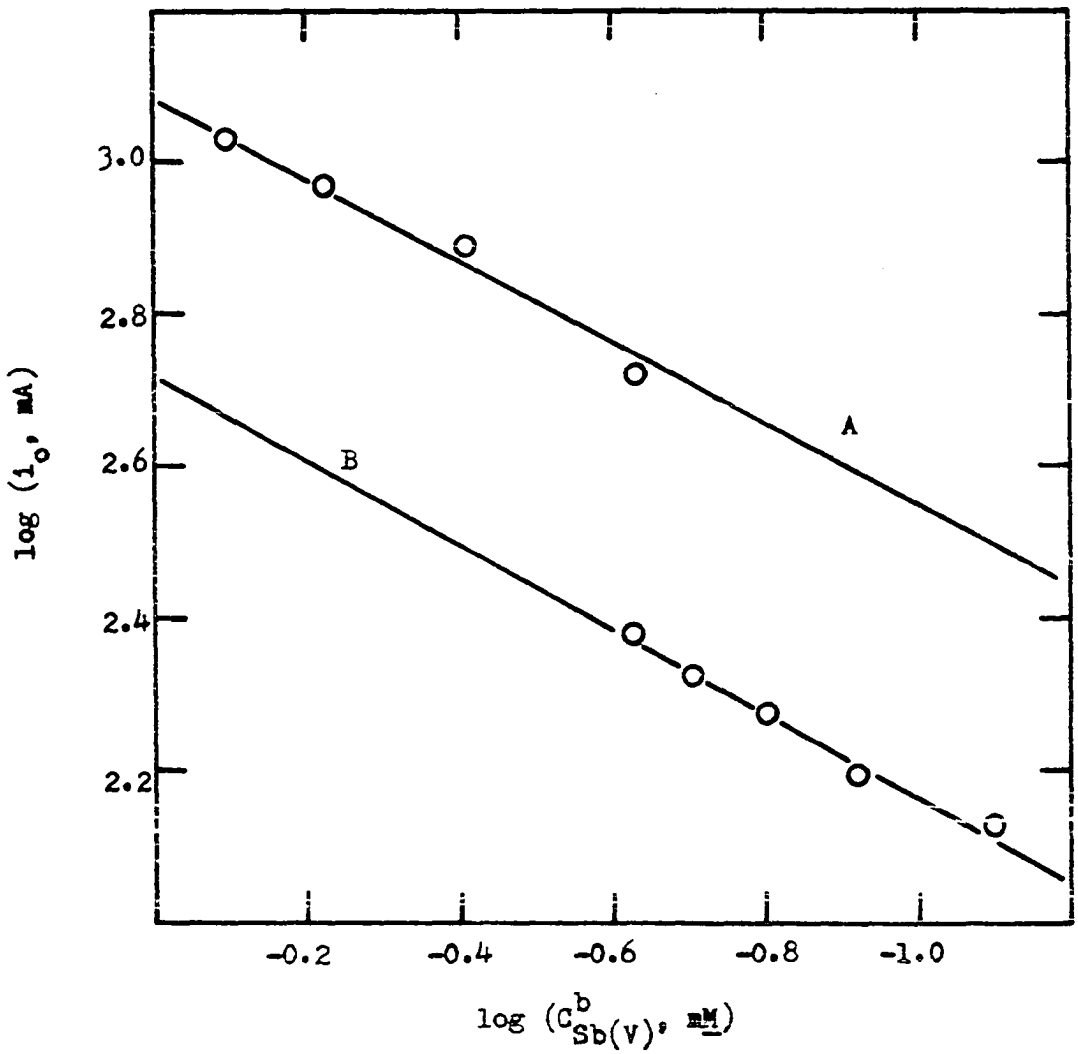

Figure V. 10. Plot of log i_o vs. log $C^b_{Sb(V)}$

12 M HCl. A - 0.44 mM Sb(III). B - 0.105 mM Sb(III).

$$\Delta \log i_o = \log(nFAk_o) + (1-\alpha)\,\Delta \log C^b_{Sb(III)} \qquad (V.\ 14)$$

$1-\alpha$, and i_o were used in Equation V. 5 to calculate k_o. Table V. 1 compares the values of k_o, α, and i_{oo} for two concentrations of NaI. The symbol i_{oo} refers to the standard exchange current density (194), which is the exchange current density which would be obtained when the concentrations of both species of the reacting couple are 1.0 M. i_{oo}, like k_o, should be a constant for any electrode reaction under a given set of conditions.

TABLE V. 1

Comparison of Values of α, i_{oo}, and k_o at Different Iodide Concentrations

$[I^-]$, M	α	k_o(cm/sec)	i_{oo}(A-l/mole-cm^2)
0.5	0.45	1.2×10^{-2}	4.6
2.0	0.54	1.5×10^{-2}	5.9

The value of k_o shown in Table V. 1 for 0.5 μM I^- was 80% of the k_o value for 2.0 μM I. As seen in the two adsorption isotherm shown in Figure V. 7, 0.5 μM I^- is about 60% and 85% of I^- concentration which will give the maximum surface coverage. This observation is in fair agreement with the k_o values reported in Table V. 1.

VI. EVALUATION OF THE COULOMETRIC DETECTOR USING THE OXIDATION OF ANTIMONY (III)

A. Introduction

A coulometric detector is one for which the electrolytic efficiency is 100%; that is, all electroactive species passing through the detector are electrolyzed. In the coulometric detector to be described, the electroactive species is transported to the electrode surface by convective-diffusional processes. Convection in the detector is caused by the velocity of the solution flowing through the detector.

The first electrodes described, which involved detection of electroactive species in electrolyte streams could not be classified as coulometric detectors because less than 0.1% of the electroactive species entering the cell are electrolyzed. Most of the detectors used a DME in a variety of different flow-through cell designs for the electroanalysis of species in electrolyte streams (19, 20, 109, 127, 179, 203, 204, 232). The applications of a DME in an electrolyte stream include analysis of gases (233), inorganic anions and cations (16, 22, 23, 65, 69, 138, 143, 157, 170), electroactive organic functional groups (23, 109, 110, 113), proteins (54), alkaloids (112), and pesticides (117, 177).

The use of solid electrodes for in-stream analysis has been investigated at platinum micro-electrodes by Muller (146), at silicone-rubber based, glassy-carbon electrodes by Joynes and Maggs (104), Nagy, et al. (147), Pungor, et al. (166), and at graphite

electrodes by Sharma and Dutt (188-190). Solid electrodes, which electrolyze more than 0.1% of the sample at 3 ml/min, but are not 100% efficient, were described by Takemori and Honda (203) and by Blaedel and Boyer (17).

The sensitivity of the detectors described previously is not very great because much less than 100% of the sample is electrolyzed. To construct a detector which has the maximum efficiency, that is a coulometric detector, the surface area of the electrode is increased and the internal volume of the electrode is decreased. The increase in surface area and decrease in internal volume is brought about by packing a tubular electrode with finely divided electrode materials (9, 20, 56, 144, 174, 193, 199, 229), plugs of wire or metallic gauze, and porous or fritted metals (191).

Coulometric detectors based on packed tubular electrodes have been constructed from platinum (144, 193), graphite (22, 191), granular carbon (9, 200), glassy carbon (20), amalgamated nickel (174), and silver (56, 191). The applications of coulometric detectors and electrochromatography has been reviewed by Fujinaga (64).

Coulometric detectors are inherently more sensitive than other electrochemical detectors because all of the sample is electrolyzed. An additional advantage of the coulometric detector is that it is not very dependent upon the flow rate of the eluent. To demonstrate this, consider the analytical relationship between I_ℓ and C^b for an unpacked tubular electrode shown in Equation VI. 1.

$$I_{\ell} = (5.24 \times 10^5) D^{2/3} L^{2/3} n V_f^{1/3} C^b \qquad \text{(VI. 1)}$$

Blaedel, et al., verified Equation VI. 1 for a tube having an inner diameter of 0.03 inches, a length L, of 1.0 inches, and for flow rates, V_f, less than 10 ml/min. A typical chromatographic peak for an unpacked tubular electrode shown in Figure VI. 1. The area under the chromatographic peak is the number of coulombs, Q. Q is found by integrating Equation VI. 1 over the time span $t_2 - t_1$, as shown in Equation VI. 2. If V_f is constant over the time span $t_2 - t$, the number of moles eluted

$$Q = (5.24 \times 10^5) n D^{2/3} L^{2/3} \int_{t_1}^{t_2} V_f^{1/3} C^b(t) dt \qquad \text{(VI. 2)}$$

is given by Equation VI. 3 and Q is given by Equation VI. 4. Equations VI. 3 and VI. 4 are combined to give Equation VI. 5.

$$\text{moles} = V_f \int_{t_1}^{t_2} C^b(t) dt \qquad \text{(VI. 3)}$$

$$Q = (5.24 \times 10^5) n D^{2/3} L^{2/3} V_f^{1/3} \int_{t_1}^{t_2} C^b(t) dt \qquad \text{(VI. 4)}$$

Thus, a plot of log Q <u>versus</u> log V_f has a slope of -0.667, demonstrating that a large dependency on flow rate does occur with an unpacked tubular electrode.

$$Q = (5.24 \times 10^5) n D^{2/3} L^{2/3} V_f^{-2/3} \text{ moles} \qquad \text{(VI. 5)}$$

For a coulometric detector Equation VI. 5 reduces to Equation VI. 6 since Q is independent of $D^{2/3}$, V_f, and $L^{2/3}$.

$$Q = n(9.65 \times 10^4) \left[\text{moles}\right] \qquad \text{(VI. 6)}$$

To determine the amount of a species eluted, one does not need a calibration curve. Since n is usually known, or easily determined, one measures Q experimentally and calculates the amount of electroactive species using Equation VI. 6.

From Equation VI. 6, one may also see that the sensitivity of the detector depends only upon the number of equivalents of electroactive species, that is, n [moles]. Thus, the coulometric detector has a uniform sensitivity for all electroactive species. This is to be contrasted to variable sensitivity detectors, such as the photometric type, whose sensitivity depends upon the nature of of the species being determined.

Results presented in this section demonstrate the utility of a coulometric detector to the determination of Sb(III) by its enhancement of the Br^- oxidation wave and by direct electrochemical oxidation.

B. Experimental

1. Chemicals and Reagents.

The following chemicals were obtained from sources given: NaBr, H_3PO_4, $HClO_4$, H_2SO_4, HNO_3, HCl, Sb_2O_3, $NiCl_2 \cdot 6H_2O$, As_2O_3, $BiCl_3$, $ZnCl_2$, $CrCl_3 \cdot 6H_2O$, $Al(NO_3)_3 \cdot 9H_2O$, $CoCl_2 \cdot 6H_2O$, and $MnCl_2$ were "Baker Analyzed" reagents; $CdCl_2 \cdot 2\frac{1}{2}H_2O$ and $HgCl_2$ were Mallinckrodt reagents; electrolytic iron and $(NH_4)_4Ce(SO_4)_4 \cdot 2H_2O$ were from G. Frederick Smith Co.; $PbCl_2$ was from Allied Chemical Co.; $CuCl_2 \cdot 2H_2O$ was from Matheson, Coleman, and Bell; and VCl_5 was from City Chemical Co. The source of selenium and $(NH_4)_4MoO_4$ was not

known.

2. Preparation of Solutions.

a. Sb(III) in 2 M HCl. Enough Sb_2O_3 was dissolved in 30 ml of concentrated HCl to make a 1.0 mM stock solution and was diluted to the mark in a volumetric flask by slowly adding a mixture of HCl and H_2O. Enough HCl was added to make the acid concentration 2.0 M.

b. Sb(III) in 1.0 M H_2SO_4. Enough Sb_2O_3 was dissolved in 30 ml of hot, concentrated H_2SO_4 to prepare a 2.0 mM stock solution. After cooling to room temperature, this solution was diluted to the mark in a volumetric flask by low addition of a mixture of H_2SO_4 and H_2O. Enough H_2SO_4 was added to make the final acid concentration 1.0 M.

c. Sb(III) in 4.0 M H_2SO_4. Enough Sb_2O_3 was dissolved in hot, concentrated H_2SO_4 to make a 5.0 mM stock solution. After cooling to room temperature, this solution was diluted to the mark in a volumetric flask by slow addition of a mixture of H_2SO_4 and H_2O. Enough H_2SO_4 was added to make the final acid concentration 4.0 M.

d. Solution Preparation for Interference Study. All solutions, except for the Pb(II) solution, were made to be 0.0100 M in the cation and 1.0 M in HCl. The Pb(II) solution was 0.00100 M in Pb(II) and 1.0 M in HCl. For most solutions either the chloride salt or some other readily available salt was dissolved in 1.0 M HCl and diluted to the mark in a volumetric flask with 1.0 M HCl.

A 0.10 M solution of Se(IV) was prepared by dissolving selenium metal in 15 ml of hot, concentrated HNO_3. This solution was diluted to one liter with H_2O. A 25.0 ml aliquot of the 0.10 M solution of Se(IV) was diluted to 250.0 ml with 0.8 ml concentrated HCl and 1.0 M HCl to make the solution 0.01 M in Se(IV) and 1.0 M in HCl. An Fe(III) solution was prepared by dissolving the appropriate amount of electrolytic iron in 12 ml of hot, concentrated 5:1 HCl-HNO_3. 6.7 ml of concentrated HCl was added and the solution diluted to 200.0 ml with H_2O. An As(III) solution was prepared by dissolving the exact amount of As_2O_3 in 10 ml of 8% NaOH. 0.8 ml of concentrated HCl was added and the solution diluted to 200.0 ml with 1.0 M HCl.

Solutions of the anions studied were made up to be 1.0 M by diluting enough of the concentrated acid to the mark in a volumetric flask with 1.0 M HCl.

3. Standardization of Sb(III) Stock Solutions.

Sb(III) stock solutions were standardized by constant current coulometric titrations with electrogenerated Br_2 as described in Section IV. B. 3.

4. Experimental Procedures.

a. Electrode Pretreatment. 1.0 M H_2SO_4 or 1.0 M HCl was passed through the packed tubular electrode and the potential was set to 1.2 V, -0.6 V, and 0.0 V for 3 minutes at each potential. The potential was changed to 0.30 V and the flow of acid solution was stopped. 10-20 ml of 0.01 M NaI was flushed through the cell

and the flow of the acid solution resumed.

b. Voltammetry. I-E curves were obtained by passing 0.989×10^{-5} M Sb(III) in 1.0 M HCl through the detector at a constant flow rate. The electronic circuitry used to obtain all I-E curves is described in Section III. A. 2.

A second procedure used to obtain I-E curves was the introduction of aliquots of 0.989×10^{-5} M Sb(III) in 1.0 M HCl into a stream of 1.0 M HCl passing through the detector at a constant flow rate. The electrode potential was increased in 50 mV steps from 0.600 V to 0.900 V. The I-t peaks were recorded on a Leeds and Northrup strip chart recorder and were integrated with a Keuffel and Esser planimeter.

c. Electrode Efficiency. Aliquots of 1.00×10^{-5} M Sb(III) in 1.0 M HCl were injected into a stream of 1.0 M HCl at a number of different flow rates and an electrode potential of 0.800 V. The electronic circuitry for all studies at a constant potential is described in Section III. A. 1. The I-t curves were recorded on a Leeds and Northrup strip chart recorder and were integrated with a planimeter.

d. Precision Study. Aliquots of 1.00×10^{-5} M Sb(III) in 1.0 M HCl were injected into a stream of 1.0 M HCl at a constant flow rate. I-t curves at an electrode potential of 0.800 V were recorded simultaneously on a Bolt, Beranek, and Newman Plotamatic X-Y recorder and on a Leeds and Northrup strip chart recorder. The peak areas were integrated with a planimeter.

e. Concentration Studies. A concentration study of the Sb(III) enhanced Br^- oxidation wave was performed using the coulometric detector described in Section III. B. Sb(III) solutions, in the concentration range from 1.0×10^{-6} M to 2.0×10^{-4} M, were prepared in 1.0 M H_2SO_4 and injected into a stream of 1.0 M H_2SO_4 at a flow rate of 1 ml/min. The stream of 1.0 M H_2SO_4 was mixed with a stream of 1.0 mM NaBr in 1.0 M H_2SO_4 before entering the detector. The flow rate of the stream containing 1.0 mM NaBr slowly decreased from 1.2 ml/min to 0.75 ml/min during the Sb(III) concentration study. The electronic circuitry used was described in Section III. A. 1. A voltage proportional to the current because of oxidation of bromide was added to an equal voltage with the opposite sign. The resulting signal was reduced by a factor of 1:10 using the voltage divider circuit described in Section III. A. 1. Current-time (I-t) curves were recorded with a Leeds and Northrup Speedomax strip chart recorder.

The concentration range over which the direct oxidation of Sb(III) was applicable was investigated by injection of 0.50 ml aliquots of Sb(III) solutions into a stream of 1.0 M HCl at a constant flow rate. The concentration of Sb(III) solutions ranged from 7.6×10^{-8} M to 4.0×10^{-5} M and were prepared by taking aliquots of the Sb(III) stock solutions in 2.0 M HCl or 1.0 M H_2SO_4 with a 2.000-ml Gilmont micrometer buret and diluting to the mark in volumetric flasks with 1.0 M HCl. The potential used

was 0.800 V and peaks were recorded using a Leeds and Northrup strip chart recorder. Peak areas were measured using the planimeter.

f. Interference Study. Solutions containing Sb(III) and the interfering ions were prepared by diluting a 1.000 ml aliquot of 1.0×10^{-3} M Sb(III) and 0.10, 1.00, and 10.00 ml of the 1.00×10^{-2} M solution of interfering ion to 100.0 ml with 1.0 M HCl. Injections of each solution were made into a stream of 1.0 M HCl at a constant flow rate. The I-t curves were integrated electronically and recorded simultaneously on a Leeds and Northrup strip chart recorder.

C. Results and Discussion

1. Voltammetry.

I-E curves were obtained using cyclic voltammetry (method 1) and by measuring the coulombs of Sb(III) oxidized in a 0.50 ml aliquot at a constant potential (method 2). The results of the two methods are shown in Figure VI. 1. Of the two methods, the use of method 2 appeared to give the best results because the observed currents were lower. The lower currents caused a smaller IR loss in the detector and therefore, less distortion in the shape of the I-E curve. For method 1, the current measured at 0.700 V was 160 μA for 0.989×10^{-5} M Sb(III) and for the second method, the peak current, measured at the same potential, was only 29.5 μ A. The cell resistance was 850 Ω and the IR losses were 0.136 V and 0.025 V for the two methods, respectively.

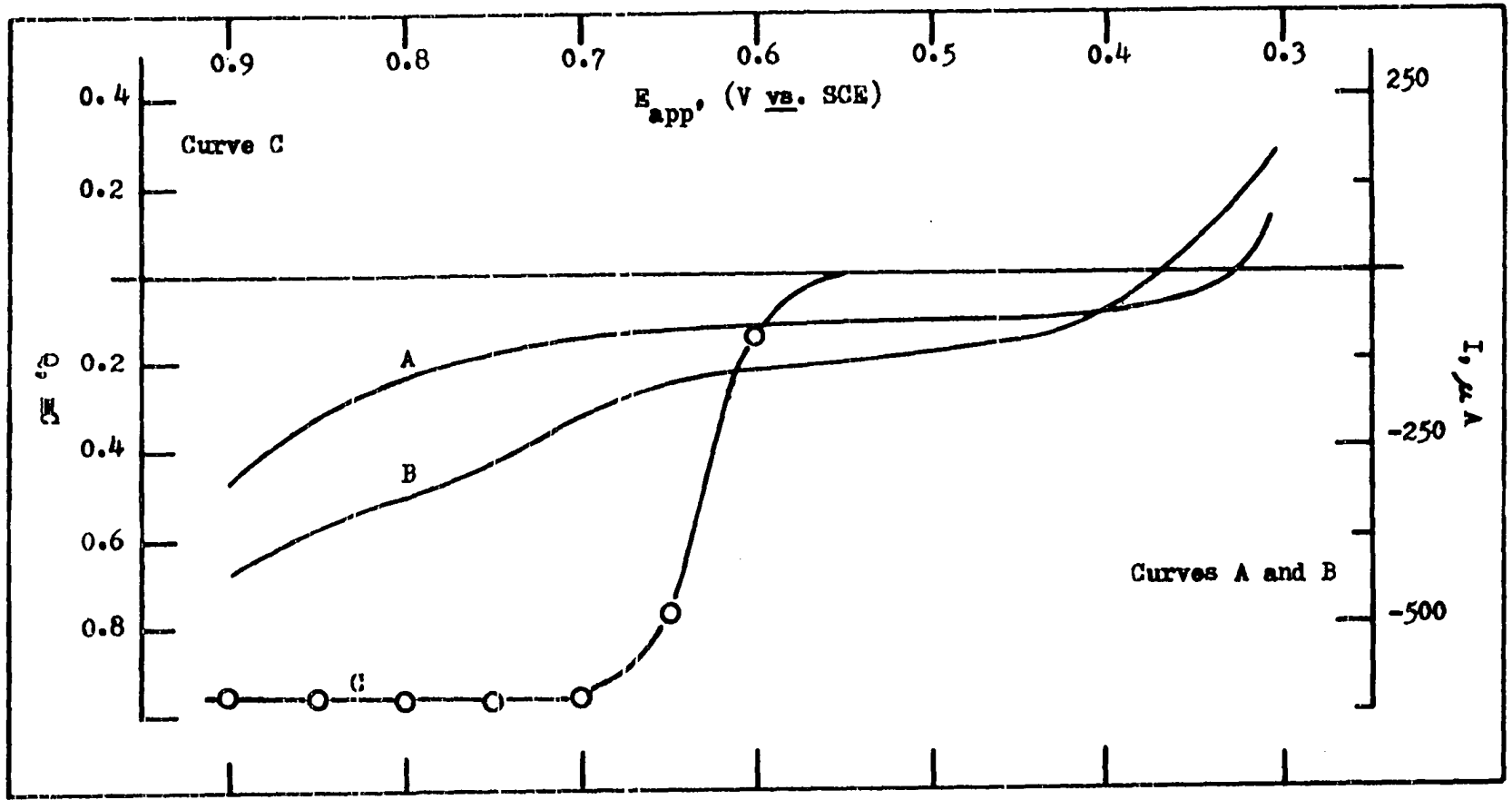

Figure VI. 1. I-E Curves of Sb(III) in 1.0 M HCl

A - 1.0 M HCl, scan rate 1.0 V/min. B - 1.0 M HCl and 0.99×10^{-5} M Sb(III), scan rate 1.0 V/min. C - 1.0 M HCl and 0.62 μg aliquots of Sb(III). Flow Rate 1.0 ml/min for all curves.

The much larger IR loss and the charging current resulting from the cyclic voltage scan in method 1 caused the observed differences between the I-E curves in Figure VI. 1.

2. Electrode Efficiency.

The tubular electrode was packed with platinum chips and wire to increase the efficiency. The efficiency of the electrode described in Section III. B. was measured and the results shown in Figure VI. 2 by plotting the coulombs of Sb(III) oxidized vs. the flow rate. No flow rate dependence was observed up to a flow of 4.1 ml/min. The results shown in Figure VI. 2 were not corrected for a blank.

3. Precision Study.

The results of fifteen 0.5065 ml injections of 1.00×10^{-5} M Sb(III) were made and the number of coulombs determined from the areas of the I-t curves obtained. Table VI. 1 shows the results obtained for the fifteen injections. Relative standard deviations of 5.0 ppt and 5.2 ppt were found for the Leeds and Northrup and Plotamatic recorders, respectively. The major source of error in this precision study was the sample loop. When the sample loop if filled, care must be taken that air bubbles do not form in the loop. If bubbles do form, the sample loop volume is decreased and the results become scattered.

4. Concentration Studies.

a. Catalytic Enhancement. A concentration study was performed using the technique of catalytic enhancement for Sb(III)

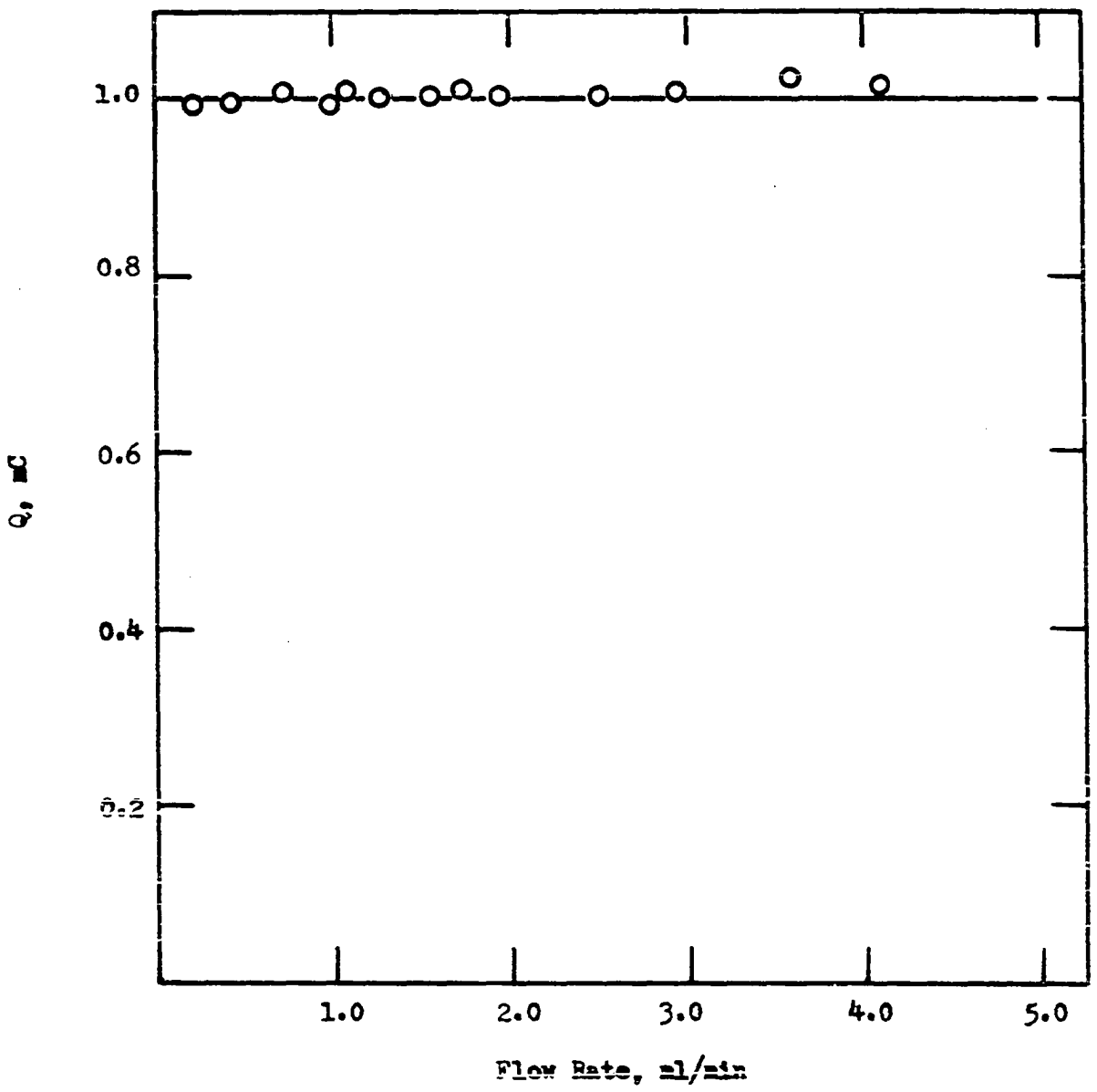

Figure VI. 2. Determination of Electrode Efficiency
1.0 M HCl. 0.62 μg aliquots of Sb(III).
Electrode Potential 0.800 V.

TABLE VI. 1

Precision Study

Arbitrary units	
Leeds & Northrup	X-Y Plotamatic
739	758[a]
733	764[a]
733	756[a]
738	773
740	773
732	781
740	774
743	782
740	778
733	783
740	776
732	783
736	772
741	778
735	780

[a] Eliminated statistically.

in 1.0 M H_2SO_4. The acid concentration was decreased from 4.0 M H_2SO_4 to 1.0 M H_2SO_4 because the Sb(III) solutions were determined to be stable in 1.0 M H_2SO_4 at concentrations below 1×10^{-4} M. The 5.00 mM Sb(III) stock solution was prepared in 4.0 M H_2SO_4.

Results of the concentration study are shown in Figure VI. 3. The agreement with the theoretical slope, indicated by the solid line, was very good for Sb(III) concentrations greater than 1.0×10^{-5} M. When the ratio of Br^- to Sb(III) became greater than 100, i. e., at Sb(III) concentrations less than 1.0×10^{-5} M, the precision and accuracy were unsatisfactory. At these low Sb(III) levels, the amplification had to be high enough to detect the Sb(III), but this high amplification also magnified the baseline noise.

Typical chromatographic peaks obtained using catalytic enhancement are shown in Figure VI. 4. The peaks in Figure VI. 4 were recorded for 0.5065 ml injections of 5.00×10^{-5} M and 2.00×10^{-6} M Sb(III) in 1.0 M H_2SO_4. The sloping baseline was integrated by following the curve as recorded and not by averaging the fluctuations. More precise results were obtained for Sb(III) concentrations below 10^{-5} M when the NaBr concentration were decreased to 1×10^{-4} M. Decreasing the Br^- concentration by a factor of 10 also decreased the baseline noise by the same amount. Thus, the ratio of enhancement current to baseline noise was increased.

b. Direct Electrochemical Oxidation. Results of a concentration study, in which injections of Sb(III) in 1.0 M HCl were made directly into a stream of 1.0 M HCl, are shown in Figure VI. 5. Theoretically, a slope of log (nFV) should be observed for a plot of log Q vs. log $C^b_{Sb(III)}$. The solid line in Figure VI. 5

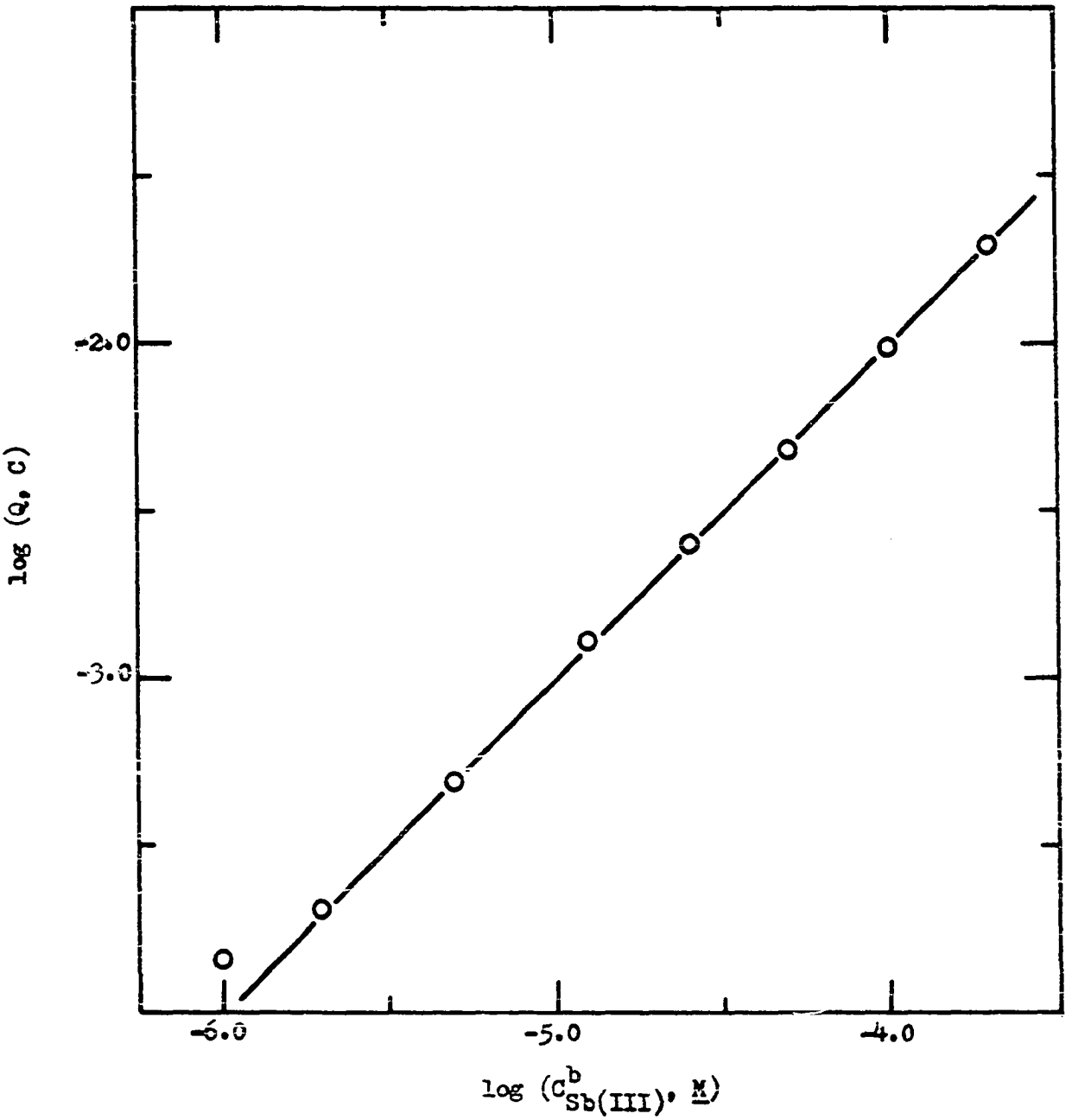

Figure VI. 3. Concentration Study for Sb(III) in 1.0 M H_2SO_4
Flow Rate of 1.0 M H_2SO_4, 1.0 ml/min. Flow Rate of 1.0 M NaBr in 1.0 M H_2SO_4, 0.75 - 1.25 ml/min. Electrode Potential 1.10 V. Sample Volume 0.5065 ml.

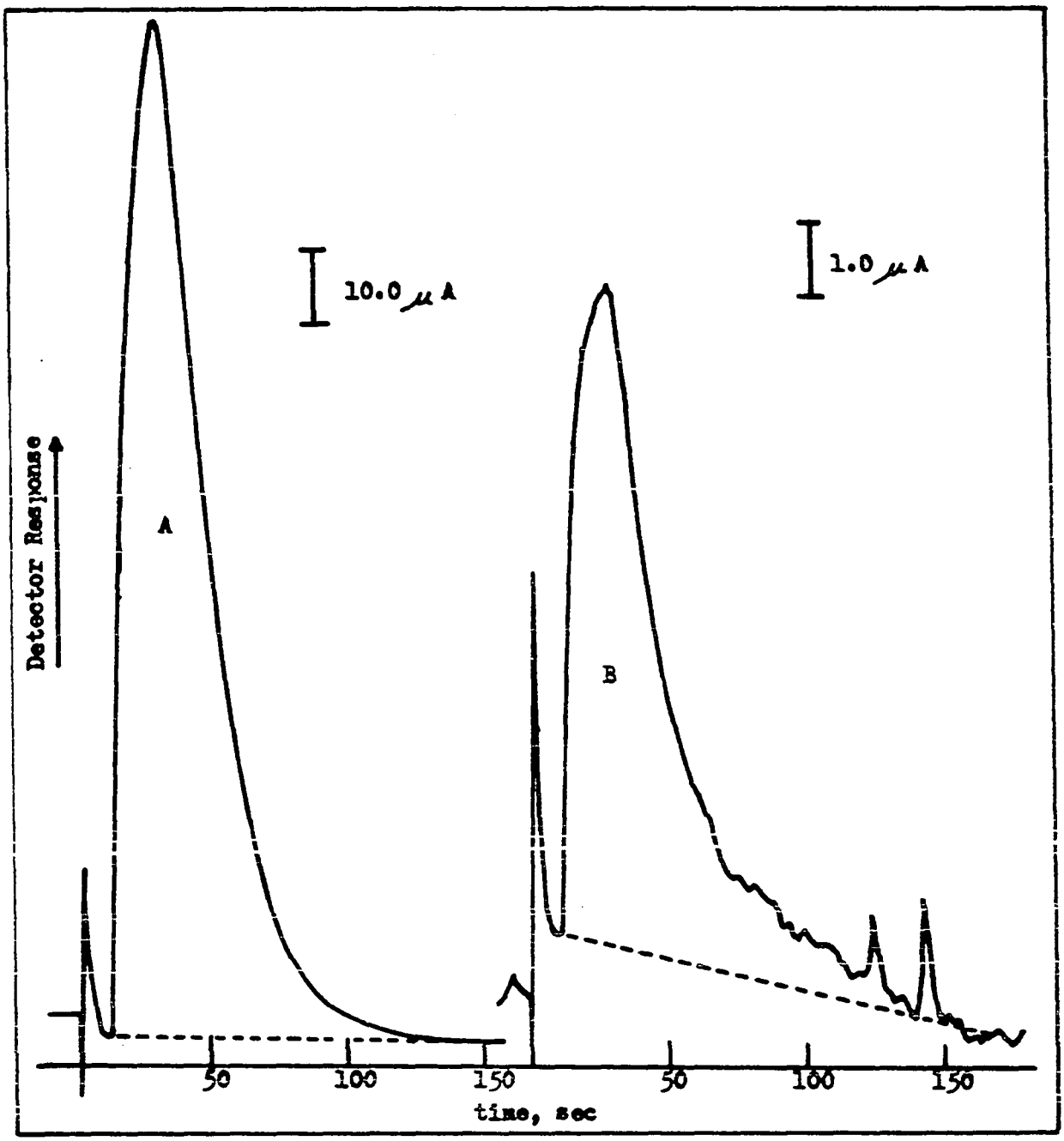

Figure VI. 4. Chromatographic Peaks Obtained for Sb(III) in 1.0 M H_2SO_4

Flow Rate of 1.0 M H_2SO_4, 1.0 ml/min. Flow Rate of 1.0 mM NaBr in 1.0 M H_2SO_4, 0.75 - 1.25 ml/min. Electrode Potential 1.10 V. A - 5.00×10^{-5} M Sb(III). B - 2.00×10^{-6} M Sb(III). Sample Volume 0.5065 ml. ---- Baseline for Integration.

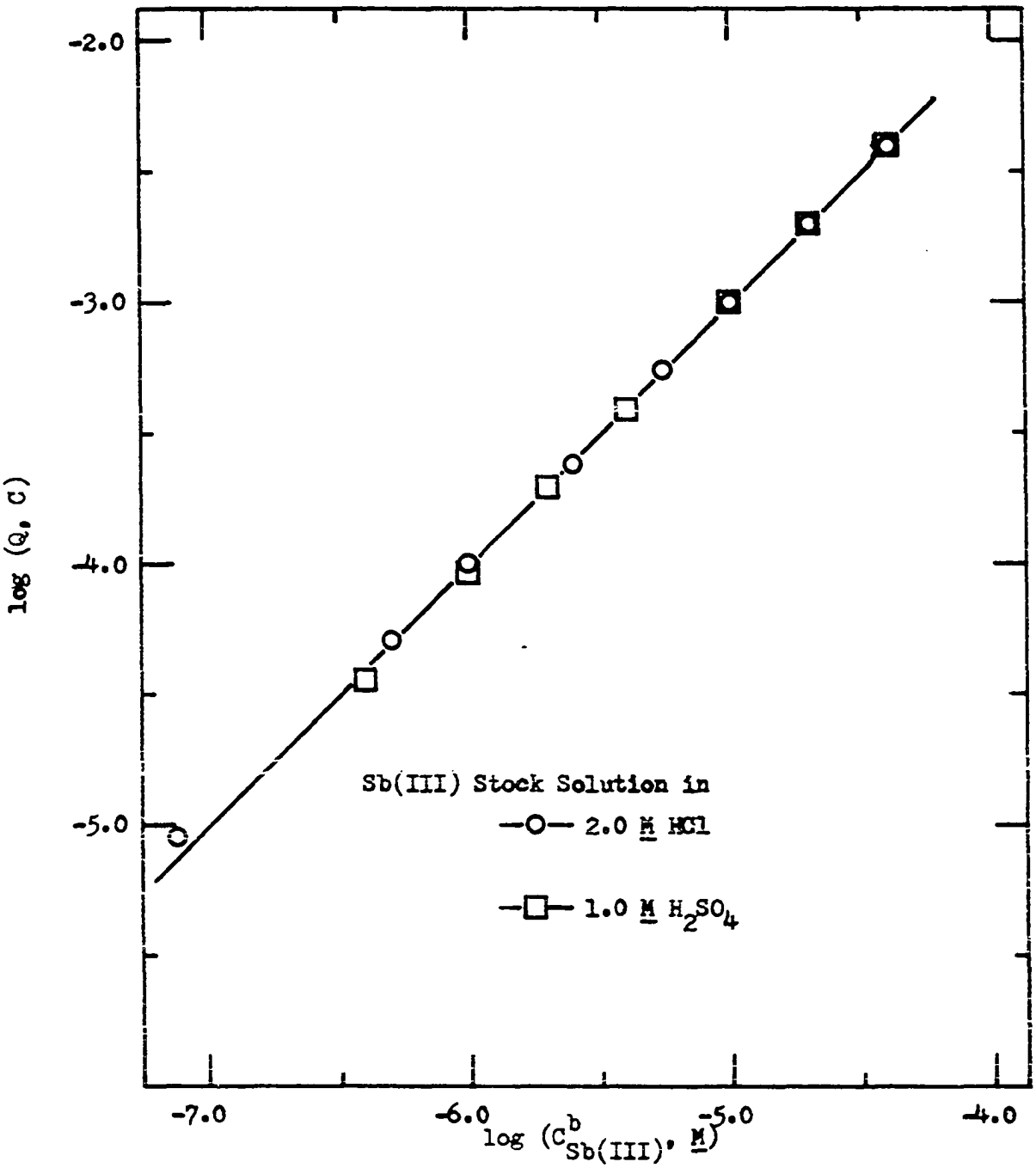

Figure VI. 5. Concentration Study for Sb(III) in 1.0 M HCl Electrode Potential 0.800 V. Sample Volume 0.5065 ml. □ - Flow Rate 1.35 ml/min. O - Flow Rate 1.05 ml/min.

has a slope equal to 1.0 and the experimental points are in very good agreement with the predicted values. The greatest degree of deviation occurs at concentrations below 5×10^{-7} M. The upper concentration limit was set by choice for Figure VI. 5.

5. Interference Study.

The interference of anions and cations on the direct electrochemical oxidation of Sb(III) was investigated and the results are shown in Table VI. 2. The results are reported as the percent Sb(III) found experimentally, that is, the coulombs of Sb(III) found divided by the coulombs of Sb(III) taken times 100%. Values greater than 100% mean the interfering ion was oxidized at the same potential as Sb(III) and values less than the interference was either reduced at 0.800 V or was adsorbed at the iodide covered platinum surface, thereby reducing the number of active sites available for oxidation of Sb(III).

Ti(III) and As(III) interfered due to oxidation at 0.800 V and Ce(IV) by reduction at 0.800 V. Cr(III) and Mn(II), which have higher oxidation states, were not oxidized at 0.800 V. Cations which interfered by non-electrochemical processes were, in order of decreasing interference, Fe(III) > Bi(III) > Hg(II) > U(VI) > Mo(VI) > Pb(II). The adsorption of these ions was reversible. After injection of a sample containing Fe(III), 1.0 M HCl was passed through the cell before injecting a sample containing Sb(III), but no Fe(III). The percent Sb(III) found was 100.

TABLE VI. 2

Effect of Interferences on the Coulometric Determination of 0.618 micrograms of Sb(III).

	Percent Sb Found		
Interference	10^{-5} M	10^{-4} M	10^{-3} M
Al(III)	101	101	100
Ti(III)	102	173	1270
Ti(IV)	100	100	102
V(V)	100	98	98
Cr(III)	100	99	101
Mn(II)	100	100	100
Fe(III)	94	81	12
Co(II)	99	99	99
Ni(II)	100	100	99
Cu(II)	99	99	99
Zn(II)	100	99	99
As(III)	100	100	108
Se(IV)	101	101	100
Mo(VI)	100	100	99
Cd(II)	101	101	100
Sn(IV)	100	100	100
Ce(IV)	93	54	-236[a]
Hg(II)	99	96	88
Pb(II)	100	99	---
Bi(III)	97	89	72
U(VI)	100	100	99
	10^{-3} M	10^{-2} M	10^{-1} M
$HClO_4$	100	100	90
HNO_3	100	99	98
H_2SO_4	99	100	99
H_3PO_4	99	98	98

[a]Negative sign means that more coulombs were found for the reduction of Ce(IV) than for the oxidation of Sb(III).

VII. DETERMINATION OF ANTIMONY (III) USING FORCED-FLOW LIQUID CHROMATOGRAPHY

A. Introduction

The determination of antimony using a coulometric detector can be accomplished by either reduction of Sb(V) or oxidation of Sb(III). Since Sb(III) species are not as easily hydrolyzed as Sb(V) species (150), the determination of antimony was carried out by oxidizing Sb(III). Several separation schemes for Sb(III) have been reported in the literature using anion exchange resins (3, 4, 13, 40, 43, 57, 60, 82, 114, 115, 121, 137, 149, 150, 187), and cation exchange resins (40, 86, 137, 198).

The method chosen for the ion exchange separation in this research was based on the cation exchange scheme described by Strelow (198). This procedure uses HCl to elute Sb(III) from the catex resin. Because Sb(III) forms a strong chloro complex, the distribution coefficient is small and Sb(III) is only weakly retained by the resin. However, in dilute $HClO_4$ solutions Sb(III) exists as SbO^+ (96) and is retained by catex resins (95). This separation procedure is used along with the direct electrochemical oxidation of Sb(III) to provide a rapid and selective method for determining antimony in a variety of different matrices and over a large range of antimony compositions.

B. Experimental

1. Chemicals and Reagents.

All chemicals used were "Baker Analyzed" reagents. Certificate values of NBS standard #53 was given in Section IV. B. 1. A

second NBS standard, #124b, was used and had the following certificate values: 83.69% Cu, 5.40% Zn, 4.93% Sn, 4.64% Pb, 0.76% Ni, 0.26% Fe, 0.20% Sb, and < 0.1% of S, P, Si, and Al. The compositions of two standard alloys prepared by Dr. John D. Verhoeven were given in Section IV. B. 1 for alloys designated ISU-1 and ISU-2. Additional standard alloys prepared by Dr. Verhoeven had the following compositions: ISU-3 contained 96.00% Sn and 4.00% Sb. TP-100C contained 95.98% Sn and 4.02% Sb.

2. Preparation of Solutions.

a. Sb(III) in 1.0 M HCl. The preparation of this stock solution was described in Section VI. B. 4. e.

b. Solution Preparation for Interference Study. The amount of $HgCl_2$ and $Bi(NO_3)_3$ necessary to prepare 0.010 M stock solutions was dissolved in 1.0 M $HClO_4$ and diluted to the mark in a volumetric flask with 1.0 M $HClO_4$. A 0.010 M stock solution of Fe(III) was prepared by the procedure described in Section V. B. 2. a.

c. Pb and Sn-Based Alloys. The dissolution procedures for these alloys are described in Section IV. B. 2. Before injection of a sample onto the column, 1.0 M aliquots were diluted to 100.0 ml with 1.0 M $HClO_4$.

d. Cu-Based Alloy. The procedures for dissolution of NBS-124d was as follows: Sufficient alloy to prepare a 1×10^{-5} M solution was dissolved in 8 ml of 1:1 HNO_3-H_2O without heating. 30 ml of 1.0 M $HClO_4$ was added and N_2 bubbled through the

solution to remove oxides of nitrogen. The solution was diluted to 100.0 ml with 1.0 M $HClO_4$.

e. Human Hair (Procedure C). Approximately 0.3 g to 1.0 g of hair was placed into a flask and dissolved in 1:1 $HClO_4$-HNO_3 according to the procedure described in Reference 47.

f. Human Hair (Procedure D). Approximately 0.3 g to 1.0 g of hair was dissolved in 10 ml of a 1:1 mixture of hot H_2SO_4-HNO_3. The HNO_3 was boiled off. If all the organic matter was not dissolved, 5 more ml of HNO_3 were added and the mixture heated until all the HNO_3 was boiled away.

After dissolution of the hair by either procedure, the Sb(V) produced was reduced to Sb(III) by the following procedure: When all visible traces of HNO_3 were removed by boiling, 10 ml of H_2O were added to the solution and it was boiled for 5 minutes. 15 ml of 1% $NaHSO_3$ were added and the solution was boiled to one-half volume to destroy the bisulphate. Samples dissolved by Procedure C were diluted to volume in a volumetric flask with water and samples dissolved by Procedure D were diluted with water and enough concentrated $HClO_4$ to give a 1.0 M $HClO_4$ solution.

g. Transistor. A power transistor was scraped from its aluminum base with a razor blade and was boiled in 5 ml of concentrated H_2SO_4 for two hours. This solution was diluted to 10.0 ml with H_2O. A 1.00 ml aliquot was diluted to 10.0 with 0.8 ml concentrated $HClO_4$ and H_2O.

3. Experimental Procedures.

a. Resin Pretreatment. The anion exchange resin used was Amberlite IRA-900. 10 g of the resin was dried, ground with a mortar and pestle and sieved. The 100-140 mesh fraction was back washed to remove any fines which remained. 0.12 g was slurried and packed into a 9 cm X 2 mm column. The resin was washed with 4.0 M HCl prior to attempting any separations.

The cation exchange resin used was Amberlite IRA-400. 10 g of the resin was dried, ground with a mortar and pestle, and sieved. The 100-140 mesh fraction was back washed to remove any fines which remained. 0.12 g was slurried and packed into a 9 cm X 2 mm column. Before injecting a sample containing Sb(III), the resin was pretreated by passing 1.0 M $HClO_4$ through the column for at least 10 minutes. After each elution with 2.0 M HCl, 1.0 M $HClO_4$ was passed through the column for a minimum of 10 minutes. Periodically the resin was stripped of all cations by passing 4.0 M HCl through the column for 10 minutes. According to Reference 197, the distribution coefficient of most metal ions in 4.0 M HCl is small.

b. Concentration Study. Aliquots of a 1.0×10^{-3} M Sb(III) stock solution in 2.0 M HCl, measured using a 2.000-ml Gilmont micrometer buret, were diluted to the mark in volumetric flasks with 1.0 M $HClO_4$. The concentration range of solutions prepared was 1.0×10^{-8} M to 1.0×10^{-4} M. Solutions could not be stored in 1.0 M $HClO_4$ for more than 24 hours because of hydrolysis to an

electrochemically inactive form or to precipitation as Sb_2O_3. The loss of Sb(III) in 24 hours was negligible.

c. Interference Study. An interference study, using a cation exchange column, was carried out with Fe(III), Bi(III), and Hg(II). These ions are also commonly found with Sb. Solutions containing 1.00×10^{-5} M Sb(III) and 1.0×10^{-4} M in the interfering ion were injected onto the catex column in 1.0 M $HClO_4$. After 1.0 min. the eluent was changed to 2.0 M HCl and then to 4.0 M HCl after an additional 2.5 min. I-t curves were recorded at 0.800 V using a Sargent Model SRG strip chart recorder and were integrated with the planimeter.

d. Analysis of Samples. After dissolution of the sample by one of the procedures described in Sections VII. B. 2. c.-g., an aliquot was diluted with 1.0 M $HClO_4$, if necessary, until the concentration was less than 5×10^{-5} M. The sample was injected onto the catex column, which had been pretreated as described in Section VII. B. 3. a. Sb(III) was eluted by changing the eluent to 2.0 M HCl 1.0 min. after injection. If a large amount of Fe(III) was present, the eluent was changed to 4.0 M HCl 3.5 min. after injection.

C. Results and Discussion

1. Investigation of Separation Schemes.

a. Anex Column. This separation scheme, which was described in Reference 187, used a mixture of $HClO_4$ and HCl to selectively elute Sb(III). Figure VII. 1 shows the I-t curve obtained at

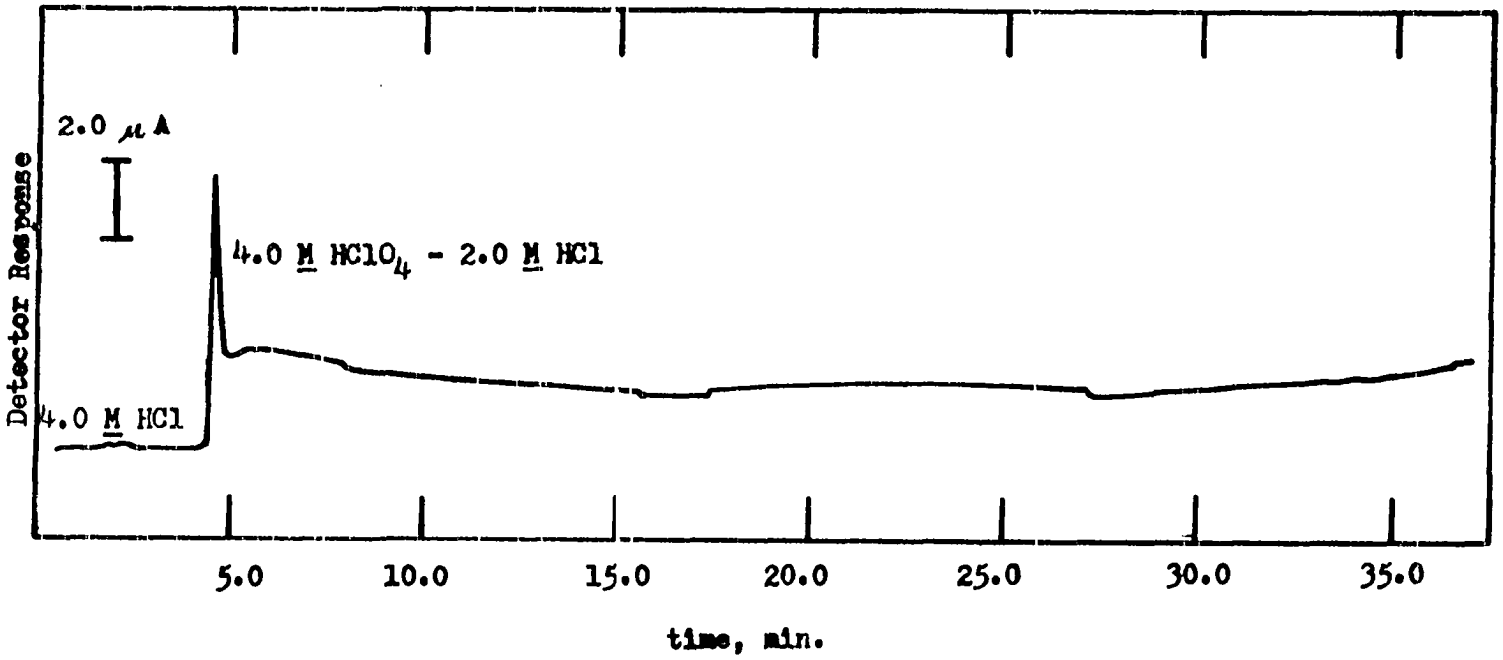

Figure VII. 1. I-t Curve for Sb(III) on an Anion Exchange Column Flow Rate of 4.0 M $HClO_4$ - 2.0 M HCl, 1.0 ml/min. 0.62 μg Sb(III). Electrode Potential 0.800 V. 100-140 Mesh Amberlite IRA-900. Column 8 cm x 2 mm.

0.800 V for the following separation. The anex resin, 100-140 mesh Amberlite IRA-900, was pretreated with 4.0 M HCl before injecting an Sb(III) sample into the stream of 4.0 M HCl. The eluent was changed to 4.0 M $HClO_4$-2.0 M HCl to elute the Sb(III), but even after 30 min., no chromatographic peak was observed for Sb(III). Direct injections of Sb(III) into 4.0 M $HClO_4$-2.0 M HCl gave peaks at the iodide covered electrode surface which were smaller than predicted for a 100% efficient electrode. No reason was able to be found to explain why Sb(III) could not be detected when an anex column was used.

b. Catex Column. This separation scheme was based on the different metal ion affinities for a strong acid catex resin in 2.0 M HCl solution. Sb(III) exists as SbO^+ in 1.0 M $HClO_4$ (184) and could be retained on 100-140 mesh Amberlite IRA-400 catex resin. In 2.0 M HCl, many metal ions have distribution coefficients above 4.0, while the Sb(III) distribution coefficient is 2.8. When Sb(III) was injected onto a catex column in 1.0 M $HClO_4$ and subsequently eluted with 2.0 M HCl at 0.5 ml/min., the Sb(III) peak was eluted 0.8 min. after the 2.0 M HCl entered the catex column as shown in Figure VII. 2. This separation scheme was very convenient because the eluent for Sb(III) was 2.0 M HCl, a strength very close to that used for preliminary investigations of the Sb(III) oxidation at the coulometric detector. Further investigation of this separation scheme using 1.0 M and 1.5 M HCl did not improve the separation so 2.0 M HCl was used for the remainder of the work described in this thesis.

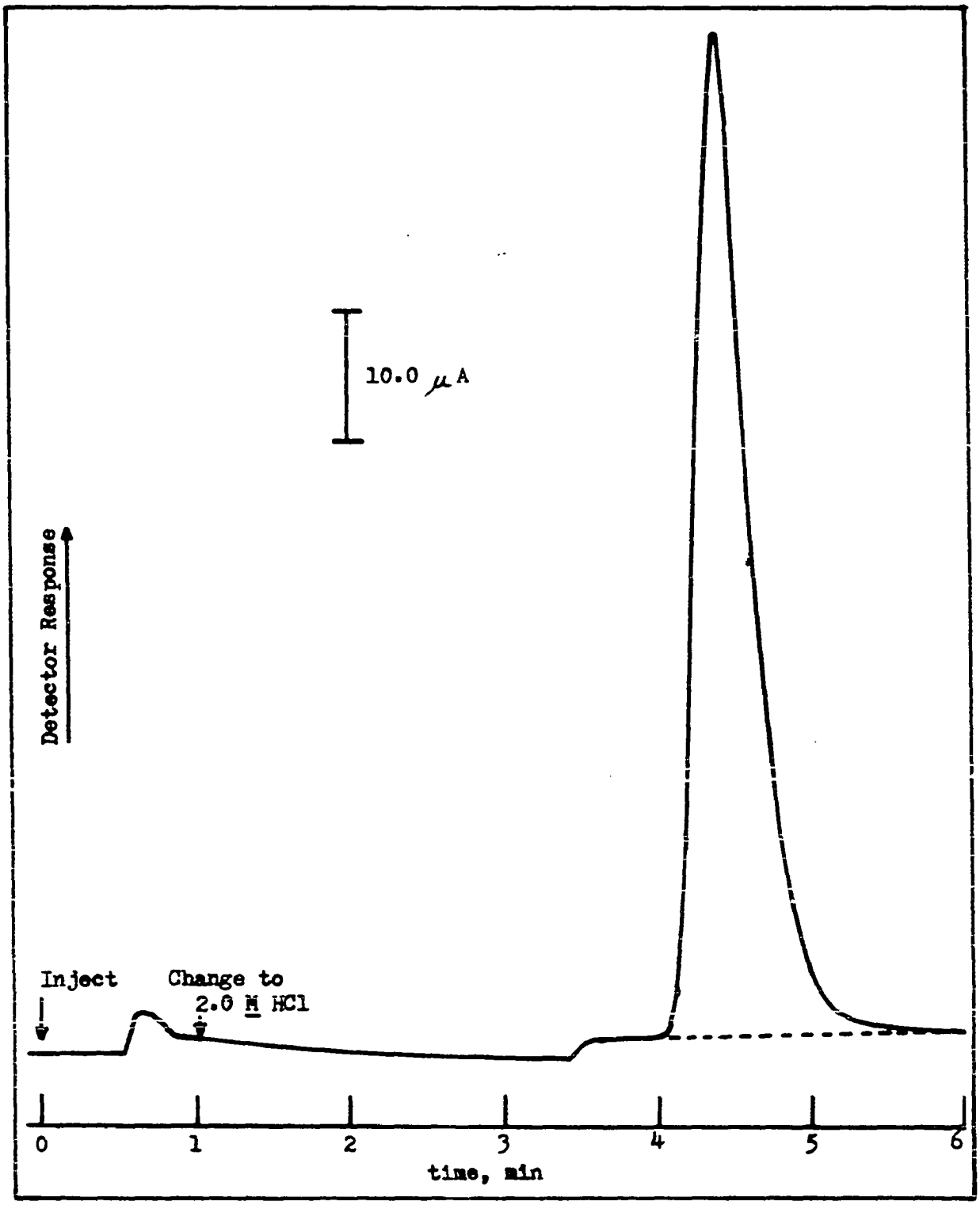

Figure VII. 2. I-t Curve for Sb(III) on a Cation Exchange Column Flow Rate of 2.0 M HCl and 1.0 M $HClO_4$, 0.5 ml/min. 0.618 μg Sb(III) in 1.0 M $HClO_4$. Electrode Potential 0.800 V. 100-140 Mesh Amberlite IRA-400. Column 8 cm x 2 mm. ---- Baseline for Integration.

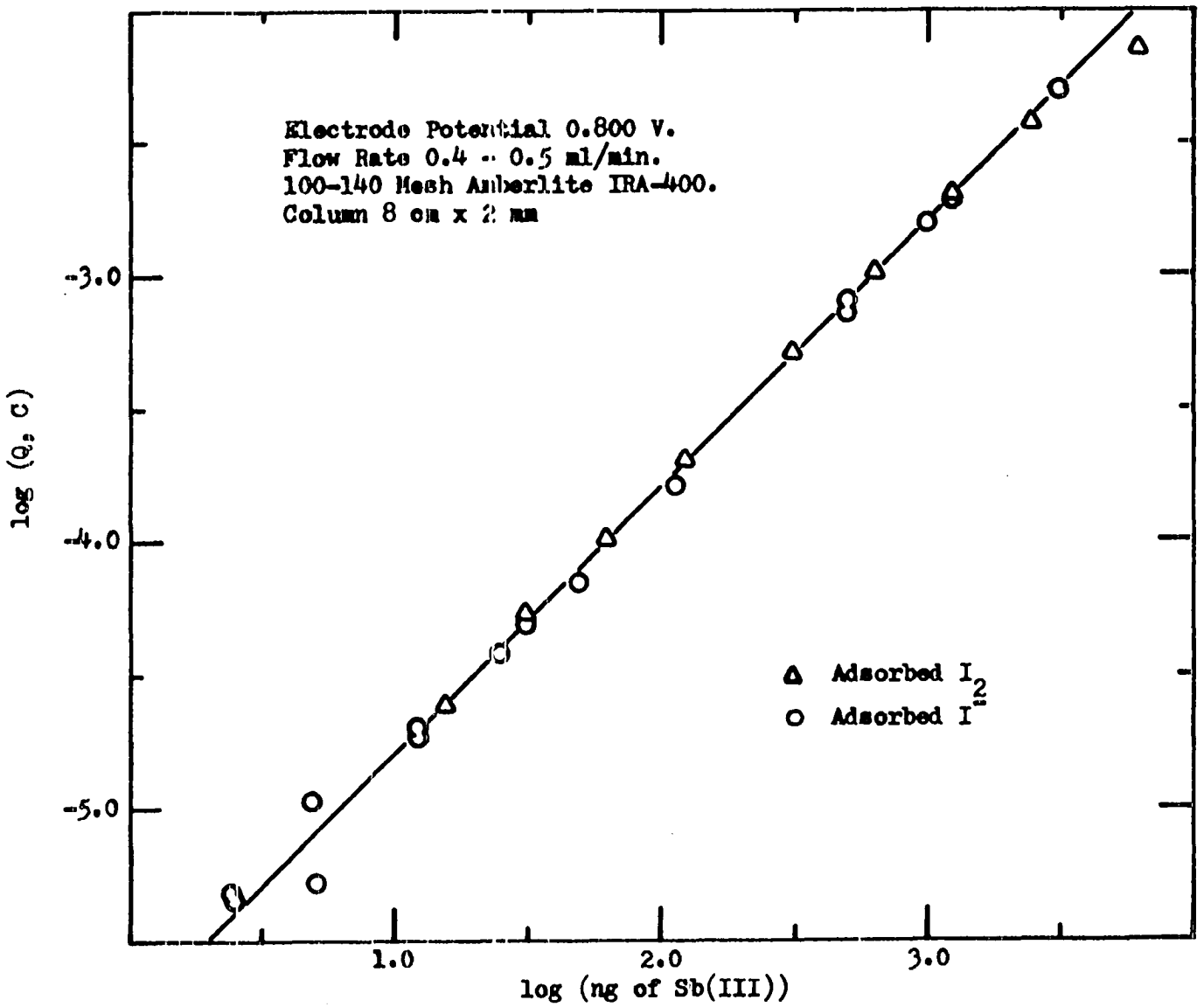

Figure VII. 3. Concentration Study for Sb(III) using a Chromatographic Separation Step

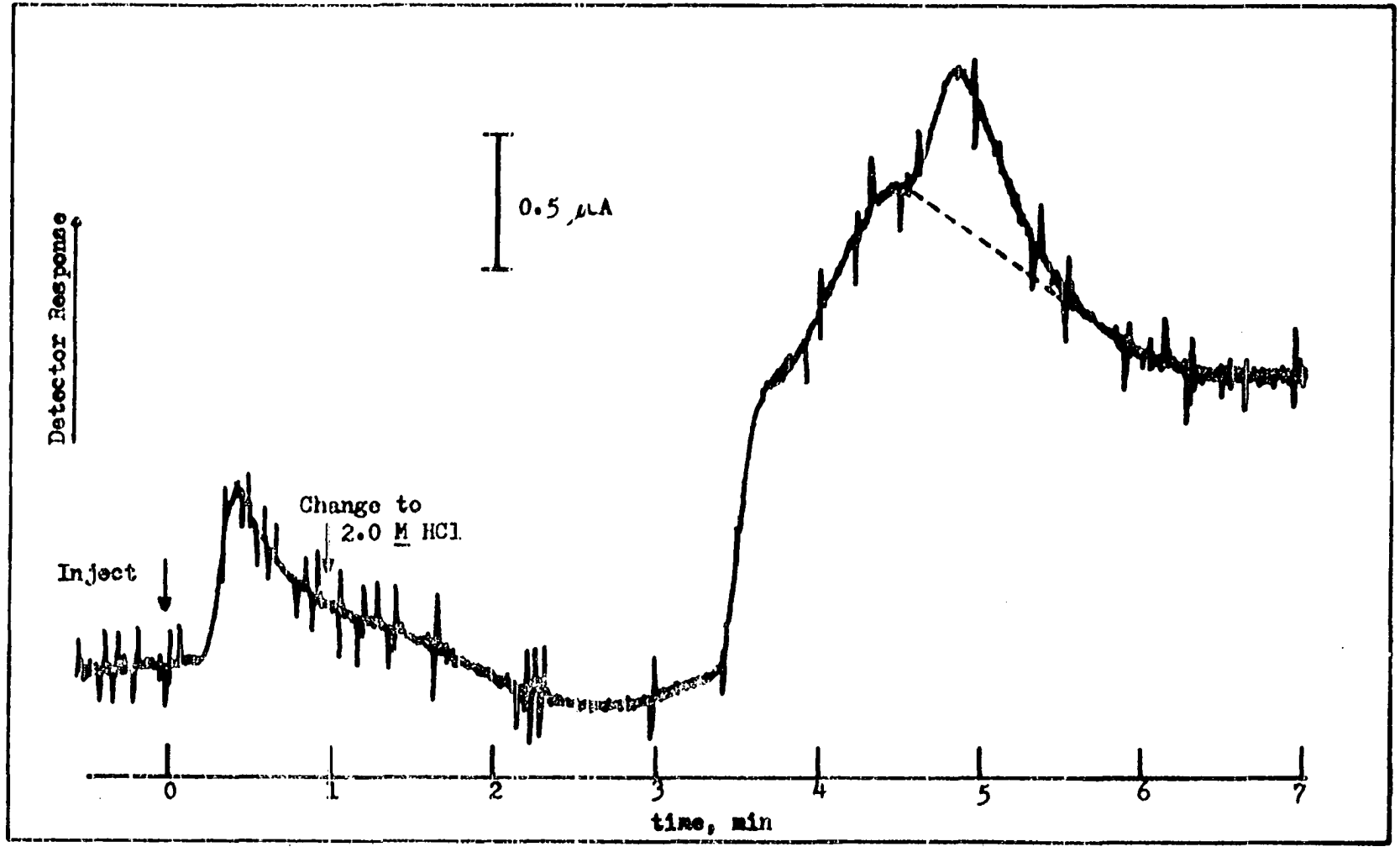

Figure VII. 4. Chromatographic Peak for 12.3 ng Sb(III) Flow Rate 0.5 ml/min. 12.3 ng Sb(III) in 1.0 M $HClO_4$. Electrode Potential 0.800 V. 100-140 Mesh Amberlite IRA-400. Column 8 cm x 2 mm. ---- Baseline for Integration.

2. Concentration Study.

The results of several concentration studies are shown in Figure VII. 3 in order to determine the linear working range. Agreement with the theoretical slope is again very good for amounts of Sb between 10.0 ng and 3.2×10^3 ng of Sb(III). At amounts of Sb(III) below 10 ng, the experimental error is large. The experimental uncertainty is caused by the large baseline change observed when changing eluents. The large baseline shift can be seen in the I-t curve for 12.3 ng of Sb(III) shown in Figure VII. 4. The deviation from 100% electrolysis at high Sb(III) concentrations may be due to either the slow heterogeneous kinetics of the Sb(III) oxidation or to an IR loss in the detector because of the high peak currents. The peak current for 1.00×10^{-4} M Sb(III) was 268 μA which resulted in an IR loss of 0.23 V. The IR loss caused part of the electrode to be at a less positive potential, at which the oxidation of Sb(III) was not 100% efficient (see Figure VI. 1).

The decreased electrode efficiency at high Sb(III) concentrations was not observed when the column was not used. At the same flow rate and Sb(III) concentration, the peak current for the I-t curve obtained using a catex column was 2.5 times higher than without a column. Consequently, the IR loss in the detector was significantly lower when the column was not used.

Another interesting feature shown in Figure VII. 3 is that either adsorbed I^- or I_2 electrocatalyze the oxidation of Sb(III).

The experimental points designated by triangles in Figure VII. 3 were obtained with adsorbed I_2. According to Reference 97, irreversibly adsorbed I^- and I_2 are distinguishable on platinum surfaces. The procedure for adsorbing I_2 was similar to the procedure described in Section VI. B. 4 a for I^-, except that the potential was held at 0.700 V when the I_2 saturated solution in 1.0 M was passed through the detector to prevent direct reduction of I_2.

3. Interference Study.

In Section VI. B. 5, the major interferences were found to be Fe(III), Bi(III), Hg(II), Ti(III), and Ce(IV). Ti and Ce do not occur frequently with Sb, so only the separation from Fe(III), Bi(III), and Hg(II) was performed using a catex column. The separation procedure described in Section VI. B. 4. f was used to determine where the Fe(III), Bi(III), and Hg(II) peaks were eluted. The electrode potential was set at 0.0 V to reduce Fe(III) and Hg(II) and at -0.200 V to reduce Bi(III). The I-t curves observed are shown in Figure VII. 5. The peak for Sb(III) is shown by the dotted line. Fe(III) and Hg(II) did not interfere under the separation conditions employed, and the Bi(III) peak tailed slightly into the Sb(III) peak causing only slight interference when the Bi(III) concentration was 10 times greater than the Sb(III) concentration.

If a better separation is desired, the column length may be increased, the flow rate may be decreased, or the resin mesh size

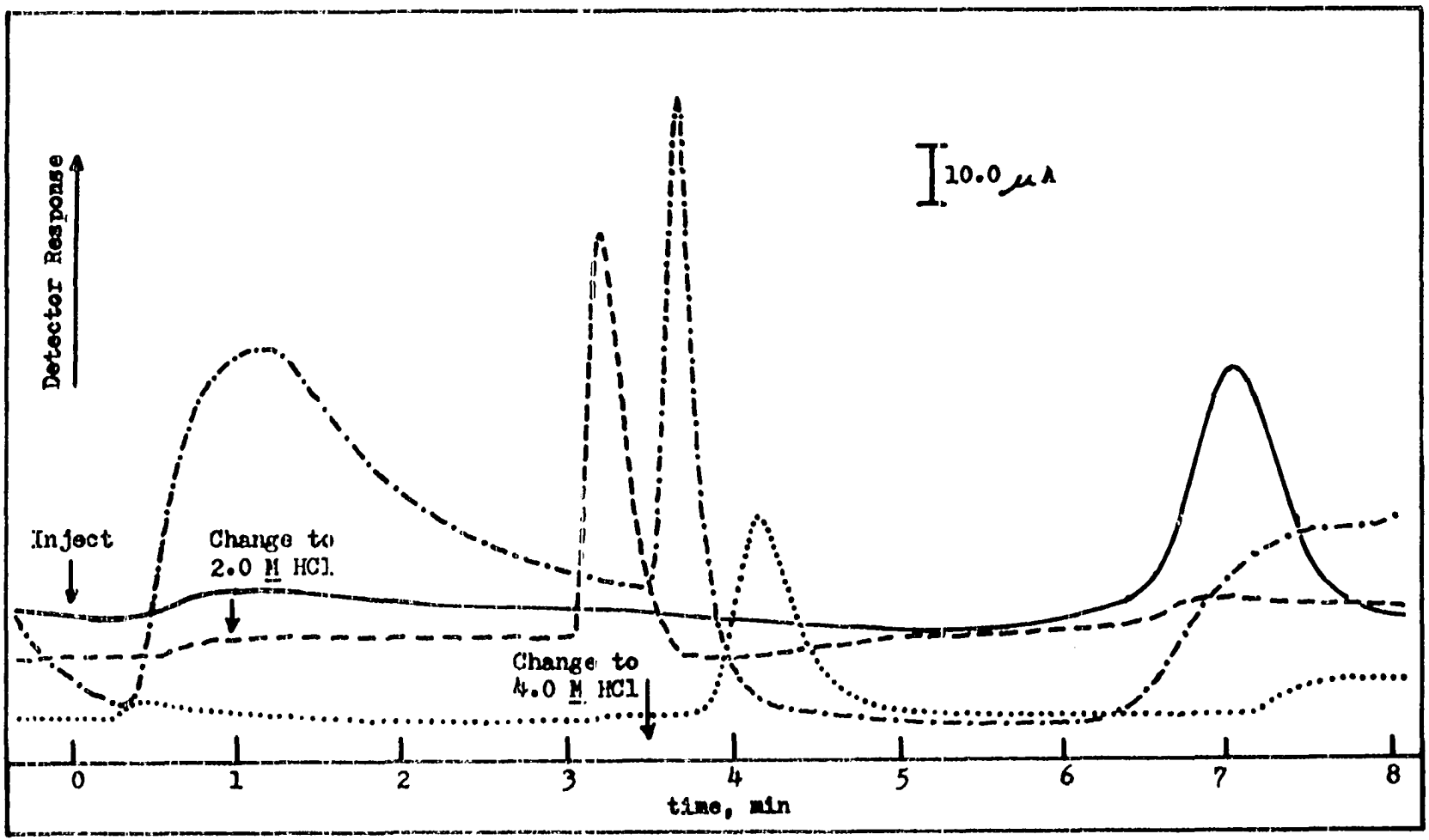

Figure VII. 5. Chromatographic Peaks for Fe(III), Bi(III), Hg(II), and Sb(III) Flow Rate .45 ml/min. ···· 1.24 μg Sb(III), 0.80 V. —— 2.84 μg Fe(III), 0.0 V. – – – 10.1 μg Hg(II), 0.0 V. -·-·- 10.6 μg Bi(III), -0.20 V. 100-140 Mesh Amberlite IRA-400. Column 8 cm x 2 mm.

increased. The separation shown in Figure VII. 5 was adequate for all experimental work described in this thesis.

4. Analysis of Samples.

One of the objectives of this thesis was to demonstrate the applicability of the coulometric detector to the determination of Sb in a variety of matrices. The results of the determinations using the procedures described in Sections VII. B. 2 and VI. B. 3. a are reported in Table VII. 1. Results of the analyses were very good. The accuracy was better than 1.0 pph in most cases and the precision was less than 2 pph.

Analyses of hair and a transistor were performed to demonstrate the usefulness of this technique for low Sb levels. The samples of hair were chosen from people having various degrees of exposure to the laboratory where all experiments were performed. The hair samples came from Larry Taylor (LRT), John LaRochelle (JHL), Marcia Taylor (MST), and Lynne LaRochelle (LKL). This was also the order of exposure to laboratory conditions. A direct correlation was found between time spent in the laboratory and the amount of antimony in the hair as shown in Table VII. 2.

The power transistor was found to have 340 ppm antimony. No reference was found which gave the amounts of antimony in different kinds of transistors.

5. Deterioration of Polyethylene Eluent Tanks.

The eluent tanks used with the high-speed liquid chromato-

TABLE VII. 1

Analysis of Alloys Containing Antimony

Eluent Flow Rate = 0.4 ml/min.

E_{app} = 0.800 V

Sample size = 0.5065 ml

Sample	% Sb	No. of Detns.	% Sb Found	Relative Precision (pph)	Relative Error (pph)
NBS-124b	0.20	1	0.20	----	0.0
NBS-124b	0.20	3	0.20	1.8	0.0
ISU-1	4.00	3	3.98	1.25	-0.55
ISU-1	4.00	5	3.95	1.6	-1.25
ISU-2	4.00	3	3.99	1.5	-0.25
ISU-3	4.00	3	3.98	1.25	-0.50
TP-100C	4.02	5	4.01	0.73	-0.25
NBS-53	10.09	4	10.09	2.1	0.0
NBS-53	10.09	4	10.2	0.57	+1.1

TABLE VII. 2

Analysis of Hair for Antimony

Eluent Flow Rate = 0.5 ml/minute

E_{app} = 0.800 V

Sample size = 2.017 ml

Hair Samples, Age	No. of Detns.	Sb Found (ppm)
LRT, 25	5	1.3 ± 0.3
JHL, 25	1	0.85
MST, 22	2	0.56 ± 0.08
LKL, 3	1	0.0

graphy are described in Section III. C. 1. After one and one half years of continuous usage in acid solutions, the bottles began to deteriorate. The first indication of trouble came when high results for the analysis of several different alloys were found. The results were consistently 20 pph high. The error could not be accounted for by interference from other components because injections of Sb(III) alone gave high results as well. The source of the error was traced to the polyethylene bottles when correct results were obtained after changing to fresh eluent solution. However, after about one week of usage, the fresh eluent solution also became contaminated.

A more direct proof that the high results were caused by deterioration of the polyethylene was obtained while determining the adsorption isotherm in Section IV. C. 2. b. 12 M HCl was passed through the packed tubular detector, which was potentiostated at 0.65 V, from a plastic syringe. The eluent was changed to 1.0 M H_2SO_4 and the potential stepped to 1.30 V. The I-t curves obtained are shown in Figure VII. 6. I-t curves b, c, and d were obtained at 3 hour intervals while storing the 12 M HCl in the plastic syringe. The longer the time the 12 M HCl was stored, the greater the area under the I-t curve became. No change with time was observed in I-t curve a, which was obtained using a glass syringe to store 12 M HCl. These results indicate that some species, which is oxidizable at potentials > 0.80 V, is leached into the acid solutions from the polyethylene bottles.

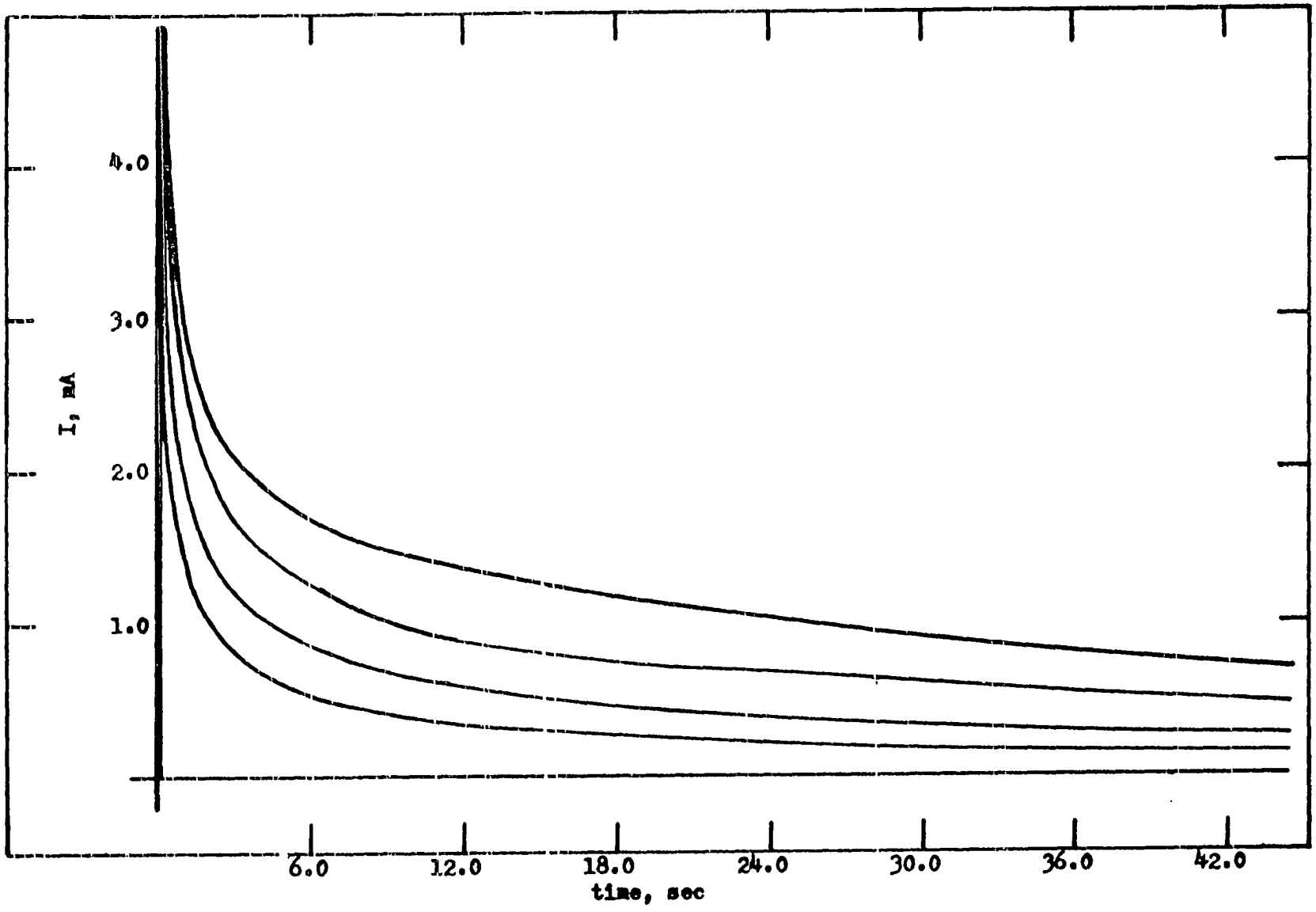

Figure VII. 6. I-t Curves Obtained After Potential Step
Potential Stepped from 0.565 V to 1.3 V. 1.0 M H_2SO_4. Flow Rate 3 ml/min.

VIII. SUMMARY

The results are given for an amperometric method for the determination of Sb(III) at an RPDE in acidic media based on the catalytic increase of the anodic current for Br^-. The method was successful provided $C^b_{Sb(III)} < C^b_{Br^-}$. Species which form slightly dissociated complexes with Br^- give a negative interference. Coulometric determinations of antimony in lead and tin-based alloys are described using the electrogeneration of Br_2 at constant current in 4.0 M H_2SO_4. No separation was required in the coulometric method.

The wave for electro-oxidation of Sb(III) at platinum electrodes was found to be electrocatalyzed by iodide adsorbed at the electrode in dilute HCl solutions. A study of the rate of the heterogeneous reaction of the Sb(III)/Sb(V) system in 12 M HCl is described. 12 M HCl was used to prevent hydrolysis of the $SbCl_6^-$. The heterogeneous kinetic parameters were determined from the slopes of I-E curves, at $\eta = 0$, as a function of the rotational velocity of the platinum disk electrode.

A packed tubular platinum electrode was evaluated as an electrochemical detector for forced-flow liquid chromatography using the catalytic increase in the bromide oxidation current and the electrocatalyzed oxidation of Sb(III) by adsorbed halides. The detector used was found to be 100% efficient at flow rates up to 4.1 ml/min. A linear working range was found over a 100 fold range of Sb(III) concentrations for the catalytic enhancement

procedures and over a 200 fold range of Sb(III) concentrations for the electrocatalysis procedure. Very few interferences were found for the electrocatalyzed oxidation of Sb(III).

Those interferences which were found were eliminated using chromatographic separations using a cation exchange resin. The linear working range found for the determination of Sb(III) using the separation step was 2.5 ng to 6.2 mg.

The coulometric detector was used with forced-flow chromatography for the determination of antimony in lead, tin and copper-based alloys, hair samples, and in a power transistor. The antimony content was calculated directly from values of peak areas on the current-time curve without using a calibration curve.

IX. SUGGESTIONS FOR FUTURE WORK

To use the independence of flow rate observed with the coulometric detector to its full advantage, the baseline changes observed must be eliminated. Baseline changes are caused by varying amounts of trace impurities in the different eluents. To eliminate these impurities the eluents could be passed through a packed tubular electrode, located before the sample injection valve, which is potentiostated at the same potential as the coulometric detector. This would specifically eliminate those impurities electrolyzed at the coulometric detector.

The elimination of baselines is necessary to extend detection limits, to enable one to electronically integrate peak areas, and to improve the precision and accuracy of the coulometric detector.

The mechanism of electrocatalysis by adsorbed ions needs to be studied in more detail. One of the key steps to determining the mechanism is to find out whether the electrocatalysis proceeds through an intermediate in which the adsorbed iodide is incorporated into the coordination sphere of the reacting ions. The replacement of the chloride ions in the Sb(III) coordination sphere by less labile ligands would slow down or eliminate the heterogeneous reaction. Another interesting investigation would be to determine the number of Sb(III) ions oxidized per ion or atom of adsorbed iodide or iodine.

Other irreversible electrode reactions which may be electro-

catalyzed by adsorbed halides are As(III), Ti(III), Ce(III), and V(V). In the case of As(III), a large amount of chloride or bromide may be necessary to convert the As(III) to a species containing labile ligands such as Cl^- or Br^-.

Since the electrogeneration of bromine proceeds very rapidly at platinum electrodes, organic species could be determined by their reaction with the electrogenerated bromine. The bromine could be generated at a constant current and monitored downstream from the generator electrode with a second coulometric electrode. After an organic species has reacted with bromine, the second electrode will detect the organic species by the decrease in the amount of bromine reaching the detector.

X. BIBLIOGRAPHY

1. J. Adam, J. Dolezal, and J. Zyka, Zh. Anal. Khim., 16, 395 (1961).

2. H. P. Agarwal, J. Electrochem. Soc., 110, 237 (1963).

3. S. B. Akki and S. M. Khopkar, Z. Anal. Chem., 255, 130 (1971).

4. T. Andersen and A. B. Knutsen, Acta Chem. Scand., 16, 849 (1962).

5. F. C. Anson, Anal. Chem., 33, 939 (1961).

6. F. C. Anson, J. Electrochem. Soc., 110, 436 (1963).

7. V. B. Avilov, Tr. Komissii Anal. Khim., Akad. Nauk SSSR, Inst. Geokhim. i Anal. Khim., 11, 44 (1960).

8. V. B. Avilov, Tr. Ural'sk Elektromakhan. Inst. Inzh. Zhelezno--Dorozhn Transp., No. 2, 74 (1959).

9. R. L. Bamberger and J. H. Strohl, Anal. Chem., 41, 1450 (1969).

10. D. J. Barclay, J. Electroanal. Chem. Interfacial Electrochem., 28, 445 (1970).

11. A. M. Baticle and F. Perdu, J. Electroanal. Chem., 12, 15 (1966).

12. D. Bauer, Bull. Soc. Chim. Fr., 3, 944 (1967).

13. F. Baumgartner, H. Stark, A. Shontag, Z. Anal. Chem., 197, 424 (1963).

14. V. Bayerle, Rec. Trav. Chim., 44, 514 (1925).

15. P. Beran, J. Cihalik, J. Dolezal, V. Simon, and J. Zyka, Chem. Listy, 47, 1315 (1953).

16. H. W. Bertran, M. W. Lerner, G. J. Petretic, E. S. Roszkowski, and C. J. Rodden, Anal. Chem., 30, 354 (1958).

17. W. J. Blaedel and S. L. Boyer, Anal. Chem., 43, 1538 (1971).

18. W. J. Blaedel and H. T. Knight, Anal. Chem., 26, 741 (1954).

19. W. J. Blaedel and J. H. Strohl, Anal. Chem., 33, 1631 (1961).

20. W. J. Blaedel and J. H. Strohl, Anal. Chem., 36, 445 (1964).

21. W. J. Blaedel and J. H. Strohl, Anal. Chem., 36, 1245 (1964).

22. W. J. Blaedel and J. W. Todd, Anal. Chem., 30, 1821 (1958).

23. W. Blaedel and J. W. Todd, Anal. Chem., 33, 205 (1961).

24. R. Bock and K. G. Hackstein, Z. Anal. Chem., 138, 339 (1953).

25. B. Breyer, H. H. Bauer, and Hacobian, Aust. J. Chem., 8, 322 (1955).

26. B. Breyer, F. Gutmann, and S. Hacobian, Aust. J. Sci. Research, A3, 567 (1950).

27. B. Breyer, F. Gutmann, and S. Hacobian, Aust. J. Sci. Research, A4, 595 (1951).

28. R. A. Brown and E. H. Swift, J. Amer. Chem. Soc., 71, 2717 (1949).

29. S. Bruckenstein and B. Miller, J. Electrochem. Soc., 117, 1040 (1970).

30. R. Cernatescu, M. Poni, R. Ralea, and I. Popescu, Acad. rep. populare Romine Filiala Iasi, Studii cercetari stiint. Ser. 1, 6, No. 3/4, 89 (1955).

31. J. H. Christie, G. Lauer, and R. A. Osteryoung, J. Electroanal. Chem., 7, 60 (1964).

32. S. P. Chuan, J. Dolezal, and J. Zyka, Collection Czech. Chem. Commun., 30, 1785 (1965).

33. G. B. Clark and G. V. Akimov, Compt. Rend. Acad. Sci., URSS, 30, 805 (1941).

34. A. F. Clifford, "Inorganic Chemistry of Qualitative Analysis," Prentice-Hall, Englewood Cliffs, New Jersey, 1961, p. 86.

35. G. Conradi and M. Kopanica, Collection Czech. Chem. Commun., 28, 1600 (1963).

36. W. D. Cooper and R. Parsons, Trans. Faraday Soc., 66, 1698 (1970).

37. D. Cozzi and S. Vivarelli, Anal. Chim. Acta, 4, 300 (1950).

38. B. D. Damaskin, O. A. Petrii, and V. V. Batrakov, "Adsorption of Organic Compounds on Electrodes," Plenum Press, New York, 1971.

39. L. Danielsson, Acta Chem. Scand., 19, 1859 (1965).

40. R. J. Davenport and D. C. Johnson, Unpublished Data.

41. H. M. Davis and R. C. Rooney, J. Polarog. Soc., 8, 25 (1962).

42. J. J. Dawson, J. Wilkinson, and M. J. Gillibrand, J. Inorg. Nucl. Chem., 32, 501 (1970).

43. A. K. De and T. Chakrabartz, Indian J. Chem., 7, 180 (1969).

44. P. Delahay and D. J. Kelsh, J. Electroanal. Chem. Interfacial Electrochem., 18, 194 (1968).

45. R. J. deLevie, J. Electrochem. Soc., 118, 185C (1971).

46. M. A. Desesa, D. N. Hume, A. C. Glamm, Jr., and D. D. DeFord, Anal. Chem., 25, 983 (1953).

47. H. Diehl, "Quantitative Analysis," Oakland Street Science Press, Ames, Iowa, 1970, pp. 315-16.

48. L. O. Dolaberidze, D. K. Kamkamidze, and V. K. Bugianishvili, Sbornik Nauch.--Tekh. Inform., Ministerstvo Geol. i Okhranz Nedr., No. 1, 128 (1955).

49. J. Dolezal and K. Janacek, Collect. Czech. Chem. Commun., 25, 885 (1960).

50. T. S. Dolzhenko and I. D. Zhdanovich, Zavodskaya Lab., 18, 46 (1952).

51. T. Dono, K. Morinaga, and T. Nomura, Bull. Nagoya Inst. Technol., 6, 156 (1954).

52. T. Dono, K. Morinaga, and T. Nomura, Bull. Nagoya Inst. Technol., 7, 165 (1955).

53. T. Dono, G. Nakagawa, and T. Nomura, Nippon Kagaku Zasshi, 83, 1249 (1962).

54. B. Drake, Acta Chem. Scand., 4, 554 (1950).

55. L. B. Dunlap and W. D. Shults, Anal. Chem., 34, 499 (1962).

56. E. L. Eckfeldt and E. W. Shaffer, Anal. Chem., 36, 2008 (1964).

57. R. A. Eroshina, G. K. Promina, T. V. Legalova, and T. M. Shebasheva, (USSR), Nauch. Tr., Leningrad. Lesotekh. Akad., No. 100, 325 (1967).

58. O. Esin, Zh. Prikl. Khim., 17, 114 (1944).

59. F. F. Faizullin and B. S. Mironov, Uch. Zap., Kazansk. Gos. Univ., 124, 53 (1964).

60. J. P. Faris, Anal. Chem., 32, 520 (1962).

61. B. Forss, Acta Acad. Aboenis, Math et Phys., 17, No. 3, 1 (1951).

62. A. N. Frumkin, O. A. Petrii, and Yu. G. Kotlov, Elektrokhimiya, 5, 1214 (1969).

63. A. Frumkin and G. Tedoradse, Z. Elektrochem., 62, 251 (1958).

64. T. Fujinaga, Pure and Applied Chem., 25, 709 (1971).

65. T. Fujinaga, S. Vugai, T. Okazaki, and C. Takagi, Chem. Soc. Jap., 84, 941 (1963).

66. H. Gerischer, Z. Elektrochem., 54, 366 (1950).

67. R. Geyer and M. Geissler, Z. Anal. Chem., 187, 251 (1962).

68. R. Geyer and M. Geissler, Z. Anal. Chem., 201, 1 (1964).

69. L. Gierst and W. Dubru, Bull. Soc. Chim. Belges, 68, 379 (1954).

70. E. Gileadi and B. E. Conway, "Modern Aspects of Electrochemistry," Vol. 3, J. O'M. Bockris and B. E. Conway, eds., Butterworth's, London, 1964.

71. V. P. Gladyshev and A. Dzhumashev, Zh. Anal. Khim., 25, 189 (1970).

72. Ya. P. Gokhstein, Zh. Fiz. Khim., 33, 1053 (1959).

73. Ya. P. Gokhstein, Zh. Fiz. Khim., 34, 1138 (1960).

74. B. E. Gordon and R. M. Tanklevskaya, Teoriya i Prakt. Polyarogh. Analiza, Akad. Nauk Moldavsk. SSR, Materialy Pervogo Vses. Soveshch, 58 (1962).

75. Yu. S. Gorodetskii, Elektrokhimiya, 2, 122 (1966).

76. G. Grube and F. Schweigardt, Z. Elektrochem., 29, 257 (1923).

77. D. Haberland and R. Landsberg, Z. Elektrochem., 70, 724 (1966).

78. K. Hagiwara, Y. Higuchi, and I. Muraki, Osaka Koggo Gijutsu Shikensho Kiho, 16, 184 (1965).

79. K. Hagiwara, Y. Higuchi, and I. Muraki, Nippon Kagaku Zasshi, 86, 205 (1965).

80. G. P. Haight, Jr., Anal. Chem., 26, 593 (1954).

81. G. P. Haight, Jr., J. Amer. Chem. Soc., 75, 3848 (1953).

82. H. Hamaguchi, N. Onuma, Y. Hirao, H. Yokoyama, S. Bando, and M. Furukawa, Geochim. Cosmochim. Acta, 33, 507 (1969).

83. A. G. Hamza and J. B. Headridge, Talanta, 13, 1397 (1966).

84. H. Hirata and T. Amemiya, Natl. Tech. Rept., 9, 319 (1963).

85. H. Hirata and T. Amemiya, Nippon Kagaku Zasshi, 85, 26 (1964).

86. M. Honda, Y. Sasaki, and H. Natsume, Japan Analyst, 4, 240 (1955).

87. H. F. Hourigan and J. W. Robinson, Anal. Chim. Acta, 10, 281 (1954).

88. A. T. Hubbard, J. Electroanal. Chem. Interfacial Electrochem., 22, 165 (1969).

89. A. T. Hubbard, R. A. Osteryoung, and F. C. Anson, Anal. Chem., 38, 692 (1966).

90. H. D. Hurwitz, J. Chem. Phys., 48, 1541 (1968).

91. M. Ishibashi, T. Fujinaga, and M. Matsuoka, J. Chem. Soc. Japan, Pure Chem. Sect., 74, 750 (1953).

92. M. Ishidate, T. Isshiki, Y. Mashiko, and N. Hosoya, Pharm. Bull. (Japan), 2, 259 (1954).

93. E. Jacobsen and T. Rojahn, Anal. Chem. Acta, 54, 261 (1971).

94. D. Jahn and W. Vielstich, J. Electrochem. Soc., 109, 849 (1962).

95. V. G. Jander and H.-J. Hartmann, Z. Anorg. Allg. Chem., 339, 239 (1965).

96. V. G. Jander and H.-J. Hartmann, Z. Anorg. Allg. Chem., 339, 256 (1965).

97. D. C. Johnson, Application of the Rotating Ring-Disc Electrode to the Study of Heterogeneous and Homogeneous Reactions, Unpublished Ph. D. Thesis, Minneapolis, Minnesota, Library, University of Minnesota, 1967.

98. D. C. Johnson, J. Electrochem. Soc., 119, 331 (1972).

99. D. C. Johnson and S. Bruckenstein, J. Electrochem. Soc., 117, 460 (1970).

100. D. C. Johnson, D. T. Napp, and S. Bruckenstein, Anal. Chem., 39, 481 (1967).

101. K. Jonas, Vezpremi Vegryipari Egyeteru Kozlemonyei, 2, 161 (1958).

102. J. Jordan, Anal. Chem., 27, 1708 (1955).

103. J. Jordan and R. A. Javick, Electrochim. Acta, 6, 23 (1962).

104. P. L. Joynes and R. J. Maggs, J. Chromatog. Sci., 8, 427, (1970).

105. Yu. M. Kargin, Teoriya i Praktika Polyarograf. Aniliza, Akad. Nauk Moldavsk. SSR, Materialy Pervogo Vses. Soveshch., 243 (1962).

106. K. Kawabuchi, H. Hamaguchi, and R. Kuroda, J. Chromatog., 17, 567 (1965).

107. H. Kazuyochi, Y. Higuchi, and I. Muraki, Nippon Kagaku Zasshi, 86, 705 (1965).

108. W. Kemula, Roczniki Chem., 26, 281 (1952).

109. W. Kemula, J. Anal. Chem., U.S.S.R., 22, 562 (1967).

110. W. Kemula, K. Bulkiewicz, and D. Sybilska, "Modern Aspects of Polarography," Plenum Press, New York, (1966), p. 36.

111. W. Kemula and Z. Kublik, Rocz. Chem., 30, 1259 (1956).

112. W. Kemula and Z. Stachurski, Rocz. Chem., 30, 1285 (1956).

113. W. Kemula and J. Witwicki, Rocz. Chem., 29, 115 (1955).

114. S. S. M. A. Khorasani and M. H. Khundkar, Anal. Chim. Acta, 25, 292 (1961).

115. W. Kiesl, Z. Anal. Chem., 227, 13 (1967).

116. L. Kiss and M. L. Varsanzi, Magy. Kem. Foly., 76, 125 (1970).

117. J. G. Koen, J. F. K. Huber, H. Poppe, and G. den Boef, J. Chromatog. Sci., 8, 192 (1970).

118. I. M. Kolthoff and C. Auerbach, J. Amer. Chem. Soc., 74, 1452 (1952).

119. I. M. Kolthoff and R. L. Probst, Anal. Chem., 21, 753 (1949).

120. A. J. Kostromin and A. A. Akhmentov, Zh. Anal. Khim., 24, 503 (1969).

121. K. A. Kraus and F. Nelson, Proceedings of the First United Nations International Conference on the Peaceful Uses of Atomic Energy, 7, 113 (1956).

122. R. Kuroda, K. Ishida, and T. Kirigama, Anal. Chem., 40, 1502 (1968).

123. M. M. Kurtepov and A. S. Fedoseeva, Doklady Akad. Nauk, SSR, 75, 563 (1950).

124. N. A. Lektorskaya and P. N. Kovalenko, Nauch. Doklady Vysshei Shkoly, Khim. i Khim. Tekhnol., 102, No. 1 (1959).

125. V. G. Levich, "Physicochemical Hydrodynamics," Prentice-Hall, Englewood Cliffs, New Jersey (1962).

126. Kh. Ya. Levitman and Z. A. Kryuchzk, Vestsi Akad. Navuk. Belarus. SSR, Ser. Fiz.--Tekh Navuk, 43, No. 2 (1958).

127. J. A. Lewis and K. C. Overton, Analyst, 79, 293 (1954).

128. J. J. Lingane, "Electroanalytical Chemistry," Interscience, New York, (1958), p. 263.

129. J. J. Lingane and C. Auerbach, Anal. Chem., 23, 986 (1951).

130. J. J. Lingane and A. J. Bard, J. Electrochem. Soc., 117, 1517 (1970).

131. J. Llopis and M. Vazquez, Electrochimica Acta, 6, 177 (1962).

132. V. V. Lov'ev, A. I. Molodov, and V. V. Gorodetski, Electrochim. Acta, 12, 475 (1967).

133. Yu. Yu. Lur'e and N. A. Filippova, Zavodskaya Lab., 14, 159 (1948).

134. Yu. S. Lyalikov, L. P. Chernaga, and V. I. Bodyn, Tr. Kishinev Politekh. Inst., No. 13, 167 (1968).

135. S. G. Mairanovskii, "Catalytic and Kinetic Waves in Polarography," Plenum Press, New York, 1968.

136. R. D. Malinina, Sb. Tr. Tsentr. Nauchn.--Issled. Inst. Chernoi Met., 31, Pt. 1, 158 (1963).

137. R. Malvano, P. Grosso, and M. Zanardi, Anal. Chim. Acta, 41, 251 (1968).

138. C. K. Mann, Anal. Chem., 29, 1385 (1957).

139. P. H. Martens and P. Nangniot, Bull. inst. agron. et stas. reserches Gembloux, 24, 285 (1956).

140. H. Matsudo and P. Delahay, Collect. Czech. Chem. Commun., 25, 2973 (1960).

141. L. Meites, "Polarographic Techniques," Interscience, New York, 1955.

142. S. N. Mladenovic, Glas. Hem. Drus. Beograd, 30, 239 (1965).

143. M. Mohnke, R. Schmunk, and H. Z. Schutze, Z. Anal. Chem., 219, 137 (1966).

144. J. Molnar, Magy. Kem. Foly., 68, 504 (1962).

145. A. G. C. Morris, Analyst, 87, 478 (1962).

146. O. H. Muller, J. Amer. Chem. Soc., 69, 2992 (1947).

147. G. Nagy, Z. S. Feher, and E. Pungor, Anal. Chim. Acta, 52, 47 (1970).

148. D. T. Napp, D. C. Johnson, and S. Bruckenstein, Anal. Chem., 39, 481 (1967).

149. F. Nelson, T. Murase, and K. A. Kraus, J. Chromatog., 13, 503 (1964).

150. F. Nelson, R. M. Rush, and K. A. Kraus, J. Amer. Chem. Soc., 82, 339 (1960).

151. H. M. Neumann, J. Amer. Chem. Soc., 76, 2611 (1954).

152. J. D. Newson and A. C. Riddiford, J. Electrochem. Soc., 108, 699 (1961).

153. R. A. Osteryoung and F. C. Anson, Anal. Chem., 36, 975 (1964).

154. G. Packman and G. F. Reynolds, Analyst, 81, 49 (1956).

155. J. E. Page and F. A. Robinson, J. Chem. Soc. Ind., 61, 93 (1942).

156. F. Pantani and P. Desideri, Gazz. Chim. Ital., 89, 1360 (1959).

157. W. J. Parker, Metal Industry, 2, 82 (1962).

158. R. Parsons, Trans. Faraday Soc., 51, 5158 (1955).

159. R. Parsons, Trans. Faraday Soc., 55, 999 (1959).

160. D. Pavlov and D. Lazarov, Doklady Akad. Nauk SSSR, 118, 103 (1958).

161. J. V. Petrocelli and A. A. Paolucci, J. Electrochem. Soc., 98, 291 (1951).

162. M. A. Portnov and V. P. Povelkina, Zhur. Anal. Khim., 3, 85 (1948).

163. K. B. Prater and A. J. Bard, J. Electrochem. Soc., 117, 1517 (1970).

164. R. Pribil, Z. Ronbal, and E. Svatek, J. Chem. Listy, 46, 396 (1952).

165. M. M. Privalova and D. I. Ryabchikov, Zh. Neorg. Khim., 7, 2537 (1962).

166. E. Pungor, Zs. Feher, and G. Nagy, Anal. Chim. Acta, 51, 417 (1970).

167. I. V. Pyatnitskii and A. Kh. Klibas, Ukr. Khim. Zh., 33, 1077 (1967).

168. J. E. B. Randles and K. W. Somerton, Trans. Faraday Soc., 48, 937 (1952).

169. A. V. Rangnekar and S. M. Khopkar, Fresenius' Z. Anal. Chem., 232, 432 (1967).

170. R. L. Rebertus, R. J. Cappell, and G. W. Bond, Anal. Chem., 30, 1825 (1958).

171. G. A. Rechnitz, "Controlled Potential Analysis," R. Belcher and L. Gordon, eds., Pergamon Press, New York, 1963.

172. E. W. Resnick, The Determination of Iron in Perchloric Acid Media Using Using Rotating Disk and Ring-Disk Electrodes, Unpublished M. S. thesis, Ames, Iowa, Library, Iowa State University, 1970.

173. L. Riccoboni and M. Zotta, Ric. Sci. Ricostruz, 17, 1169 (1947).

174. D. K. Roe, Anal. Chem., 36, 2371 (1964).

175. M. T. Rossetti, Atti ist. Veneto Sci., 103, Pt II, 77 (1943-44).

176. A. Saito, Nippon Kagaku Zasshi, 82, 715 (1961).

177. E. Sandi, Z. Anal. Chem., 167, 241 (1959).

178. K. Sasaki, I. Izumi, K. Ohashi, T. Uemura, and S. Nagaura, Nippon Kagaku Zasshi, 87, 918 (1966).

179. E. Scarano, M. G. Bonicelli, and M. Forina, Anal. Chem., 42, 1470 (1970).

180. O. Scarpa, Atti Accad. Italia., Rend. Classe Sci. Fis. Mat. Nat. [7], 1, 204 (1939).

181. O. Scarpa, Atti Accad. Italia., Rend. Classe Sci. Fis. Mat. Nat. [7], 1, 443 (1940).

182. E. Scheffler and S. Ziegenbalg, Freiberger Forschungsh, B83, 111 (1963).

183. J. R. Scholes and K. H. Denmead, Metallurgia, 71, 295 (1965).

184. R. Schulmann, J. Amer. Chem. Soc., 46, 52 (1924).

185. K. Schwabe and W. Schwenke, Electrochim. Acta, 9, 1003 (1964).

186. V. V. Senkevich, L. P. Chernega, V. I. Badzer, and Yu. S. Lyalikov, Zavod. Lab., 34, 1176 (1968).

187. M. D. Seymour, Rapid Separation and Determination of Heavy Metals in Hydrochloric Acid by Forced-flow Anion Exchange Chromatography, Unpublished Ph. D. Thesis, Ames, Iowa, Library, Iowa State University, 1972.

188. L. R. Sharma and J. Dutt, Indian J. Chem., 6, 593, 597 (1968).

169. L. R. Sharma and J. Dutt, Indian J. Chem., 7, 485 (1969).

190. L. R. Sharma and J. Dutt, Indian J. Chem., 8, 170 (1970).

191. J. A. Shropshire, J. Electroanal. Chem., 9, 90 (1965).

192. R. E. Sioda, Electrochim. Acta, 13, 375 (1968).

193. R. E. Sioda, Electrochim. Acta, 13, 1559 (1968).

194. M. Spiro, Electrochim. Acta, 9, 1531 (1964).

195. S. Srinivasan and E. Gileadi, Electrochim. Acta, 11, 321 (1966).

196. S. Srinivasan and H. Wroblowa, Advances in Catalysis, 17, 351 (1951).

197. J. T. Stock, "Amperometric Titrations," Interscience, New York, 1965.

198. F. W. E. Strelow, Anal. Chem., 32, 1185 (1960).

199. J. H. Strohl and T. A. Polutanovich, Anal. Letters, 2, 423 (1969).

200. M. V. Susic, Bull. Inst. Nuclear Sci. "Boris Kidrich", 5, 65 (1955).

201. T. Takada, K. Nakana, A. Yamada, and K. Morinaga, Denki Kagaku, 31, 125 (1963).

202. Y. Takashi, Nippon Kagaku Zasshi, 82, 1012 (1961).

203. Y. Takemori and M. Honda, Rev. Polarog. Jap., 16, 96 (1970).

204. R. Tamamushi, S. Momiyama, and N. Tanaka, Anal. Chim. Acta, 23, 585 (1960).

205. N. Tanaka and R. Tamamushi, Electrochim. Acta, 9, 963 (1964).

206. V. V. Ten'kovtsev, J. Appl. Chem. USSR, 30, 1161 (1957).

207. V. M. Tioshits and A. I. Levin (USSR), Tr. Ural. Politekh. Inst., No. 170, 76 (1968).

208. P. E. Toren, Anal. Chem., 40, 1152 (1968).

209. S. Trasatti, Chimica e Industria, 51, 1063 (1969).

210. A. M. Trukhan, Yu. M. Povanov, and P. D. Lukovtsev, Elektrokhimiya, 4, 763 (1968).

211. M. Tsuiki, Denki Kagaku, 28, 687 (1965).

212. M. Tsuiki, Denki Kagaku, 29, 42 (1965).

213. M. Tsuiki and T. Kawase, Gifu Daigaku Nogakubu Kenkyu Hohoku, No. 10, 26 (1960).

214. A. Turco, Gazz. Chim. Ital., 83, 231 (1953).

215. S. Tustanowski, J. Chromatog., 31, 266 (1967).

216. L. N. Vasil'eva, R. G. Pats, and A. A. Pozduzakova, Zh. Anal. Khim., 22, 1659 (1957).

217. L. N. Vasil'eva and Z. L. Yustus, Sb. Nauch. Tr. Gos. Nauch-Issled. Inst. Isvet. Metal, No. 27, 40 (1967).

218. J. Veber, D. Pirtskhalova, Yu. B. Vasil'ev, and V. S. Bagotskii, Elektrokhimiya, 5, 1037 (1969).

219. K. J. Vetter, Z. Phys. Chem., 196, 360 (1951).

220. K. J. Vetter, Z. Elektrochem., 56, 797 (1952).

221. K. J. Vetter, Z. Phys. Chem., 199, 285 (1952).

222. K. J. Vetter and G. Manecke, Z. Phys. Chem., 195, 270 (1950).

223. K. J. Vetter and G. Manecke, Z. Phys. Chem., 195, 337 (1950).

224. K. J. Vetter and G. Thiemke, Z. Elektrochem., 64, 805 (1960).

225. L. Vignoli, B. Cristau, and F. Govezo, Chim. Anal., 43, 439 (1961).

226. S. Vivarelli and D. Cozzi, Soc. Ital. Progr. Sci., Atti iunione, 44th Meeting, Perugia (1952) Summ: Chimica e ndustria, 34, 684 (1952).

227. A. J. Vogel, "Quantitative Inorganic Analysis," 3rd ed., Wiley, New York, 1961, p. 369.

228. J. A. Voloshchenko, Ukr. Khim. Zh., 25, 576 (1959).

229. J. D. Voorhies and S. M. Davis, Anal. Chem., 32, 1855 (1960).

230. E.-K. Wang and J. P. Chang, Hua Hsueh Hsueh Pao, 31, 18 (1965).

231. E.-K. Wang and C. H. Shang, Hua Hsueh Hsueh Pao, 31, 464 (1965).

232. L. D. Wilson and R. J. Smith, Anal. Chem., 25, 218 (1953).

233. L. D. Wilson and R. J. Smith, Anal. Chem., 25, 334 (1953).

234. W. M. Wise and J. P. Williams, Anal. Chem., 36, 1863 (1964).

235. R. A. Whiteker and N. R. Davidson, J. Amer. Chem. Soc., 75, 3081 (1953).

236. L. A. Wooten and C. L. Luke, Ind. Eng. Chem., 13, 771 (1941).

237. P. Ya. Yakovlev, R. D. Malinina, G. P. Razumova, and M. S. Dymova, Teoriya i Praktika Polyarograf. Aniliza, Akad. Nauk Moldavsk, SSR, Materialy Perrogo Vses. Soveslich., 198 (1962).

238. S. Yamauchi, Bunseki Kagaku, 15, 466 (1966).

239. T. Yoshino, Nippon Kagaku Zasshi, 82, 1012 (1961).

240. M. D. Seymour, J. P. Sickafoose, and J. S. Fritz, Anal. Chem., 43, 1734 (1963).

241. F. Albert Cotton and G. Wilkinson, F. R. S., "Advanced Inorganic Chemistry", Interscience, New York, 1962, p. 568.

XI. ACKNOWLEDGEMENTS

The author would like to express his deep appreciation to Dr. Dennis C. Johnson for his assistance and guidance throughout the course of my research and graduate study. His high ideals and expectations provided the necessary inspiration to make my research and teaching challenging and rewarding experiences.

The author thanks the National Science Foundation for financial support during the summer of 1971 and Pine Instrument Company, Grove City, Pennsylvania, for financial support during the summer of 1972.

The author would like to thank Ronald Davenport and Bruce Parkinson for their contributions to my research.

Finally, the author thanks his wife, Marcia, for her support and understanding during my graduate study. I am also grateful for her assistance in the typing of this manuscript.